5. SITE 485[1]

Shipboard Scientific Party[2]

HOLE 485

Date occupied: March 5, 1979

Date departed: March 6, 1979

Time on hole: 19 hours

Position: 22°44.95′N; 107°54.21′W

Water depth (sea level; corrected m, echo-sounding): 2981.0

Water depth (rig floor; corrected m, echo-sounding): 2991.0

Bottom felt (m, drill pipe): 2996.5

Penetration (m): 50.5

Number of cores: 6

Total length of cored section (m): 50.5

Total core recovered (m): 36.93

Core recovery (%): 73

Oldest sediment cored:
Depth sub-bottom (m): 50.5
Nature: Silty clay
Age: Quaternary
Measured velocity (km/s): About 1.5

Principal results: 50 meters of soft to firm, grayish olive clay with minor layers of silty clay, clayey silt, and silty sand were recovered. All of the sediments are Quaternary in age.

HOLE 485A

Date occupied: March 6, 1979

Date departed: March 12, 1979

Time on hole: 7 days

Position: 22°44.92′N; 107°54.23′W

Water depth (sea level; corrected m, echo-sounding): 2981.0

Water depth (rig floor; corrected m, echo-sounding): 2991.0

Bottom felt (m, drill pipe): 2996.5

Penetration (m): 331.0

Number of cores: 39

Total length of cored section (m): 280.5

Total core recovered (m): 136.1

Core recovery (%): 49

Oldest sediment cored:
Depth sub-bottom (m): 314.5
Nature: Mudstone
Age: Quaternary
Measured velocity (km/s): 2.17

Basement:
Depth sub-bottom (m): 153.5
Nature: Basalt
Velocity range (km/s): 4.99–6.20

Principal results: 153 meters of hemipelagic clay, silty clay, and sandy silt of Quaternary age overlay acoustic basement. The basement was cored for 280.6 meters and found to consist of interlayered massive basalts and sediments composed largely of silty claystone.

BACKGROUND AND OBJECTIVES

Having completed drilling operations at Site 484, we decided to drill and log one additional hole and run the oblique seismic experiment before returning to port. We considered two locations near Site 483 as possible drilling sites, but since previous drilling at this site and at Site 474 (drilled on Leg 64) indicated that the basement was relatively uniform in this part of the Gulf, we decided that some other site might provide more useful information. From a scientific standpoint we thought that a mirror-image site, directly across the median rift from Site 482, would be most valuable. But this site had only about 60 m of sediment, and drilling difficulties at Site 484 had indicated that a sediment thickness of at least 100 m was necessary to start a hole into basement.

Site 485 was therefore selected in the first sediment pond east of that where Site 482 was located. This site has about 120 to 150 meters of sediments overlying basement, a high heat flow, and some basement reflectors, suggesting pillow piles at the sediment/basement contact. This was also judged the best location in which to carry out the oblique seismic experiment because of its proximity to Hole 482C, in which the Hawaiian downhole seismometer was already emplaced.

The primary objectives at Site 485 were to determine the nature of the basement (specifically to determine whether the upper basement consists of pillows or interlayered massive basalts and sediments), to investigate the width of the axial intrusion zone using magnetic reversal stratigraphy, to determine the temperature gradient in the sediments and in the underlying basement, and to study the structure of the upper crust by repeat-

[1] Lewis, B. T. R., Robinson, P., et al., *Init. Repts. DSDP*, 65: Washington (U.S. Govt. Printing Office).

[2] Brian T. R. Lewis (Co-Chief Scientist), Department of Oceanography, University of Washington, Seattle, Washington; Paul T. Robinson (Co-Chief Scientist), Department of Earth Sciences, University of California, Riverside, California (present address: Department of Geology, Dalhousie University, Halifax, Nova Scotia, Canada); Richard N. Benson, Delaware Geological Survey, University of Delaware, Newark, Delaware; Grant Blackinton, Hawaii Institute of Geophysics, University of Hawaii at Manoa, Honolulu, Hawaii; Ron Day, Department of Geological Sciences, University of California, Santa Barbara, California (present address: Arco Oil and Gas Company, Dallas, Texas); Frederick K. Duennebier, Hawaii Institute of Geophysics, University of Hawaii at Manoa, Honolulu, Hawaii; Martin Flower, Department of Mineral Sciences, Museum of Natural History, Smithsonian Institution, Washington, D.C. (present address: Department of Geological Sciences, University of Illinois at Chicago Circle, Chicago, Illinois); Mario Gutiérrez-Estrada, Instituto de Ciencias del Mar y Limnología, Universidad Nacionál Autónoma de Mexico, Mexico City, Mexico (present address: Estación de Investigaciones Mazatlán, Universidad Nacionál Autónoma de Mexico, Mazatlán, Sinaloa, Mexico); John Hattner, Department of Geology, Florida State University; Tallahassee, Florida (present address: Chevron Oil Company, Lafayette, Louisiana); Albert M. Kudo, Department of Geology, University of New Mexico, Albuquerque, New Mexico; M. Ann Morrison, Department of Geology, Imperial College, London, England (present address: Department of Geological Sciences, University of Birmingham, Birmingham, England); Claude Rangin, Laboratoire Tectonique, Universite Pierre et Marie Curie, Paris, France; Matthew H. Salisbury, Deep Sea Drilling Project, Scripps Institution of Oceanography, La Jolla, California; Hans-Ulrich Schmincke, Institut fur Mineralogie, Ruhr-Universitat, Bochum, Federal Republic of Germany; Ralph Stephen, Department of Geology and Geophysics, Woods Hole Oceanographic Institution, Woods Hole, Massachusetts; Boris P. Zolotarev, Geological Institute, U.S.S.R. Academy of Sciences, Moscow, U.S.S.R.

ing the oblique seismic experiment conducted on Leg 52 (Stephen et al., 1980). To accomplish these objectives, we decided to drill a single-bit hole to the maximum possible depth in the time available and to run a complete set of downhole logs prior to undertaking the seismic experiment.

OPERATIONS

After profiling from Site 484 and making three runs across the sediment valley at Site 485, we dropped the beacon in 2981 meters of water at 22°45′N, 107°54′W at 0650 hours on March 5. Figure 1 illustrates the general location of the site, and Figure 2 shows the reflection profile taken on board the *Glomar Challenger* while passing over the site. We took a mud line core for Hole 485 at 1430 hours and, after five more sediment cores had been taken, attempted a temperature run. Since we were unable to recover the probe, we suspected that its tip had been bent outside the bit. We therefore pulled the pipe and, at 0200 hours on March 6, found that the probe was indeed bent and that the electronics package had sprung a leak.

After offsetting 50 ft. to the east, we began Hole 485A, obtaining our first core at 1100 hours on March 6 after washing down to about 50 meters sub-bottom (Table 1). Acoustic basement was reached about 10 hours later at a sub-bottom depth of 153.5 meters. The drilling went smoothly thereafter, until it was stopped because of time constraints at 0330 hours on March 10 at a sub-bottom depth of about 330 meters. After washing and cleaning the hole, we released the bit at 0830 hours.

After the logging had been completed, we checked out, on the rig floor, the three-component borehole geophone that was to be used in the oblique seismic experiment and then lowered it to a depth of 3215 meters (134 meters sub-bottom). While testing in the hole, we observed unity gain seismic signals for all three components, though no seismic signals were observed on the amplifier channels. We therefore brought the geophone back to the surface, where testing on deck confirmed that the amplifiers were not working properly.

After we had made an unsuccessful attempt to deploy a high-pressure hydrophone in the hole, we successfully emplaced a vertical component geophone at 1345 hours on March 11, and the *Kana Keoki* conducted a prearranged shooting pattern around the site. As discussed by Stephen et al. (this volume), we successfully completed the experiment with the recovery of the seismometer at 0830 on March 12.

A final logging run to measure the temperature at the bottom of the hole was begun at 0830 hours and finished at 1130. The pipe was then pulled, and the ship headed for port in Mazatlán, bringing the leg to an end on March 13, 1979.

SEDIMENT LITHOLOGY

As can be seen in Figures 1 and 2, the two holes drilled at Site 485 are located just to the east of Site 482 in a valley parallel to the rift axis. Hole 485 was cored continuously from the mud line to a sub-bottom depth of 50.5 meters sub-bottom, whereas Hole 485A was washed from the mud line to a depth of 50.5 meters and then cored continuously to a total depth of 331.0 meters sub-bottom.

The uppermost sediment/basalt contact, which we interpret as the acoustic basement, occurs at 153.5 meters, but thick layers of sediments were found between the various basalt units below the contact (Fig. 3). Recovery in the sediments was good to a depth of 65 meters, but only moderate to poor at greater depths. In the following discussion, the sediments will be described in terms of those found, respectively, above and below the uppermost basalt. Since Holes 485 and 485A were drilled only a few meters apart, the sediments from the two holes will be described together.

Sediments Overlying Basement

Sediments overlying the uppermost basalt are mainly hemipelagic with minor terrigenous material. We recognized two units in the sediments on the basis of the relative content of hemipelagic versus terrigenous material as well as the thickness and frequency of the more coarse-grained layers interpreted as distal turbidites (Table 2).

Unit I (0–79.0 m)

Unit I consists of two subunits. The uppermost subunit (IA), which ranges from 0 to 31.5 meters sub-bottom, is composed of fine-grained hemipelagic sediments interbedded with fine-grained turbidite sequences. The turbidites display sharp contacts with the underlying fine-grained hemipelagic material, grading upward to thin fine-grained sediments.

The fine-grained material in Unit IA is represented by soft to firm grayish olive (10Y4/2) clay with small, white, siliceous-sponge spicule concretions, black strands of pyrite, and a low (5%) silt-size detrital mineral content. The turbidite layers, which range from a few centimeters to a few tens of centimeters in thickness, are composed of grayish olive (10Y4/2) or olive gray (5Y3/2) silty clay, clayey silt, and sandy silt. The reworked minerals in these layers are mainly quartz, feldspar, pyrite, and heavy minerals. The thickest turbidite layers are generally the most coarse grained.

The lower subunit (IB), which ranges from 31.5 to 79.0 meters sub-bottom, is similar to Unit IA except that the fine-grained layers have a higher silt-size detrital mineral content (15%), and the more coarse-grained material displays a lower content of detrital minerals than do corresponding layers in the subunit above. Nonetheless, the sandy fraction is higher (20%) and present more frequently than in the turbidite layers of the upper subunit. The thickness of these turbidite layers (10–50 cm) is greater than in the subunit above, and plant fragments are present in a few of the layers (Fig. 4).

In a general way, the coarse-grained material increases with depth throughout Unit I, and only the uppermost 35 meters of the unit are unconsolidated. The increase in consolidation below this depth could be related to local diagenesis, since centimeter-size pieces of

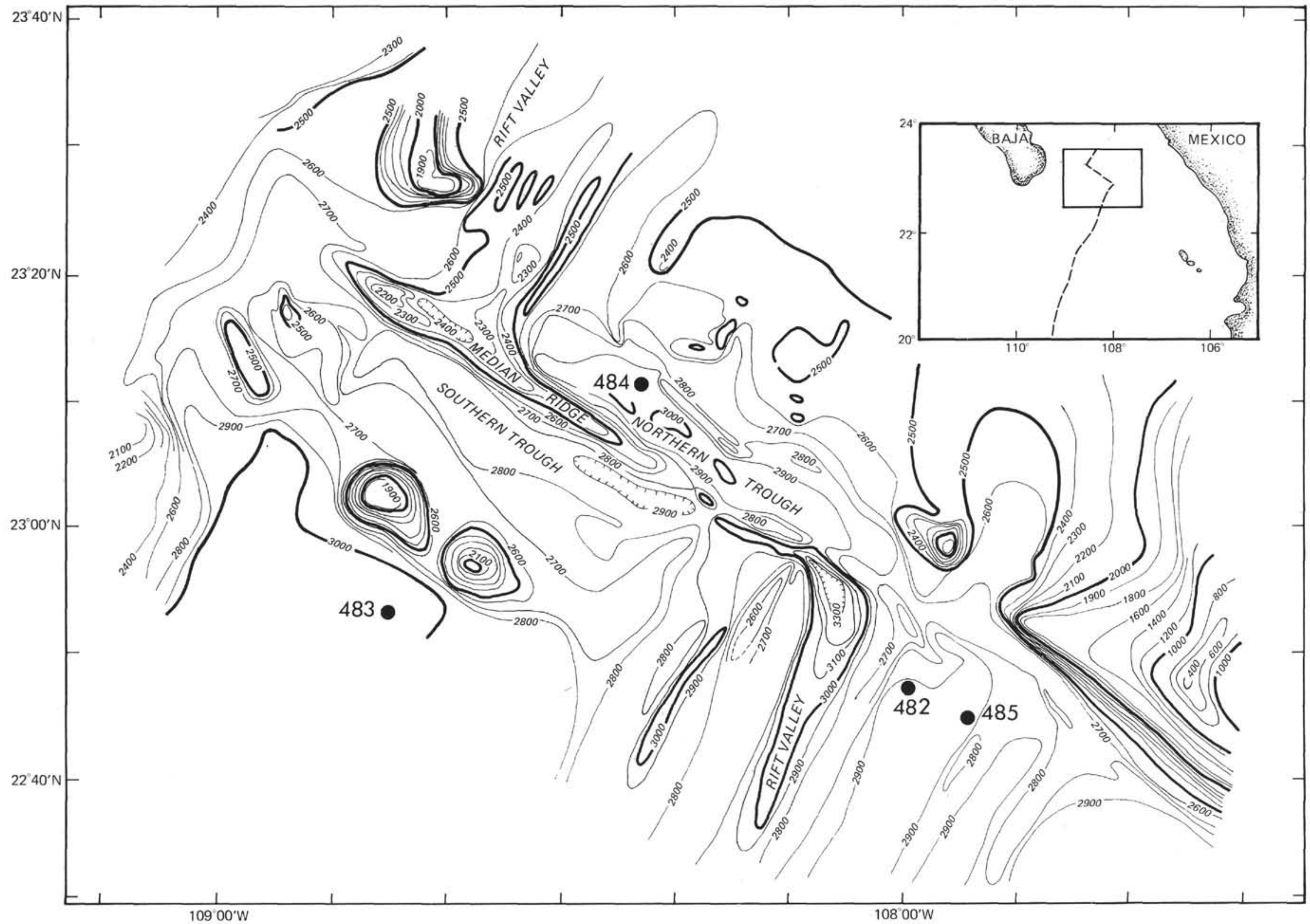

Figure 1. Bathymetry map of the Tamayo Fracture Zone showing location of Site 485.

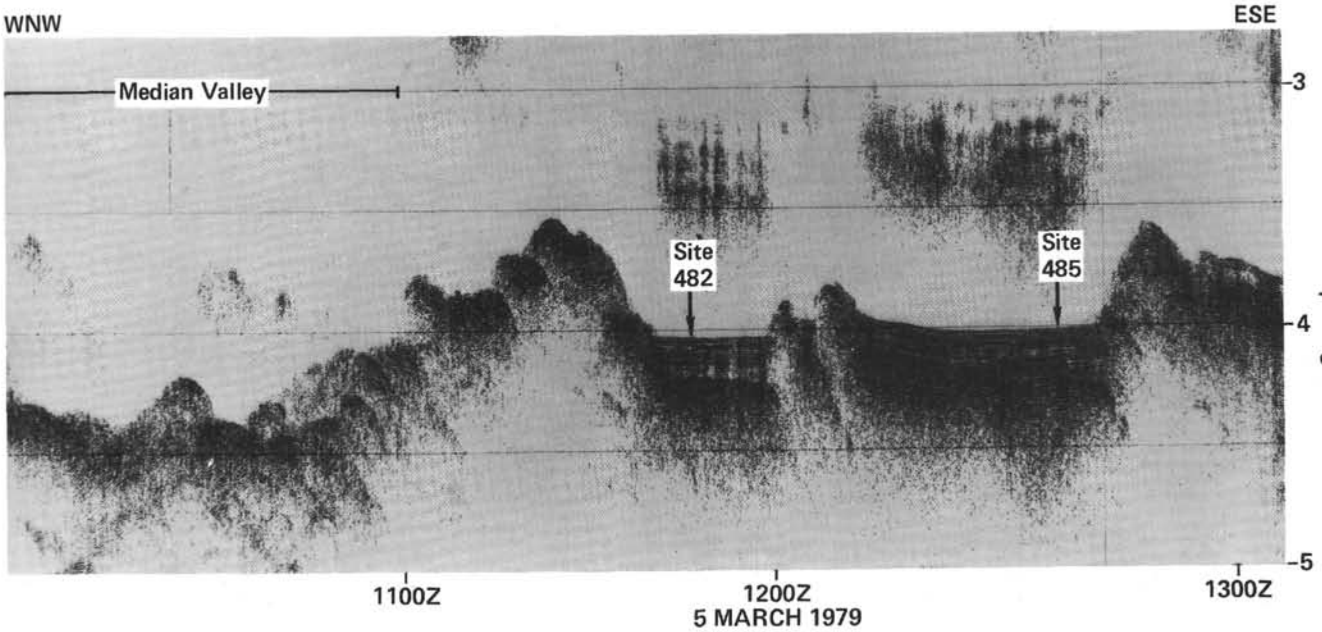

Figure 2. Seismic reflection profile recorded aboard *Glomar Challenger* through Sites 482 and 485, using an air-gun sound source. (Vertical scale in seconds of two-way reflection time. Horizontal scale is given in time along ship's track. One hour represents about 10 km.)

Table 1. Coring summary, Site 485.

Core	Date	Time	Depth from Drill Floor (m)	Depth below Seafloor (m)	Length Cored (m)	Length Recovered (m)	Recovery (%)
Hole 485							
1	3/5/79	1510	2996.5-2999.5	0.0-3.0	3.0	2.69	90
2	3/5/79	1608	2999.5-3009.0	3.0-12.5	9.5	4.90	52
3	3/5/79	1658	3009.0-3018.5	12.5-22.0	9.5	9.62	101
4	3/5/79	1756	3018.5-3028.0	22.0-31.5	9.5	3.90	41
5	3/5/79	1847	3028.0-3037.5	31.5-41.0	9.5	6.27	66
6	3/5/79	1943	3037.5-3047.0	41.0-50.5	9.5	9.55	101
Hole 485A							
1	3/6/79	1151	3047.0-3056.5	50.5-60.0	9.5	9.60	101
2	3/6/79	1253	3056.5-3066.0	60.0-69.5	9.5	5.89	62
3	3/6/79	1357	3066.0-3075.5	69.5-79.0	9.5	3.44	36
4	3/6/79	1448	3075.5-3085.0	79.0-88.5	9.5	1.14	12
5	3/6/79	1548	3085.0-3094.5	88.5-98.0	9.5	5.18	55
6	3/6/79	1652	3094.5-3104.0	98.0-107.5	9.5	4.40	46
7	3/6/79	1745	3104.0-3113.5	107.5-117.0	9.5	2.23	23
8	3/6/79	1846	3113.5-3123.0	117.0-126.5	9.5	3.34	35
9	3/6/79	2005	3123.0-3132.5	126.5-136.0	9.5	3.48	37
10	3/6/79	2128	3132.5-3142.0	136.0-145.5	9.5	3.70	39
11	3/7/79	0008	3142.0-3151.5	145.5-155.0	9.5	4.36	46
12	3/7/79	0755	3151.5-3154.5	155.0-158.0	3.0	1.38	46
13	3/7/79	1211	3154.5-3156.0	158.0-159.5	1.5	1.35	90
14	3/7/79	1350	3156.0-3160.5	159.5-164.0	4.5	0.61	14
15	3/7/79	1456	3160.5-3170.0	164.0-173.5	9.5	0.00	0
16	3/7/79	1639	3170.0-3177.0	173.5-180.5	7.0	0.05	0.7
17	3/7/79	1914	3177.0-3180.0	180.5-183.5	3.0	2.25	75
18	3/7/79	2037	3180.0-3184.5	183.5-188.0	4.5	1.50	33
19	3/7/79	2143	3184.5-3189.0	188.0-192.5	4.5	1.67	37
20	3/7/79	2307	3189.0-3193.5	192.5-197.0	4.5	2.12	47
21	3/8/79	0011	3193.5-3198.0	197.0-201.5	4.5	0.12	3
22	3/8/79	0203	3198.0-3208.0	201.5-211.5	10.0	8.57	86
23	3/8/79	0600	3208.0-3212.5	211.5-216.0	4.5	4.34	96
24	3/8/79	1040	3212.5-3217.5	216.0-221.0	5.0	4.65	93
25	3/8/79	1405	3217.5-3222.5	221.0-226.0	5.0	3.21	64
26	3/8/79	1527	3222.5-3227.0	226.0-230.5	4.5	1.75	39
27	3/8/79	1647	3227.0-3231.5	230.5-235.0	4.5	1.48	33
28	3/8/79	1749	3231.5-3236.0	235.0-239.5	4.5	0.90	20
29	3/8/79	2204	3236.0-3246.0	239.5-249.5	10.0	5.40	54
30	3/9/79	0115	3246.0-3251.0	249.5-254.5	5.0	4.60	92
31	3/9/79	0331	3251.0-3255.5	254.5-259.0	4.5	4.01	89
32	3/9/79	0640	3255.5-3264.5	259.0-268.0	9.0	8.04	89
33	3/9/79	0902	3264.5-3273.5	268.0-277.0	9.0	2.37	26
34	3/9/79	1119	3273.5-3282.5	277.0-286.0	9.0	2.39	27
35	3/9/79	1547	3282.5-3291.5	286.0-295.0	9.0	7.69	85
36	3/9/79	1738	3291.5-3300.5	295.0-304.0	9.0	3.87	43
37	3/9/79	1910	3300.5-3309.5	304.0-313.0	9.0	1.95	22
38	3/9/79	2321	3309.5-3318.5	313.0-322.0	9.0	7.48	83
39	3/10/79	0355	3318.5-3327.5	322.0-331.0	9.0	5.80	64
					280.5	136.31	49

limestone composed of silt-size calcite grains and minor dolomite occur in Core 6 from Hole 485.

Unit II (79.0–153.5 m)

Unit II is composed of alternating layers of firm to very firm and stiff, partially dehydrated, fine-grained hemipelagic material and thick layers of poorly compacted, fine-grained terrigenous material interpreted as turbidites. The fine-grained hemipelagic material is composed of gray to grayish olive clay and silty clay with a silt-size detrital mineral content of about 10% throughout most of the section except near the base of the unit, where it increases to 40%. As at many other sites in the ocean basins, the fine-grained sediments near the sediment/basement contact are relatively stiff and dehydrated.

The coarse-grained fraction in the turbidite layers is generally soft and poorly recovered. When present, it is composed of silty sand (60% sand, 35% silt) and is rich in foraminifers (15%). Silt-size grains of authigenic calcite and minor dolomite also occur (10–20%). Carbonate enrichment is common in the coarser-grained material and is particularly marked near the sediment/basalt contact.

Sediments Interlayered in Basement

We drilled thick sediment layers within the basalts between 153.5 and 331.0 meters. Although the recovery in these sediments was low, the logging results suggest that the basement section at Site 485 consists of nearly equal proportions of sediments and basalts distributed among seven sediment and eight basalt units, not all of which were successfully sampled. Although these are all shown in Figure 3, the sediment descriptions, which follow (and are summarized in Table 2) are necessarily based on

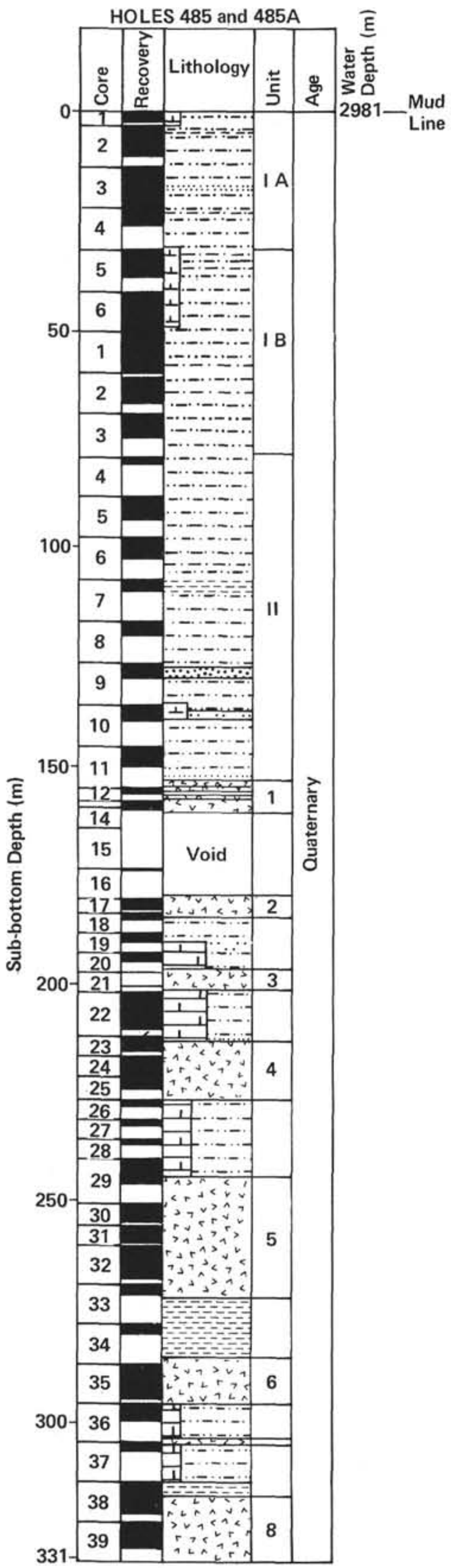

Figure 3. Sediment and basement stratigraphy, Site 485. (For explanation of symbols, see Explanatory Notes, this volume.)

the sediments recovered. It should be noted that we made no attempt to divide the sediments found in the basement into formal units or subunits, since the most obvious basis for making such a division, the presence of interlayered basalts, appears to be unrelated to sedimentation.

160.7–179.3 m: The presence of a 19-meter-thick layer of sediments between 7 and 26 meters sub-basement may be inferred from both logging (Salisbury, this volume) and from the high rate of penetration achieved while drilling through this interval. Though we recovered no sediments, these are inferred to be Quaternary in age on the basis of the age of underlying sediments.

183.7–195.8 m: Sediments in this interval consist of a soft, olive gray sandy mud underlain by a stiff, dehydrated, muddy nannofossil chalk, containing pyrite concretions. The boundary between these two lithologies is marked by an 80-cm-thick turbidite, composed of sandy mud and displaying a sharp contact with the underlying chalk. The contacts with the overlying and underlying basalts were not recovered.

201.0–212.5 m: The next sediment interval consists of olive gray, muddy nannofossil chalk and ooze with pyrite-filled burrows (Fig. 5) and interbedded turbidites composed of sandy mud and redeposited calcareous nannofossils. The turbidites we recovered are between 15 and 45 cm thick; since they tend to be less cohesive than the hemipelagic sediments, however, and may have been partially washed out during drilling, the turbidite layers may be thicker *in situ*.

The hemipelagic sediments in the upper 10 cm of Core 23 are rich in silt-size grains of calcite and minor dolomite and display evidence of carbonate dissolution and cementation, whereas the calcareous nannofossils in the same interval display several stages of recrystallization. The contacts with the overlying and underlying basalts are also marked by carbonates; we found pieces of limestone formed by dissolution and recrystallization of calcareous nannofossils below pieces of aphyric basalt along the upper contact, as well as a 10-cm-thick layer of hard, calcareous sandstone overlying the basalt at the base of the interval.

226.4–243.6 m: The recovered sediments in this interval consist of hard, black, nannofossil-bearing silty claystone. Since the recovery was low, however, this lithology may not be representative of the entire interval.

270.7–284.5 m: The next sediment interval consists of hard, black claystone with relatively few calcareous nannofossils. As in the sediments recovered between 201 and 212 meters, the scarcity of calcareous microfossils suggests that dissolution has taken place. Since the recovery was again low, the lithology reported may be biased.

294.5–303.2 m: Sediments in the next interval consist of olive black, nannofossil-bearing silty claystones with finely laminated sandy mudstones near the top of the section, which may be turbidites. The turbidites(?) are inclined about 10° and contain numerous pyrite-filled burrows. The carbonate content increases sharply about 6 cm above the basal contact, and limestone coats the uppermost piece of the underlying basalt.

Table 2. Sedimentary lithologic units, Site 485.

Unit	Lithology	Age	Depth (m)	Thickness (m)	Sample (level in cm)
Sediments overlying basement					
IA	Silty clay with thin turbidites composed of sandy silt and sandy mud	late Quaternary	0–31.5	31.5	485-1-1, 0 through 4,CC
IB	Silty clay and nannofossil-bearing silty clay with thin turbidites composed of sandy mud	late Quaternary	31.5–79.0	47.5	485-5-1, 0 through 485A-3,CC
II	Silty clay with thick turbidites composed of sandy mud, silt, and sand	Quaternary	79.0–153.5	74.5	485A-4-1, 0 to 11-3, 55
Sediments interlayered in basement					
	Not sampled	—	160.7–179.3	18.6	485A-14-1, 65 to 17-1, 0
	Sandy mud and muddy nannofossil chalk	Quaternary	183.7–195.8	12.1	485A-18-1, 58 to 22-1, 0
	Muddy nannofossil chalk	Quaternary	201.0–212.5	11.5	485A-22-1, 3 to 23-1, 50
	Nannofossil-bearing silty claystone	Quaternary	226.4–243.6	17.2	485A-26-1, 20 to 29-1, 0
	Claystone	Quaternary	270.7–284.5	13.8	485A-33-2, 95 to 34-1, 56
	Nannofossil-bearing silty claystone	Quaternary	294.5–303.2	8.7	485A-35-6, 55 to 36-3, 64
	Nannofossil-bearing silty claystone and claystone	Quaternary	304.2–315.0	10.8	485A-36,CC, 31 to 38-2, 2

304.2–315.0 m: The deepest sediments we recovered at Site 485 consist of very firm to hard, olive black claystones and nannofossil-bearing silty claystones. Zeolites are present in the clay matrix, and pyrite occurs as vein fillings (Fig. 6) and as a thin coating along the basal sediment/basalt contact.

In conclusion, the sedimentation at Site 485 is predominantly hemipelagic, but fine-grained, distal, and probably redeposited turbidite layers occur throughout the section. The abundance of the turbidites and their average grain size increase progressively from the mud line to the top of the uppermost basalt. Turbidites are still present within the sediments interlayered in the basement, but they decrease in frequency and grain size between 184 and 213 meters, below which sediments are more fine grained to the base of the section.

The sediment/basalt contacts are generally poorly preserved below the basalt layers because of drilling disturbance. On the other hand, sediments immediately overlying the basalts generally show dissolution of calcareous nannofossils, a change in color, and local carbonate cementation, which could indicate diagenesis.

BIOSTRATIGRAPHY

Calcareous nannofossils and moderately well to well-preserved foraminifers occur in most of the samples we examined from Site 485 (Fig. 7). The calcareous nannofossils are also moderately well to well preserved, except in the sediments interlayered in basalt, where the preservation is poor. Radiolarians are common to abundant only in the uppermost 80 meters of sediment. This depth corresponds to the late Quaternary increase in radiolarian faunal abundance noted at Site 482 (this volume).

The sediments between 0 and 36 meters sub-bottom (Core 485-1 through the upper part of Core 5) are assigned to Zone NN20/21 (undifferentiated) and are thus less than 0.41 million years old. The radiolarian *Axoprunum angelinum* has its highest occurrence (0.41 m.y.) at a sub-bottom depth of 35.31 meters (Sample 485-5-3, 80–82 cm) and is present to a depth of 73 meters (Section 485A-3,CC) and again at a depth of 227.10 meters (Sample 485A-34-1, 9–11 cm). Calcareous nannofossil Zone NN19 (0.44–1.65 m.y.) is recognized from the lower part of Core 485-5 through the lowest sediment unit recovered at the site (Section 485A-38-1 at a depth of 314 m). Based on negative evidence (the absence of the coccolith *Helicopontosphaera sellii*), the oldest sediment units drilled at Site 485 are no older than 1.22 m.y.

Calcareous Nannofossils

We analyzed nannofossils, planktonic foraminifers, and radiolarians in all of the sediment-bearing cores from Site 485. Since calcareous nannofossils were the most abundant fossil taxa observed, and are present almost throughout, they were used as the principal biostratigraphic control. Species identification was sometimes difficult, however, because of the small size and poor preservation of the nannofossils in some intervals.

Nannofossil assemblages and zonal succession at Site 485 are the same as those observed at Sites 483 and 484 except for changes caused by preferential dissolution in the sediments recovered near or within the basement sequence. Generally, the cores contain common to abundant nannofossils which are well to moderately well preserved. Within the basement sequence, however, the preservation was poor to moderate and tended to decrease downhole. In some of the same intervals, there were large amounts of unspecified carbonate. We observed one barren interval between 315 and 316 meters in Core 485A-38.

As was noted above, Cores 485-1 through 485-5 are assigned to Zone NN20/21. The boundary between Zones NN20/21 and NN19 occurs between Sample 485-5-4, 50–52 cm and Sample 485-5-4, 141 cm at a depth of 36–37 meters. No lower boundary was determined for Zone NN19. Since we observed no *Helicopontosphaera sellii*, a maximum age of 1.22 m.y. can be assigned to the recovered sedimentary section.

Foraminifers

Foraminifers are present in most of the samples but are abundant in only three (Fig. 7). In general, the tests are moderately well to well preserved.

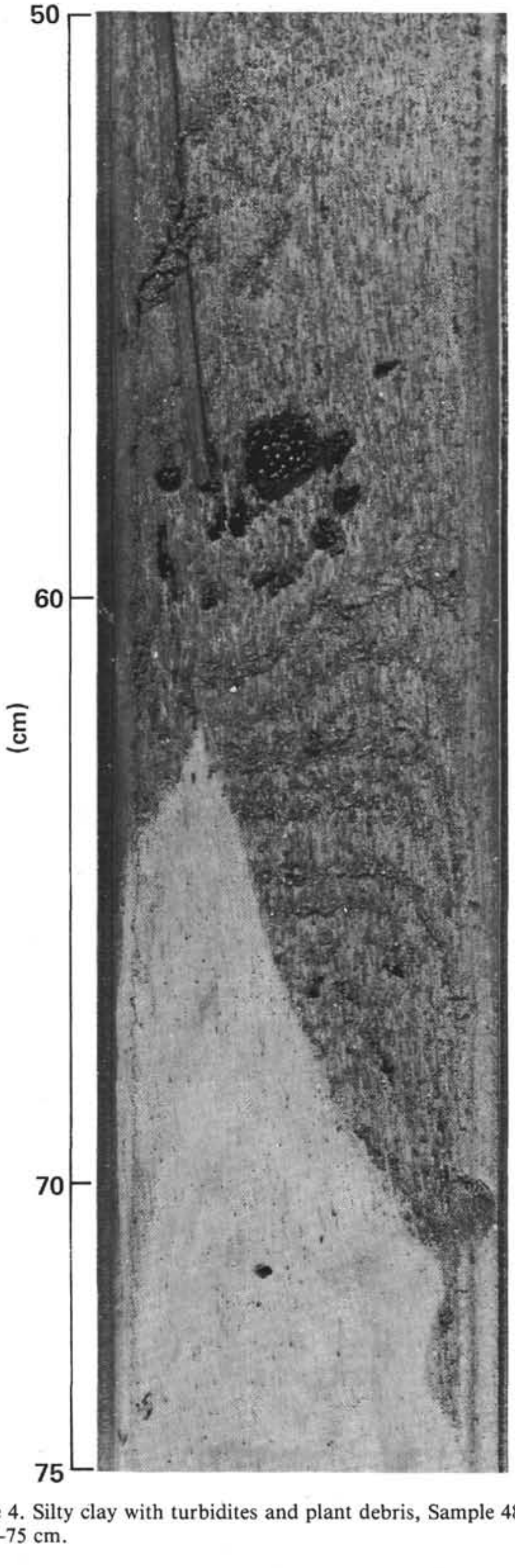

Figure 4. Silty clay with turbidites and plant debris, Sample 485-5-2, 50–75 cm.

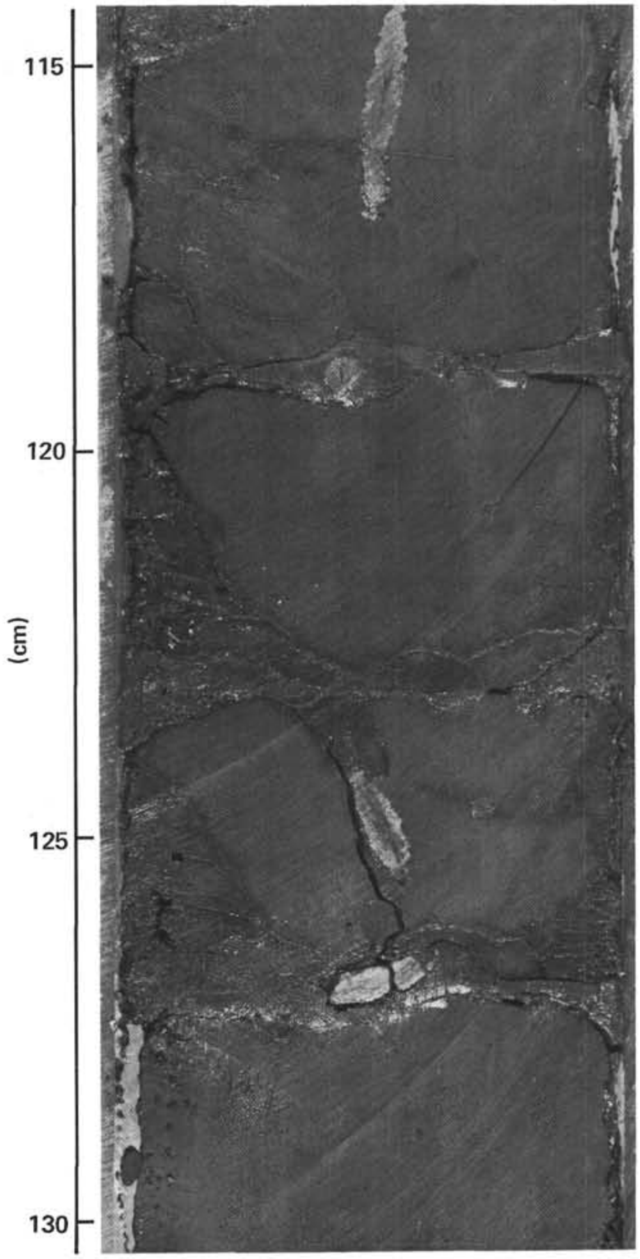

Figure 5. Pyrite-filled burrows in muddy nannofossil chalk, Sample 485A-22-1, 115–130 cm.

We observed lower bathyal to abyssal foraminiferal assemblages characteristic of water depths of about 3000 meters (*Melonis pompilioides, Uvigerina senticosa,* plus those listed for Site 483) in only 10 of the samples. In all others, assemblages displaced from upper bathyal and/or neritic environments are present. Many consist primarily of small juvenile specimens, which suggests that size-sorting, perhaps by turbidity or contour currents, has occurred. The displaced benthic foraminifers, therefore, support the interpretation that much of the sedimentary section at Site 485 consists of turbidites. The high rate of sediment accumulation also supports this view.

The most abundant and diverse planktonic foraminiferal assemblages generally occur in those samples containing *in situ*, lower bathyal to abyssal benthic species. The dominant species are *Globigerina bulloides, Globigerinoides ruber, G. sacculifer, Globoquadrina dutertrei*, and *G. pachyderma* (right-coiling). *Pulleniatina obliquiloculata* is common only in Core 485-1 at

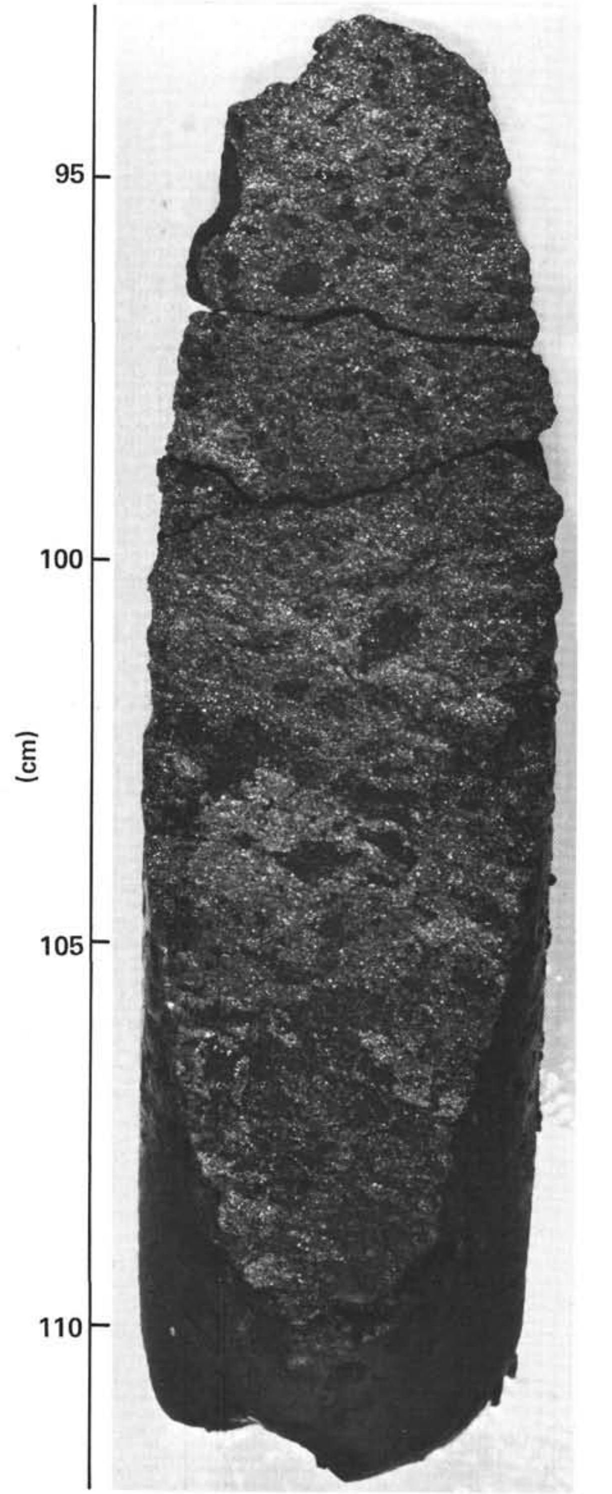

Figure 6. Pyrite vein filling in claystone, Sample 485A-38-1, 92–112 cm.

a depth of 2.3 meters. The assemblages thus appear to be characteristic of the California Current system.

No planktonic foraminiferal species indicative of a pre-Quaternary age were observed. Tests of *Globigerinoides ruber* with obliquely appressed later chambers suggestive of *G. obliquus*, a species that became extinct

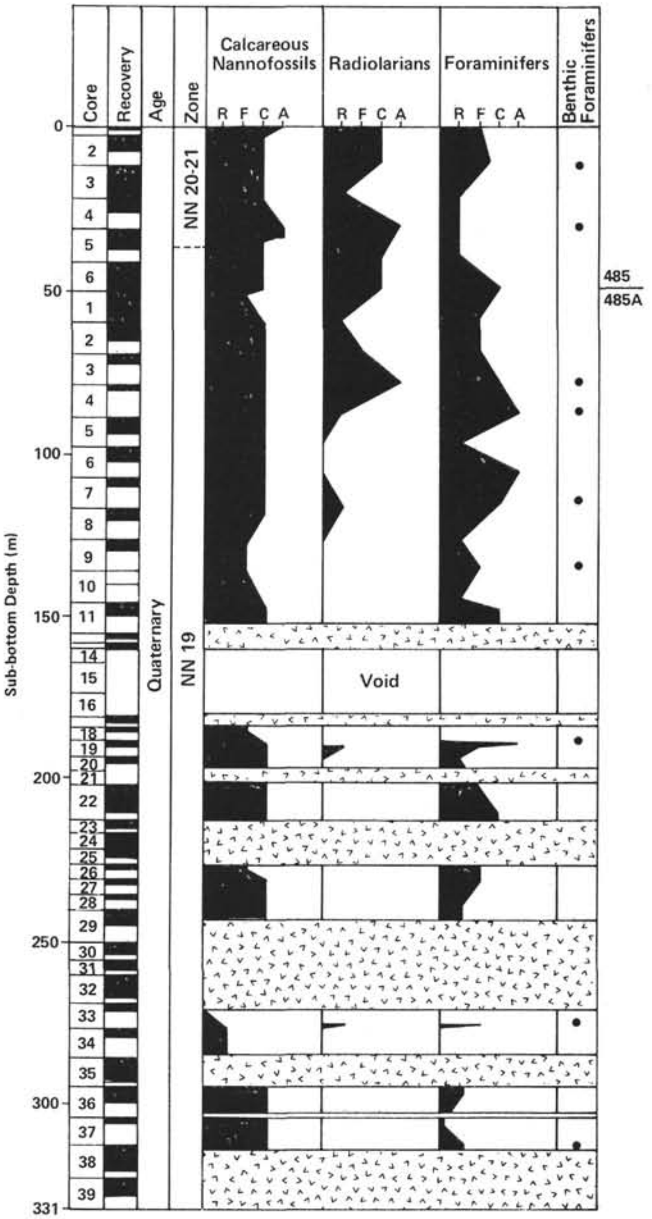

Figure 7. Biostratigraphic summary, Site 485. (R = rare, F = few, C = common, A = abundant.)

in the early Pleistocene, first occur in Section 485A-4,CC at a depth of 88.5 meters. Further study must be conducted to determine whether or not these forms are stratigraphically significant in the region of the Gulf of California.

Radiolarians

Radiolarians are common to abundant in the upper 80 meters of sediment at Site 485. Below this, they are rare to absent. Preservation is generally good.

The most abundant and diverse assemblages, typical of the Quaternary assemblages reported for other Leg 65 sites, are from the more pelagic sediments, characterized by the presence of *in situ*, lower bathyal to abyssal, benthic foraminiferal species. In the intervals above 80 meters in which radiolarians are uncommon

(Fig. 7), they appear to have been diluted by rapidly deposited terrigenous sediments, i.e., fine-grained turbidites. Below 80 meters, they are rare or absent even in the more pelagic sediments. In terms of estimated sediment accumulation rates for Site 485, this suggests that a true faunal increase occurred about 0.5 to 0.6 million years ago. This is consistent with the estimated dates of radiolarian faunal increases noted at DSDP sites southeast of the axis of the East Pacific Rise (Benson, this volume).

The highest occurrence of *Axoprunum angelinum* (= *Stylatractus universus*) is in Sample 485-5-3, 80–82 cm. The extinction level of this species (0.41 m.y.) is thus placed at about 35 meters sub-bottom. The only other level below 79 meters sub-bottom in which the species was found was at a depth of 277.10 meters (Sample 485A-34-1, 9–11 cm).

SEDIMENT ACCUMULATION RATE

We determined only two paleontologic datum points at Site 485, both of about the same age. The highest occurrence of *Axoprunum angelinum*, which became extinct 0.41 million years ago, is at a sub-bottom depth of 35.31 meters (Sample 485-5-3, 80–92 cm). The boundary between calcareous nannofossil Zones NN19 and NN20/21 (0.44 m.y.) occurs at about 36–37 meters sub-bottom in Section 485-5-4, between 51 and 141 cm. The rate of accumulation of the upper 37 meters of sediments is thus 88 m/m.y. (Fig. 8).

The thickness of sediments drilled below the uppermost basalt is 100 meters. This, together with the 154 meters drilled above the basement, totals 254 meters. Since the oldest sediment dated by calcareous nannofossils is younger than a minimum age of 1.2 m.y., the minimum average rate of sediment accumulation below 37 meters sub-bottom is 280 m/m.y.

Our interpretation of the magnetic anomaly pattern places a further constraint on the maximum age of the crust at Site 485. The site lies approximately in the middle of the Reversed Matuyama Epoch, lying between the Normal Brunhes Epoch and the Jaramillo Normal Event. The maximum crustal age is therefore about 0.8 m.y. Using this date, and allowing for an estimate of 30–40 meters of undrilled sediment below the base of the hole, the maximum sedimentation rate below 37 meters is about 625 m/m.y.

SEDIMENT GEOCHEMISTRY

As we had at the other sites drilled on Leg 65, we made numerous measurements using the shipboard Carbonate Bomb (Müller and Gastner, 1971) and CHN analyzer to determine the $CaCO_3$ and reduced (organic) carbon content of the sediments (Table 3). These were supplemented by shore-based measurements of total carbon, organic carbon, and $CaCO_3$ (Table 4) made with a LECO WR-12 analyzer, using the technique described by Bader et al. (1970) and Boyce and Bode (1972). As can be seen in Tables 3 and 4, the $CaCO_3$ content reaches a value of 20% in Section 485-4-2 but is relatively low (<10%) throughout the rest of the hole. The organic carbon content is also relatively low

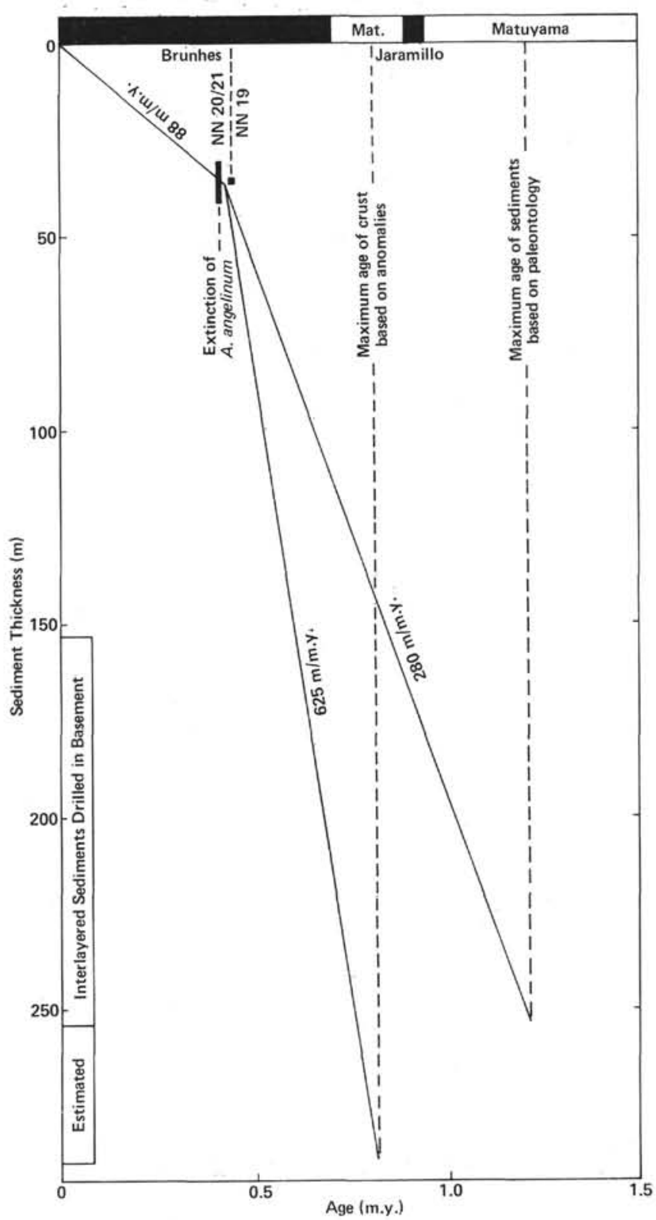

Figure 8. Sediment accumulation rates, Site 485.

(<3%), showing a slight tendency to decrease with depth.

SEDIMENT PHYSICAL PROPERTIES

Sediments above Basement

We made detailed physical property measurements on the sediments recovered at Site 485, as we had at Sites 482 through 484, using the techniques outlined previously (Site 482, this volume). As can be seen in Table 5 and Figure 9, wet-bulk density increases irregularly from about 1.4 g/cm^3 near the mud line to about 1.9 g/cm^3 near the basement contact, compressional-wave velocity increases from 1.5 km/s (the velocity of water) to about 1.7 km/s, shear strength increases from 0.05 to about 1 ton/ft.^{2}, and porosity decreases from 75% to about 45% over the same interval. Although these trends are

Table 3. $CaCO_3$ (bomb) and reduced carbon determinations, Site 485.

Sample (interval in cm)	$CaCO_3$ (%)	Reduced Carbon (%)	Lithology
Hole 485			
1-2, 0-2	6	—	Nannofossil-bearing silty clay
1-2, 8-10	6	2.2	Nannofossil-bearing silty clay
2-1, 30-32	2	2.9	Clay
2-1, 38-40	3	—	Clay
3-3, 43-45	5	2.5	Silty clay
3-3, 52-54	6	—	Silty clay
4-2, 10-12	17	—	Nannofossil-bearing sandy mud
4-2, 19-21	16	2.0	Nannofossil-bearing sandy mud
5-3, 51-53	3	—	Nannofossil-bearing silty clay
5-3, 62-64	3	2.0	Nannofossil-bearing silty clay
6-2, 18-20	4	1.9	Silty clay
6-2, 26-28	4	—	Silty clay
Hole 485A			
1-2, 20-22	2	—	Nannofossil-bearing silty clay
1-2, 28-30	6	1.5	Nannofossil-bearing silty clay
2-2, 19-21	4	2.6	Nannofossil-bearing silty clay
2-2, 28-30	3.5	—	Nannofossil-bearing silty clay
3-2, 30-32	3	—	Nannofossil-bearing silty clay
3-2, 44-46	5	2.4	Nannofossil-bearing silty clay
4-1, 70-72	2.5	—	Silty clay
4-1, 72-74	2.5	2.9	Silty clay
5-3, 13-15	4	—	Nannofossil-bearing silty clay
5-3, 24-26	4	1.5	Nannofossil-bearing silty clay
6-2, 28-30	4	1.5	Nannofossil-bearing silty clay
7-2, 42-44	3	—	Nannofossil-bearing clay
7-2, 52-54	2.5	1.1	Nannofossil-bearing clay
8-2, 19-21	4.5	—	Nannofossil-bearing silty clay
8-2, 28-30	5	1.9	Nannofossil-bearing silty clay
9-2, 78-80	2.5	—	Silty sand
9-2, 87-89	2.5	0.3	Silty sand
10-2, 30-32	3	2.3	Silty nannofossil ooze
10-2, 38-40	3	—	Silty nannofossil ooze
11-2, 85-87	3	—	Calcareous clayey silt
Hole 485A			
11-2, 93-95	4	0.8	Calcareous clayey silt
22-1, 47-50	4.5	1.9	Muddy nannofossil chalk
22-1, 50-52	4.5	—	Muddy nannofossil chalk
22-6, 32-34	4	—	Muddy nannofossil chalk
22-6, 38-40	5	1.7	Muddy nannofossil chalk

Note: — = not determined.

Table 4. Carbon and carbonate analyses, Site 485.

Sample (level in cm)	Depth (m)	Total Carbon (%)	Organic Carbon (%)	$CaCO_3$	Lithology
Hole 485					
1-2, 11	1.64	2.7	1.9	7	Nannofossil-bearing silty clay
2-1, 29	3.29	2.8	2.0	7	Silty clay
3-3, 42	15.92	2.7	1.6	9	Silty clay
4-2, 8	23.58	3.6	1.2	20	Nannofossil-bearing sandy mud
5-3, 59	35.09	2.2	1.5	5	Nannofossil-bearing silty clay
6-2, 16	42.66	2.0	1.5	4	Silty clay
Hole 485A					
2-2, 18	61.68	2.7	1.9	7	Nannofossil-bearing silty clay
4-1, 68	79.68	2.7	2.0	5	Silty clay
5-3, 22	91.72	2.0	1.1	7	Nannofossil-bearing silty clay
8-2, 18	118.68	2.5	1.4	9	Nannofossil-bearing silty clay

clearly related to clay compaction (the section consists predominantly of silty clay), several features in Figure 9 deserve further comment:

1) At Sites 482 and 483 (and, in fact, at most DSDP sites), the physical properties of the recovered sediments are uniform to a depth of 50–70 meters because of drilling disturbance in the unconsolidated sediments at the top of the section. At Site 485, however, the uppermost sediments display traces of bedding, and the physical properties change monotonically from the mud line to the basement. This suggests that the uppermost sediments are relatively undisturbed and that the physical properties shown in Figure 9 for the upper levels of the hole may approach those *in situ*.

2) The velocities measured in the sediments recovered between 50 and 100 meters sub-bottom were anomalously low (and the signal attenuation high) because of the presence of gas (H_2S). Since H_2S is unlikely to be in the gaseous state *in situ*, the velocities shown for this interval in Figure 9 are probably not representative of *in situ* conditions.

3) The section consists largely of clay, but silt and sand are important constituents at the base of each turbidite sequence. Since silt and sand will reduce the shear strength of the sediments, the base of each turbidite is likely to be a zone of washouts and low recovery, particularly toward the base of the section, where high pump pressures were used in drilling.

Sediments Interlayered in Basement

Within the interlayered sediments below the uppermost basalts, physical properties continue to change with depth in response to increasing compaction, with wet bulk density, velocity, and shear strength of the silty clays and claystones reaching values as high as 1.93 g/cm^3, 2.17 km/s, and 1.87 tons/ft.^{2}, respectively, and porosity reaching values as low as 42%. As in the overlying sediments, the physical properties of the sandy layers are noticeably different from those of the more clay-rich material; in particular, the unconsolidated sandy layers have extremely low shear strengths (about 0.3 tons/ft.^{2} in Cores 18-1 and 19-2) whereas the more cemented sandy layers (Sections 20,CC and 22-3) have high densities and velocities and low porosities. Since the latter are not volumetrically important, however, they do not contribute significantly to the physical properties of the formation.

IGNEOUS PETROGRAPHY

We drilled Hole 485A to a total depth of 331 meters, of which the lower 178 meters (Cores 11 through 39) were a sequence of interlayered sediments and basalts that we interpret as acoustic basement. The average recovery below the uppermost basalt was 51%, but we estimate from the results of logging (Salisbury, this volume) that between 80 and 90% of the basalt was recovered and that the cores with little recovery were mostly sediment.

As can be seen in Figure 3, the basement section consists of about 100 meters of sediment and 78 meters of basalt. The upper 90 meters consists largely (70%) of sediments (sandy mud, muddy nannofossil chalk, and silty claystone) with interlayered massive and pillow basalts, whereas the lower 88 meters is composed largely (60%) of relatively thick, massive basalt units inter-

Table 5. Sediment physical properties, Site 485.

Sample (interval in cm)	Wet-Bulk Density (g/cm^3)	P-Wave[a] Velocity (km/s)	Acoustic Impedance ($\times 10^5$ g/cm^2·s)	Shear[b] Strength (tons/ft.^{2})	Porosity[c] (vol.%)	Remarks
Hole 485						
1-1, 109-113	—	—	—	0.03	—	Soft
1-2, 64-77	1.34	1.50	2.01	0.05	79	Soft
2-1, 73-77	—	—	—	0.07	—	Soft
2-2, 102-105	—	—	—	0.05	—	Soft
2-3, 71-110	1.46	1.50	2.19	0.18	71	Stiff
3-2, 119-121	—	—	—	0.10	—	Soft
3-4, 22-24	—	—	—	0.14	—	Stiff
3-6, 95-110	1.49	1.50	2.24	0.14	69	Stiff
4-3, 32-47	1.50	1.51	2.27	0.25	69	Stiff
5-2, 44-46	—	—	—	0.19	—	Sandy layer in turbidite
5-2, 86-88	—	—	—	0.25	—	Clay-rich layer in turbidite
5-4, 36-47	1.74	1.57	2.73	0.10	54	Sandy layer in turbidite
5-4, 124-137	1.59	1.53	2.43	0.30	63	Clay-rich layer in turbidite
6-2, 82-84	—	—	—	0.20	—	Stiff
6-4, 120-122	—	—	—	0.13	—	Stiff
6-5, 138-140	—	—	—	0.17	—	Stiff
6-7, 3-19	1.54	1.48	2.28	0.33	66	Firm
Hole 485A						
1-2, 70-72	—	—	—	0.32	—	Gassy
1-4, 63-65	—	—	—	0.29	—	Gassy
1-6, 130-145	1.61	1.52	2.45	0.46	62	Gassy
2-3, 107-109	—	—	—	0.35	—	Gassy
2-4, 48-59	1.65	1.49	2.46	0.48	59	Gassy
3-2, 110-118	1.57	—	—	0.45	64	Gassy
3-3, 41-44	—	1.45	—	—	—	Gassy
4-1, 42-70	1.65	1.49	2.46	0.54	59	Gassy
5-3, 110-123	1.82	1.55	2.82	0.53	49	Gassy
5-4, 32-48	1.84	1.57	2.89	0.38	48	Clayey silt turbidite
6-3, 42-77	1.83	1.61	2.95	0.55	48	Stiff
6-3, 100-107	1.80	1.55	2.79	—	50	Sandy mud
7-2, 7-10	1.73	1.69	2.92	—	54	Clayey silt turbidite
7-2, 17-20	—	—	—	0.69	—	Stiff
8-2, 103-125	1.80	1.60	2.88	1.05	50	Stiff
9-2, 87-104	1.93	1.71	3.34	0.06	42	Disturbed silty sand
10-1, 121-130	1.64	—	—	0.33	—	Sandy silt turbidite
10-2, 62-78	1.78	1.65	2.94	1.03	51	Stiff
11-1, 104-140	1.78	1.67	2.97	—	53	Hard
18-1, 103-112	1.92	—	—	0.24	43	Disturbed sandy mud
19-2, 16-42	1.85	1.54	2.85	0.40	47	Soft sandy mud
19-2, 78-137	1.82	1.66	3.02	1.00	49	Firm
20-1, 95-121	1.83	1.84	3.37	—	51	Hard
20,CC, 21-23	2.57	5.00	12.85	—	8	Chalk
22-1, 77-80	1.80	1.83	3.29	—	54	Hard
22-3, 138-143	1.84	2.57	4.73	—	49	Sandy mud
26-1, 51-118	1.79	1.62	2.90	—	51	Firm
27-1, 121-128	1.81	1.72	3.11	—	50	Firm
28-1, 113-134	1.84	1.75	3.22	—	48	Firm
34-1, 41-43	1.93	1.86	3.59	1.47	42	Claystone
36-1, 20-23	—	2.40	—	—	—	Limestone
36-1, 101-140	1.93	1.95	3.76	1.45	46	Silty claystone
37-1, 41-70	1.87	2.03	3.80	1.87	46	Silty claystone
38-1, 18-19	—	2.17	—	—	—	Claystone

[a] Measured at atmospheric pressure.
[b] Torvane measurement.
[c] Assuming a grain density of 2.60 g/cm^3.

layered with claystones. Within these broad divisions, we distinguished seven lithologic units (Table 6) on the basis of drilling breaks, logging, the recovery of sediments, and such features as grain-size changes in the cores themselves. With the exception of Unit 1, which appears to be composed of five individual cooling units, each of the lithologic units shown in Table 6 represents a separate cooling unit.

As in the previous holes drilled on Leg 65, the phenocryst content in the basalts is generally low (<5%) but variable and includes the assemblages olivine and spinel, plagioclase > clinopyroxene > olivine, and plagioclase > olivine, with the uppermost unit being most variable. As would be expected, the basalts are fine grained near the margins of the massive basalts, medium to coarse grained near the centers, and very coarse grained to gabbroic in the thickest unit (Unit 5).

Lithologic Units

Unit 1

Unit 1 (Section 11-3, 55 cm to 14-1, 65 cm; 153.5 to 160.7 m) consists of four thin, massive cooling units at the top, each 1 meter or less in thickness, and a lower cooling unit slightly greater than 3 meters thick. The contact with the overlying sediment displays a 3-mm thick glassy margin and a crust of brecciated, indurated silty sand, containing deformed foraminifers, shards of glass, and feldspar (Fig. 10). The texture, phenocryst content, and chemistry of the cooling units are highly variable. The phenocrysts in the first cooling unit (1a) are: olivine > spinel; those in the third (1c) are: plagioclase > clinopyroxene > olivine; and those in the fifth (1e) are olivine > plagioclase. This contrast is somewhat surprising in that the cooling breaks separating the units

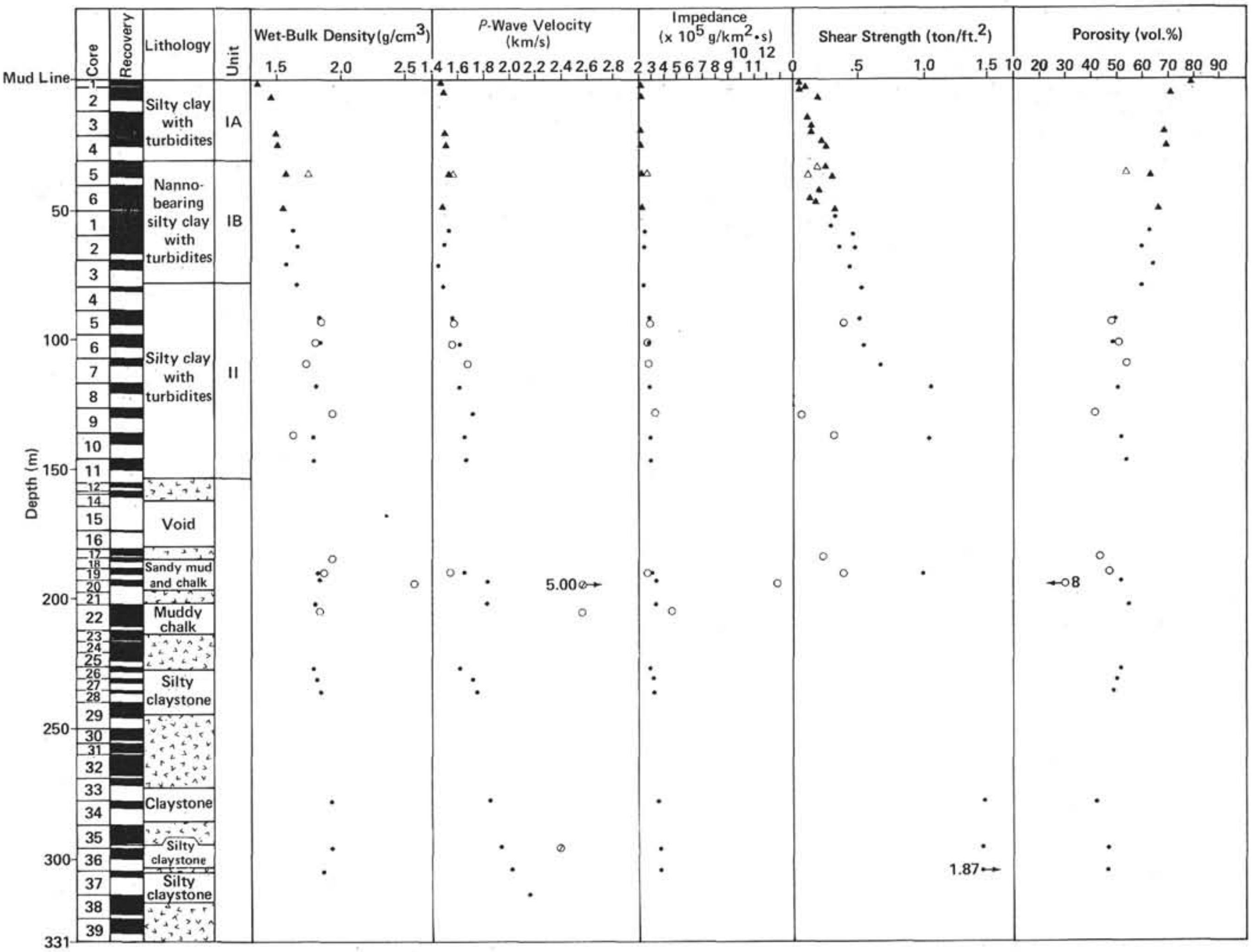

Figure 9. Sediment physical properties, Site 485. (Triangles and circles correspond to Holes 485 and 485A, respectively; filled symbols represent clay; open symbols represent sand or silt; ⊘ = limestone.

Table 6. Basement lithologic units, Hole 485A.

Unit	Top (m) a	Top (m) b	Base (m) a	Base (m) b	Thickness (m) a	Thickness (m) b	Type of Cooling Unit	Phenocryst Assemblage	Sample (level in cm)
1a	153.5	153.5	154.4	ND	0.9	ND	Massive basalt	Olivine-Plagioclase	11-3, 55 to 11-3, 140
1b	154.4	ND	155.5	ND	1.1	ND	Massive basalt	Plagioclase-Olivine	11-3, 140 to 12-1, 51
1c	155.5	ND	155.9	ND	0.4	ND	Massive basalt	Plagioclase-Clinopyroxene-Olivine	12-1, 51 to 12-1, 90
1d	155.9	ND	156.1	ND	0.2	ND	Massive basalt	Plagioclase-Olivine	12-1, 90 to 12-1, 114
1e	156.1	ND	159.4	160.7	3.3	ND	Massive basalt	Olivine-Plagioclase	12-1, 114 to 14-1, 65
	Interlayered Sediment								
2	180.5	179.3	184.0	183.7	3.5	4.4	Massive basalt	Plagioclase	17-1, 0 to 18-1, 58
	Interlayered Sediment								
3	201.5	195.8	201.5	201.0	0.03	5.2	Pillow basalt?	Plagioclase	22-1, 0 to 22-1, 3
	Interlayered Sediment								
4	212.0	212.5	226.2	226.4	14.2	13.9	Massive basalt	Plagioclase-Olivine	23-1, 50 to 26-1, 20
	Interlayered Sediment								
5	239.5	243.6	270.4	270.7	30.9	27.1	Massive basalt	Plagioclase	29-1, 0 to 33-2, 95
	Interlayered Sediment								
6	277.5	284.5	294.0	294.5	16.5	10.0	Massive basalt	Plagioclase-Olivine	34-1, 56 to 35-6, 55
	Interlayered Sediment								
7	298.6	303.2	298.7	304.2	0.1	1.0	Massive basalt	Plagioclase	36-3, 64 to 36,CC
	Interlayered Sediment								
8	314.5	315.0	328.5	331.0	14.0	16.0	Massive basalt	Plagioclase	38-2, 2 to 39-5, 60

Note: ND = not determined.
[a] Calculated from core, corrected for spacers.
[b] Calculated from drilling rate and downhole logs.

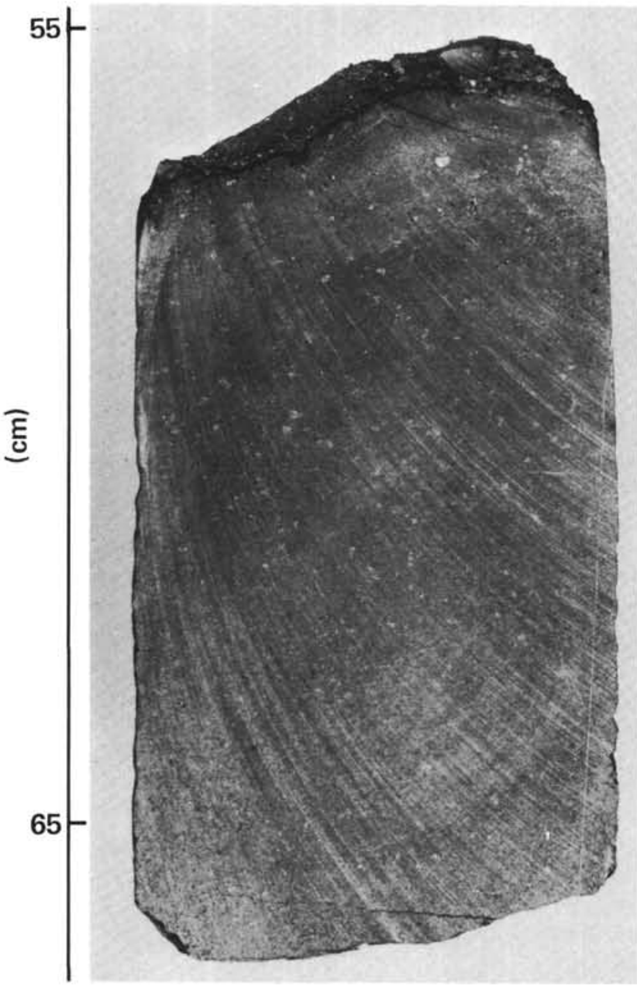

Figure 10. Sediment/basalt contact at the top of Unit 1, showing glassy margin and indurated crust of brecciated silty sand, Sample 485A-11-3, 55–67 cm.

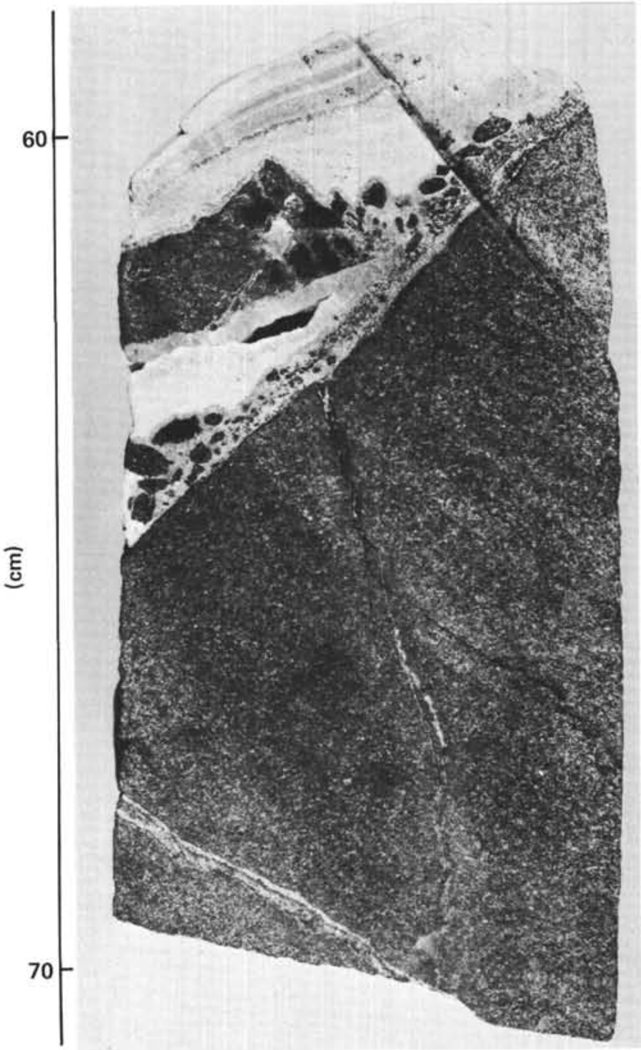

Figure 11. Calcite-cemented Benioff Zone in massive basalt, Sample 485A-17-2, 58–72 cm.

are only poorly developed. The base of Unit 1 is separated from Unit 2 by about 20 meters of sediment, of which none was recovered.

Unit 2

Unit 2 (Section 17-1, 0 cm to 18-1, 58 cm; 179.3 to 183.7 m) consists of one (or possibly two) cooling unit(s) composed of massive, aphyric, medium- to coarse-grained basalt characterized by thick carbonate veins and a calcite-cemented breccia in Section 17-2 (Fig. 11). Because the basalt is coarse grained on both sides of the breccia, we did not assign a cooling unit boundary to the brecciated interval. The density log shows three peaks, which we attribute to the brecciated nature of the basalt rather than to different cooling units. Unit 2 is separated from Unit 3 by about 12.5 meters of sandy mud and muddy nannofossil chalk.

Unit 3

Unit 3 (Section 22-1, 0–3 cm; 195.8 to 201.0 m) consists of an upper unit of cemented sediments and/or basalt and an even thinner lower unit composed of basalt interbedded in sediments. Although both units can be discerned in the logs, the only basalt recovered from either consists of a small pillow of plagioclase-phyric basalt from the lower unit. Unit 3 is separated from Unit 4 by about 11.5 meters of sediment.

Unit 4

Unit 4 (Section 23-1, 50 cm to 26-1, 20 cm; 212.5 to 226.4 m) is a thick, massive, sparsely plagioclase–olivine-phyric basalt displaying a coarse-grained gabbroic texture with groundmass clinopyroxene up to 5 mm in length in the center of the unit (Core 24). The grain size decreases gradually from the top of Section 25-2 to the base of the unit.

The uppermost sediment/basalt contact is well preserved and consists of a 1-mm thick rind of devitrified glass covered by calcite-cemented (baked?) sandstone displaying horizontal bedding about 1 cm above the contact. The base of the unit is marked by a sharp contact between sediments and fine-grained basalt. Lithologic Unit 4 is separated from Unit 5 by about 17.5 meters of sediment.

Unit 5

Unit 5 (Section 29-1, 0 cm to 33-2, 95 cm; 243.6 to 270.7 m) is a massive, coarse-grained, very sparsely plagioclase-olivine-phyric basalt. The unit is tentatively interpreted as a single very thick cooling unit because no definite cooling breaks were observed within or between cores; the recovery is very high for the entire unit. Some rapid changes in grain size (from coarse to very coarse) and a variable phenocryst content suggest, however, that the unit may consist of several flow or intrusive batches that were emplaced sufficiently rapidly to form a single but complex cooling unit. The grain size increases away from both margins over a distance of several meters and is coarsest (and the alteration most pronounced) near the top of the unit (Sections 30-2 through 4), where ophitic clinopyroxene grains up to 2.5 cm in length occur in the groundmass. Plagioclase and olivine phenocrysts, including some rounded plagiocrysts up to 1.5 cm in length, are slightly more abundant in the lower few meters of the unit but are small and rare in the basal 30 cm. Titanomagnetite exceeds 1 mm in length in the coarse-grained rocks but gradually decreases in the lower 5 to 10 meters. The unit is separated from Unit 6 by about 11 meters of sediment, of which only 60 cm were recovered.

Unit 6

Unit 6 (Section 34-1, 56 cm to 35-6, 55 cm; 284.5 to 294.5 m) consists of a massive basalt with fewer than 2% plagioclase phenocrysts and a finer grain size than Units 1 and 2. The upper sediment/basalt contact is similar to that at the top of Unit 1 in that the basalt displays a thin rim of devitrified glass. The basal contact was not recovered, but the grain size decreases notably toward the base of the unit. Unit 6 is underlain by about 9 meters of indurated silty claystone.

Unit 7

Unit 7 (Section 36-3, 65 cm to CC; 303.2 to 304.2 m) consists of approximately 30 cm of plagioclase-phyric basalt with chilled rinds of devitrified glass. The contact between the basalt and the overlying sediment is marked by a strongly cemented or baked limestone and is interpreted as intrusive. Unit 7 is underlain by about 12 meters of silty claystone.

Unit 8

Unit 8 (Section 38-2, 2 cm to 39-5, 60 cm; 315.0 to 331.0 m), the deepest unit encountered in Hole 485A, consists of a sparsely plagioclase-phyric, medium- to coarse-grained basalt occurring in a single complex cooling unit or in two cooling units with an indistinct cooling break between Cores 38 and 39. The uppermost sediment/basalt contact, which resembles but is more irregular than the intrusive(?) contact at the top of Unit 7, is marked by indurated (baked?) sediments composed of limestone, silty clay, smectite, sulfides, chalcedony, and fragments of basalt with rinds of devitrified glass. Because we terminated drilling in this unit, we did not recover the lower sediment/basalt contact.

Mineralogy and Petrography

The most common phenocrysts at Site 485 are plagioclase and olivine. Minor clinopyroxene and spinel also occur, but these are usually found in glomerocrysts with the former minerals. The largest phenocrysts (up to 6 mm) are usually plagioclase, whereas olivine is usually less than 2 mm across, and clinopyroxene, less than 3 mm. The paragenetic sequences observed at Site 485 include the following:

plagioclase → olivine → clinopyroxene → spinel
olivine → plagioclase → clinopyroxene → spinel
olivine → plagioclase → spinel → clinopyroxene

Groundmass textures also vary considerably throughout the section. Grain size is particularly coarse in Cores 23 through 32, with both plagioclase and clinopyroxene ranging up to 4 or 5 mm in length. Pigeonite occurs in the cores of Ca-rich pyroxenes and as single crystals in the more coarse-grained basalts, i.e., those with gabbroic textures. Quartz and tridymite occur in late stage interstitial patches.

Mode of Emplacement

As at Sites 482 and 483, the mode of emplacement of the massive basalts is uncertain. Most of the contacts recovered are equivocal, but some probable intrusive as well as depositional contacts were found. The coarse gabbroic texture observed in part of Lithologic Unit 5 suggests the slow cooling expected in a sill. Similarly, the downhole logs suggest that anomalously dense sedimentary rocks occur for several meters above Units 1 and 2 and in many cases the natural gamma ray peaks are higher in the sediments adjacent to the massive basalts. In the case of Unit 5, however, the sediments are anomalously dense immediately below the basalt. It is thus difficult to interpret these data unequivocally in terms of either thermal metamorphism or cementation adjacent to cooling—or leached—basalts. Even if all or most of the massive basalts could be shown to be intrusive, they might have started as surface flows which then burrowed into soft sediments.

Alteration

As at Sites 482 and 483, there was evidence for both low and high temperature alteration in the basalts at Site 485. In general, the basalts are more extensively altered than at the other sites—no fresh olivine was observed in any of the thin sections—nevertheless, we observed no regular increase of alteration grade with depth.

The low-temperature assemblage consists of smectite, carbonate, sulfides, and occasional zeolites or a trace of silica, deposited in veins and vesicles. Olivine and interstitial glass are replaced by smectites and in some cases by calcite. Diffuse alteration haloes containing sulfides also occur adjacent to veins in Sections 23-1 and 39-2. In the lower part of the hole (Cores 29 through 35) secondary vein sulfides are most abundant immediately below the sediment/basalt contact, but in the upper part of the section we did not observe a clear relationship between the interlayered sediments and the abundance of secondary minerals.

Higher-temperature secondary minerals occurred in Cores 17 and 24 through 33, in all of which chlorite was replacing smectite. The center of Unit 5 is pervasively altered, with epidote visible in hand specimen (Section 30-3), actinolite replacing pyroxene (Section 31-2), and a mixture of chlorite, sulfides, and an amorphous opaque material replacing patches 1–2 cm in diameter. This correlates with a decrease in density in the center of the unit. The alteration in this particular unit is probably deuteric, but some hydrothermal alteration may also be present.

There was clearer evidence of high temperature alteration in Cores 17 and 24. The basalt in Core 24 contains 15–20% chlorite and smectite and is cut by a smectite-pyrite vein in which epidote crystals are clearly visible. Core 17 is cut by numerous calcite veins and a calcite-cemented breccia. The basalt has a low density and in places contains up to 20% chlorite and smectite. Since the material on either side of the breccia is coarse-grained, Core 17 is thought to contain only a single cooling unit. Adjacent to the basalt, the breccia contains numerous angular fragments of altered basalt, isolated crystals of plagioclase and pyroxene, the latter with altered margins, and abundant chlorite. Farther away from the basalt contact, the breccia consists almost entirely of calcite within which appears traces of biotite and rare angular grains of quartz. These fragments bear more resemblance to detrital grains than to cryptocrystalline deposits of secondary silica, indicating that some sedimentary material may have fallen into the open fractures.

BASALT GEOCHEMISTRY

We analyzed a total of 12 basalt samples from Units 1a, 1c, 1e, 2, 4, and 5. These data are presented for each sample in Table 7. Average analyses corrected for carbonate content and normalized to dry weight are summarized by unit in Table 8 and plotted individually in magnesia variation diagrams in Figure 12.

The basalts are more uniform in composition than at the other sites drilled on Leg 65, generally displaying a relatively narrow range of MgO (7.0–7.9%). One nearly aphyric basalt from cooling Unit 1a has 10% MgO and probably reflects a mafic liquid magma. The other basalts could be related to a similar, but not identical, parent magma by crystal fractionation.

Most of the basalts exhibit low temperature alteration characterized by the replacement of olivine and interstitial glass by smectite and minor carbonate. Veins and sparse vesicles are usually filled with smectite, carbonate, and pyrite; more rarely they contain minor epidote. The coarse-grained rocks exhibit extensive evidence of deuteric alteration, with actinolite and minor epidote replacing clinopyroxene. In a few basalts, chlorite replaces smectite, suggesting that some higher temperature hydrothermal alteration has occurred.

Table 7. Shipboard X-ray fluorescence analyses of basalts, Hole 485A.

Sample	Major Elements (wt.%)											Volatiles (wt.%)			Trace Elements (ppm)		
(interval in cm)	SiO_2	TiO_2	Al_2O_3	Fe_2O_3*	MnO	MgO	CaO	Na_2O	K_2O	P_2O_5	Total	LOI	H_2O^{+a}	CO_2[a]	Ni	Sr	Zr
11-3, 82–83	47.93	1.45	15.70	10.46	0.15	9.80	11.55	2.44	0.02	0.10	99.60	1.80	0.86	0.26	220	135	90
12-1, 62–64	49.15	2.10	13.45	13.35	0.21	7.00	11.51	2.40	0.04	0.21	99.42	0.83	0.33	0.47	69	90	134
13-1, 103–105	49.24	1.98	13.76	13.03	0.20	6.99	11.62	2.31	0.05	0.18	99.36	1.32	0.38	0.62	76	107	132
17-1, 112–114	49.06	2.21	14.65	12.50	0.17	6.93	11.02	2.51	0.06	0.20	99.31	1.73	0.87	0.35	101	105	151
23-1, 118–120	48.92	2.19	14.46	12.81	0.18	6.96	11.10	2.48	0.08	0.20	99.38	1.46	0.87	0.22	84	109	145
24-1, 89–91	49.17	1.99	14.87	11.73	0.18	7.24	11.60	2.49	0.05	0.18	99.50	1.11	0.68	0.21	90	105	136
25-3, 14–16	49.05	2.13	14.20	12.67	0.20	7.44	11.31	2.36	0.07	0.20	99.63	1.46	1.00	0.32	91	155	144
29-2, 122–124	49.40	2.21	13.92	13.00	0.18	7.61	10.87	2.41	0.11	0.20	99.91	1.52	1.02	0.18	91	94	142
29-4, 62–64	49.30	2.21	13.19	13.31	0.21	7.65	11.10	2.30	0.07	0.19	99.53	1.59	0.88	0.16	65	94	143
30-1, 39–41	49.52	2.23	13.21	13.26	0.20	7.42	11.25	2.25	0.06	0.19	99.59	1.32	0.65	0.17	59	97	142
30-3, 103–105	49.20	2.06	14.75	12.50	0.19	6.56	11.05	2.55	0.07	0.20	99.13	1.18	0.62	0.19	75	106	151
31-2, 81–83	49.38	1.82	14.26	11.80	0.19	7.77	12.02	2.33	0.12	0.17	99.86	1.11	0.51	0.14	102	96	119

[a] % composition after baking off H_2O^-
* Total iron as Fe_2O_3.

Table 8. Average composition of basalt units, Hole 485A.[a]

Unit	Major Elements (wt.%)										Trace Elements (ppm)			Ratios					Number of Analysis
	SiO_2	Al_2O_3	FeO*	MgO	CaO	Na_2O	K_2O	TiO_2	P_2O_5	MnO	Ni	Sr	Zr	$\frac{TiO_2}{Al_2O_3}$	Mg No.	$\frac{Ti}{Zr}$	$\frac{Zr}{Ni}$	$\frac{P}{Zr}$	
1a	48.75	15.99	9.56	9.96	11.40	2.48	0.02	1.47	0.10	0.15	220	135	90	0.092	0.673	97.9	0.41	4.88	1
1c and 1e	50.48	13.98	12.16	7.16	11.14	2.41	0.05	2.09	0.20	0.21	73	99	133	0.150	0.538	94.2	1.82	6.61	2
2	50.19	14.99	11.51	7.09	10.82	2.57	0.06	2.26	0.20	0.17	101	105	151	0.151	0.549	89.7	1.50	5.82	1
4	50.04	14.80	11.37	7.35	11.23	2.49	0.07	2.15	0.19	0.18	88	123	142	0.145	0.561	90.8	1.61	5.57	3
5[b]	50.33	14.05	11.92	7.44	11.04	2.41	0.08	2.22	0.20	0.20	73	98	145	0.158	0.552	91.8	1.99	6.06	4
Sample 31-2, 81–83 cm	50.13	14.47	10.74	7.87	11.99	2.36	0.12	1.84	0.17	0.19	102	96	119	0.127	0.591	92.7	1.17	7.02	1

[a] Carbonate-corrected, normalized to dry weight.
[b] Exclusive of Sample 485A-31-2, 81–83 cm.
* Total iron oxide as FeO.

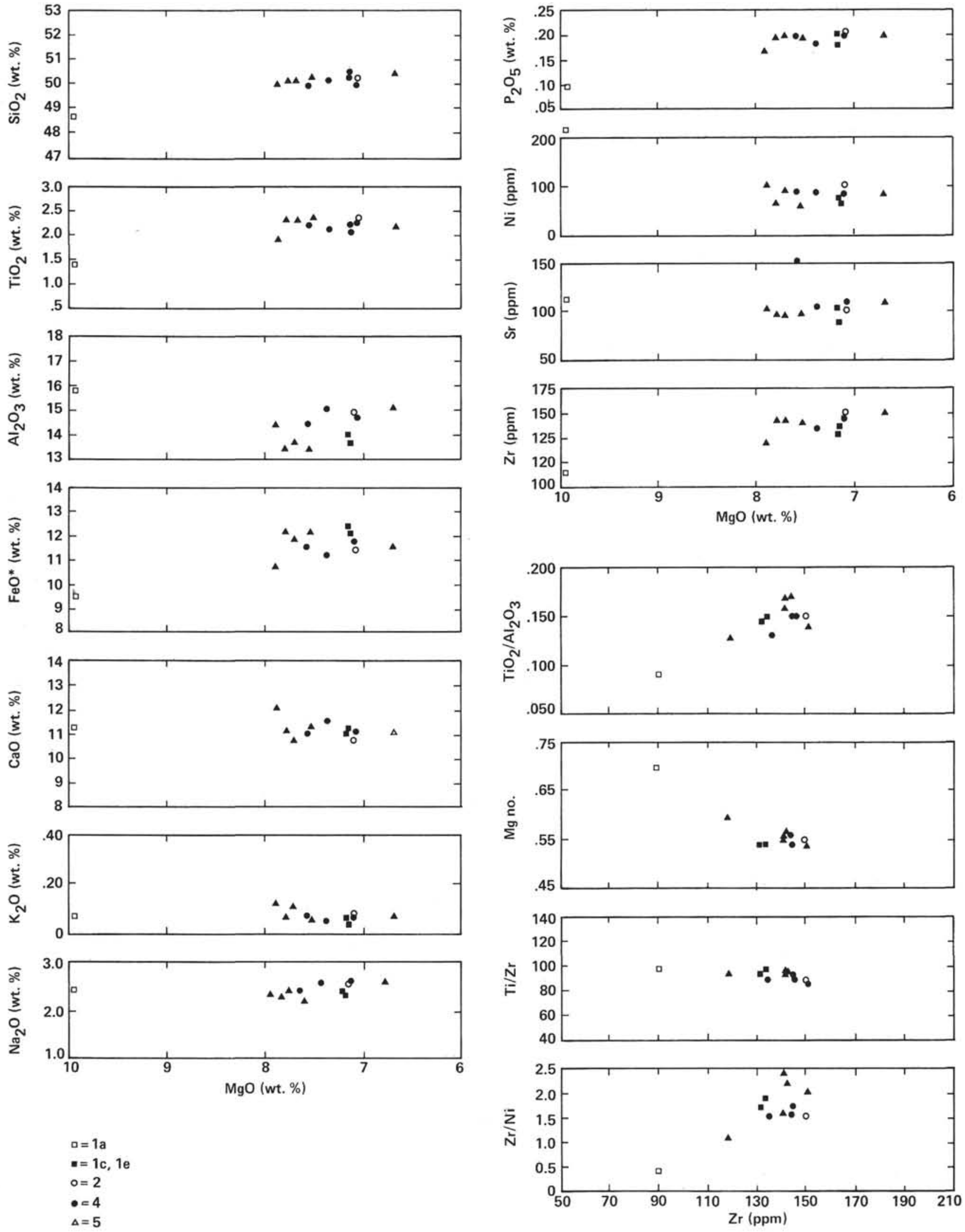

Figure 12. Major oxides, minor oxides, and trace elements versus MgO for basement lithologic units and cooling units in Hole 485A. (Enclosed field represents range of compositions displayed by samples from Unit 4; triangles represent samples from Unit 5. Also shown are ratios of oxides and trace elements versus Zr content. Dotted lines show possible fractionation trends connecting individual samples or cooling units; open circle represents Sample 485A-31-2, 81–83 cm. Oxide values in weight percent; trace elements in ppm.)

As can be seen in Tables 7 and 8, the sample from cooling Unit 1a (Sample 485A-11-3, 82–83 cm) has an MgO content of 10% and thus a composition close to that of a magnesian liquid magma. The thin section for the sample shows about 3% olivine phenocrysts which, even if cumulate, could not alone explain the mafic character of the rock.

The remaining samples, however, display a comparatively small range of MgO content (7.0–7.9 wt.%). Cooling Units 1c and 1e are chemically distinct from Unit 1a (despite similar phenocryst contents) but are almost identical to each other and to Unit 2, although the latter has a slightly higher Al_2O_3 content and lower FeO* (i.e., total iron oxide) and CaO content (Fig. 12).

Lithologic Unit 4, which displays a coarse-grained gabbroic texture with sparse plagioclase phenocrysts, shows only minor intra-unit variation in MgO content (7.1–7.6%) among the three samples examined. Of these, the sample with the lowest MgO content is virtually indistinguishable from Lithologic Unit 2 and from the cooling units observed in the lower part of Unit 1.

Unit 5 shows more intra-unit variation than the others, perhaps because of the presence of multiple cooling units or high temperature alteration. The deepest sample (Sample 485A-31-2, 81–83 cm), shown separately in Table 8 for purposes of comparison, is slightly enriched in MgO and shows a significantly lower content in TiO_2, P_2O_5, and Zr and a higher CaO and Al_2O_3 content for equivalent MgO than the other samples from the unit. Although the basalts in Unit 5 are sparsely phyric and show little evidence of crystal accumulation, the compositions of all but the most magnesian sample plot along a simple fractionation trend. The discrepancy between this trend and the composition of the relatively magnesian sample might be partially explained by the addition of MgO during alteration.

Although the basalts at Site 485 are, for the most part, too similar to be distinguished by chemical type, variations in the Ti/Zr ratio and the average ratios of TiO_2/Al_2O_3, $Mg/(Mg + Fe^{+2})$, Zr/Ni, and Ti/Zr versus Zr for individual units or groups of units permit constraints to be placed on the interrelationships between units (Fig. 12). Unit 1a and Units 1c and e, for example, show qualitatively compatible crystal fractionation trends. Similarly, the subdivisions of Unit 5 indicated in Table 8 show a similar qualitative relation, suggesting that the alteration is not required to explain all of the chemical variations observed in the unit. Since no simple hypothesis involving the redistribution of olivine, plagioclase, and clinopyroxene can explain the decrease in the Zr/Ni ratio observed with increasing Zr between Units 1, 2, 4, and 5, they appear to belong to separate fractionation trends.

BASALT PHYSICAL PROPERTIES

The physical properties of the basalts recovered in Hole 485A are basically similar to those measured at Sites 482 and 483. Wet-bulk density ranges from 2.80 to 3.02 g/cm^3 about a mean of approximately 2.95 g/cm^3, grain density averages about 3.06 g/cm^3, compressional wave velocity ranges from 5.0 to 6.2 km/s, with most values falling between 5.8 and 6.0 km/s, and porosity averages between 3% and 4%.

Although the physical properties of the basalts shown in Table 9 and Figure 13 display no particular pattern with depth in the hole, they are very sensitive to alteration within specific units. The altered basalt from Core 17, for example, has the lowest density (2.80 g/cm^3) and the lowest velocity (5.0 km/s) observed in the hole. Similarly, the relatively fresh basalts at the top and bottom of Unit 5 have high wet-bulk densities, but the deuterically altered, coarse-grained (almost gabbroic) samples from the center of the unit have relatively low densities and velocities.

BASALT PALEOMAGNETISM

The paleomagnetic properties of 34 oriented basalt samples from Hole 485A were studied by stepwise demagnetization to help determine the age and structural history of the site (Table 10). As can be seen in Table 11, the mean stable inclination is $+34°$, a value only slightly less than that of the present-day axial dipole ($+40°$). The mean initial inclination was $+39°$, indicating that a steeper secondary component was removed from the stable primary component. There is a positive correlation between changes in inclination and the petrologic boundaries in Units 1 through 6. The NRM in Unit 8, however, was very unstable, and a meaningful inclination could not be obtained although it appeared to be reversely magnetized. The mean NRM intensity and the mean MDF are respectively 5.31×10^{-3} gauss (G) and 79 Oe, both of which values are similar to those obtained for the massive basalts at Sites 482 and 483.

The magnetic properties observed in Hole 485A are consistent with coarse-grained basalts. The MDF values of 20 to 40 Oe in Unit 8, for example, are very low. It is interesting to note, however, that several samples from Unit 5, the thickest unit cored, display the highest MDF values. This implies, as suggested elsewhere, that this is not a simple cooling unit. The nearly constant inclinations measured in Unit 5, however, indicate that it cooled in a short period compared to secular variation.

As discussed earlier, the maximum age of the basement at Site 485, based on paleontologic data, is 1.22 m.y. Spreading rate calculations (assuming a half spreading rate of 2.7 cm/y.) yield an age of 0.74 m.y. The time spanned by these estimates falls within the Matuyama Reversed Polarity Epoch (0.7–2.4 m.y.), and the site itself lies in the Matuyama Magnetic Anomaly. Since all of the units were normally polarized, with the possible exception of Unit 8 and Unit 7 (which wasn't sampled), three possibilities exist; either (1) we drilled into basalts which erupted less than 0.7 million years ago during the Brunhes Normal Epoch; (2) we drilled into basalts which erupted about 0.9 million years ago during the 60,000-year-long Normal Jaramillo Event (which would imply that our maximum sediment accumulation rate is low by a factor of two within the basement section); or (3) the magnetization has not faithfully recorded the paleomagnetic field at this site.

Table 9. Basalt physical properties, Hole 485A.

Sample (interval in cm)	Density Wet-Bulk (g/cm^3)	Density Grain[a] (g/cm^3)	P-Wave Velocity[b] (km/s)	Acoustic Impedance ($\times 10^5 g/cm^2 \cdot s$)	Porosity[a] (vol.%)	Remarks
11-3, 90-92	2.92	3.03	6.13	17.9	3.5	
12-1, 145-147	3.00	3.05	6.20	18.6	1.5	
17-1, 48-50	2.80	3.07	4.99	14.0	8.8	Altered
18-1, 39-41	2.89	3.05	—	—	5.1	
23-1, 114-116	2.94	3.04	5.91	17.4	3.4	
23-3, 41-43	2.95	3.03	5.87	17.3	2.8	
24-4, 42-44	2.97	3.07	6.03	17.9	3.4	
25-2, 118-120	2.96	3.06	5.99	17.7	2.9	
29-2, 20-22	2.95	3.05	5.80	17.1	3.4	
30-1, 50-52	2.94	3.09	5.61	16.5	5.0	
31-3, 102-104	2.91	3.09	5.78	16.8	5.8	Deuterically altered
32-3, 40-42	2.90	3.06	5.81	16.8	5.1	Deuterically altered
33-2, 52-54	2.98	3.03	6.12	18.2	1.7	
34-2, 56-58	3.03	3.15	5.90	17.9	3.8	
35-4, 41-43	2.95	3.04	6.01	17.7	2.9	
38-5, 39-41	2.95	3.05	5.92	17.5	3.2	
39-5, 34-37	3.02	3.13	6.00	18.1	3.6	

[a] Determined by heating in air for 24 hours at 110°C.
[b] Measured at atmospheric pressure.
[c] From wet-bulk density and P-wave velocity.

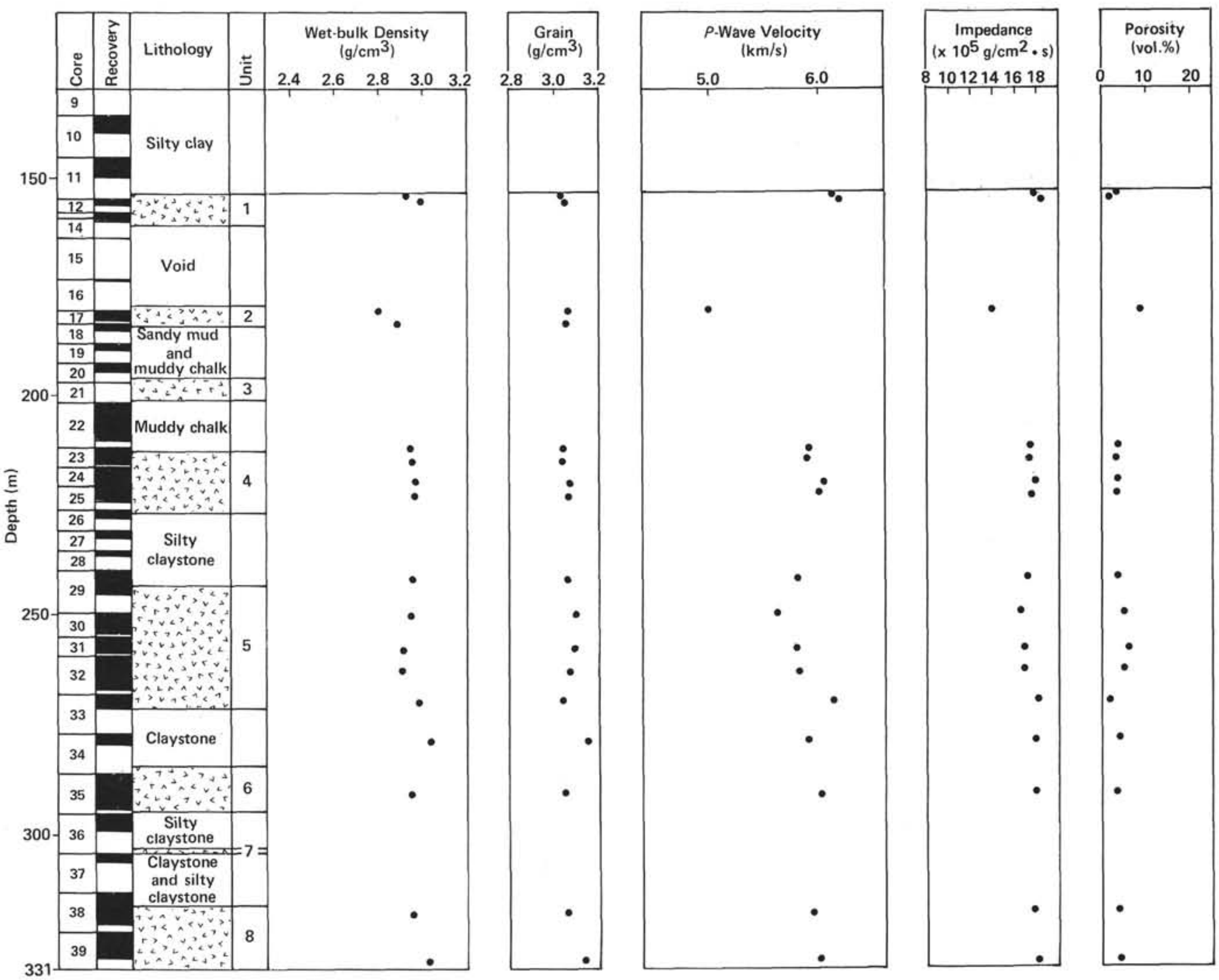

Figure 13. Basalt physical properties, Hole 485A.

Table 10. Paleomagnetic properties of basalts from Hole 485A.

Unit	Sample (level in cm)	Depth (m)	Declination (°)	Inclination (°)	NRM Intensity ($\times 10^{-3}$G)	Stable Inclination (°)	Susceptibility ($\times 10^{-3}$G/Oe)	Median Destructive Field (Oe)	Koenigsberger[a] Ratio, ϕ
1a	11-3, 79	149.29	125	35	2.90	32	1.51	62	4.3
1c	12-1, 59	155.59	264	57	12.47	49	2.62	65	10.6
1e	13-1, 96	158.96	218	55	6.42	49	3.35	40	4.3
	14-1, 60	160.10	69	52	7.48	42	3.17	60	5.3
2	17-1, 108	182.30	83	32	10.06	31	2.80	90	8.0
	17-2, 77	182.77	23	39	9.16	33	4.29	64	4.7
	18-1, 29	183.79	64	36	7.21	31	4.46	45	3.6
4	23-1, 99	212.49	96	38	8.07	36	3.60	70	5.0
	23-4, 12	216.12	109	31	6.60	32	2.49	43	4.2
	24-2, 21	217.71	335	58	5.08	55	2.97	62	3.8
	25-2, 29	222.79	217	46	6.92	46	4.00	55	3.8
	25-3, 29	224.29	157	46	7.18	44	3.42	70	4.6
5	29-1, 20	239.70	235	41	1.87	38	—	155	—
	29-2, 123	242.23	338	27	3.78	20	2.66	179	3.2
	29-4, 48	244.48	264	33	7.03	30	3.68	117	4.3
	30-1, 43	249.93	3	27	9.34	24	3.26	155	6.4
	30-3, 105	253.55	136	27	5.60	19	2.98	75	4.2
	31-2, 85	256.85	266	24	5.77	20	2.89	115	4.4
	32-1, 10	259.10	358	27	5.30	25	2.41	140	4.9
	32-3, 58	262.58	22	18	2.25	22	3.09	123	1.6
	32-5, 138	266.38	76	30	3.18	22	3.07	130	2.3
	32-6, 69	267.19	30	32	2.37	22	3.01	148	1.8
	33-2, 81	278.31	230	30	2.64	25	2.95	110	2.0
6	34-2, 68	279.18	26	48	6.79	39	3.49	34	4.33
	35-1, 26	286.26	333	53	6.40	38	—	45	—
	35-3, 72	289.72	307	48	6.29	38	3.77	55	3.7
	35-4, 47	290.97	191	50	5.38	39	3.38	45	3.5
	35-6, 44	293.94	234	54	5.68	38	—	40	—
8	38-2, 76	315.17	133	−23	0.83	−55	2.20	135	0.8
	38-4, 102	318.52	216	52	1.16	−43	2.86	22	0.9
	38-6, 35	320.85	199	62	2.31	—	3.22	35	1.6
	39-2, 77	324.27	319	80	2.78	—	3.13	28	2.0
	39-4, 22	326.72	187	65	2.98	—	—	40	—
	39-5, 8	328.80	354	60	1.14	—	2.71	20	0.9

[a] H = 0.45 Oe.

Table 11. Average of paleomagnetic properties, Hole 485A.

		n
Inclination before demagnetization	39°	28
Stable inclination	34°	28
NRM intensity	5.31×10^{-3} gauss	34
Median destructive field (MDF)	79 Oe	34
Susceptibility	3.14×10^{-3} gauss/Oe	32
Koenigsberger ratio (ϕ)	3.8	30

SUMMARY AND CONCLUSIONS

We drilled two holes at Site 485. Hole 485 was cored from the mud line to 50.5 meters sub-bottom, and Hole 485A was continuously cored from 50.5 to 331.0 meters sub-bottom. The average recovery in Hole 485 was about 73% and that in Hole 485A was about 50%.

The section overlying the basement consists of 153 meters of hemipelagic clay with minor terrigenous material. We recognized two units in this section, based on the frequency and thickness of sandy and silty layers interpreted as distal turbidites. The upper unit, extending from the mud line to 79 meters sub-bottom, is composed of soft to firm, grayish olive clay with between 5 and 15% silt. A few layers of silty clay, clayey silt, and sandy silt range up to 30 cm in thickness. These layers contain detrital quartz, feldspar, heavy minerals, and some plant material.

The lower unit, extending from 70.5 to 153.5 meters sub-bottom, is similar to the upper one except that clayey silts and silty sands comprise 35 to 40% of the unit. Most of the sandy and silty layers are poorly indurated and poorly recovered. On average, the clayey layers contain 15 to 20% calcareous nannofossils.

Physical properties of the sediment at this site are somewhat different from those measured at Sites 482 and 483. Instead of remaining constant in the upper 50–70 meters of the section, they change regularly from the mud line to the basement. Wet-bulk density ranges from about 1.4 to 1.9 g/cm^3, compressional wave velocity ranges from 1.5 to 1.7 km/s, and porosity ranges from 75 to 45%. Since this pattern suggests that little drilling disturbance has occurred in the upper part of the section, these measured values may approximate *in situ* values.

All of the sediments, both above and within the basement, are Quaternary in age. The upper 36 meters are assigned to nannofossil Zone NN20/21 (undifferentiated). The highest occurrence of *Axoprunum angelinum* was found at 35 meters sub-bottom. The lowest sediment recovered at this site (314 m sub-bottom) is assigned to nannofossil Zone NN19. These sediments are probably no older than 1.22 m.y.

The basement was cored from 153.5 to 331.0 meters sub-bottom with an average recovery of 51%. As at Sites 482 and 483, the upper part of basement consists of interlayered massive basalts (44%) and sediments (56%). Because of poor recovery in the sediments, we used both the drilling record and downhole logs to define basement stratigraphy.

The interlayered sediments consist of moderately indurated, clayey siltstones with minor sandstone and claystone. Nannofossil marls are present in a few cores, and several pieces of limestone were recovered in Core 22. Pyrite-filled burrows and concretions are fairly common.

The massive basalts are similar to those found at Sites 482 and 483 except that they are often thicker, are sometimes much coarser-grained, and often show evidence of intrusive contacts. Eight basalt units are recognized on the basis of the criteria used at Site 483. Possible baked contacts occur at the top of Units 4, 7, and 8; Units 4 and 8 have coarse-grained "gabbroic" textures similar to those expected from slow cooling in a sill.

The basalts are sparsely to moderately phyric with mainly plagioclase and olivine phenocrysts; minor clinopyroxene and spinel sometimes occur in glomerophyric clots with plagioclase. The coarse-grained basalts have ophitic "gabbroic" textures and are characterized by the presence of both pigeonite and augite as well as interstitial groundmass quartz.

The basalts are more uniform in composition than at the other sites drilled on Leg 65, generally displaying a relatively narrow range of MgO (7.0-7.9%). One nearly aphyric basalt from cooling Unit 1a has 10% MgO and probably reflects a mafic liquid magma. The other basalts could be related to a similar, but not identical, parent magma by crystal fractionation.

Most of the basalts exhibit low temperature alteration characterized by the replacement of olivine and interstitial glass by smectite and minor carbonate. Veins and sparse vesicles are usually filled with smectite, carbonate, and pyrite; more rarely they contain minor epidote. The coarse-grained rocks exhibit extensive evidence of deuteric alteration, with actinolite and minor epidote replacing clinopyroxene. In a few basalts, chlorite replaces smectite, suggesting that some higher temperature hydrothermal alteration has occurred.

Physical properties of the basalts are also similar to those at Sites 482 and 483. Wet-bulk density ranges from 2.80 to 3.02 g/cm^3, compressional wave velocity varies from 5.0 to 6.2 km, and porosity ranges from 1 to 8%. These variations reflect alteration rather than regular downhole trends.

Overall, the basement at Site 485 is similar to that at Sites 482 and 483, but the thickness of the upper section composed of interlayered sediment and basalt is greater, probably because of a higher sedimentation rate. Many of the basalts at this site are probably or definitely intrusive and have developed textures and mineralogies reflecting slow cooling.

REFERENCES

Bader, R. G., Gerard, R. D., et al., 1970. *Init. Repts. DSDP*, 4: Washington (U.S. Govt. Printing Office).

Boyce, R. E., and Bode, G. W., 1972. Carbon and carbonate analyses, Leg 9, Deep Sea Drilling Project. *In* Hays, J. D., et al., *Init. Repts. DSDP*, 9: Washington (U.S. Govt. Printing Office), 797-816.

Müller, G., and Gastner, M., 1971. The "Carbonate Bomb," a simple device for the determination of the carbonate content in sediments, soils and other materials. *N. Jahrb. Mineral.*, 10:466-469.

Stephen, R. A., Louden, K. E., and Matthews, D. H., 1980. The oblique seismic experiment on DSDP Leg 52. *Geophys. J. R. Astron. Soc.*, 60:289-300.

SITE 485 HOLE CORE 1 CORED INTERVAL 0.0–3.0 m

TIME – ROCK UNIT	BIOSTRATIGRAPHIC ZONE	FOSSIL CHARACTER: FORAMINIFERS	NANNOFOSSILS	RADIOLARIANS	DIATOMS
UPPER QUATERNARY	NN20–21 (N)	FG	AG	CM	

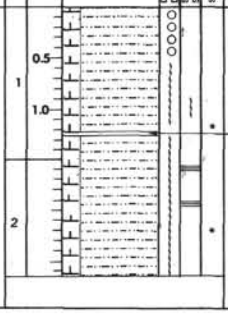

LITHOLOGIC DESCRIPTION

10Y 4/2

5B 9/1

VOID

10Y 5/2

Soft, grayish olive NANNOFOSSIL-bearing SILTY CLAY containing small (mm) bluish white sponge spicule concretions and black streaks of pyrite.

SMEAR SLIDE SUMMARY

	1-120	2-75
TEXTURE:		
Sand	–	–
Silt	37	39
Clay	63	61
COMPOSITION:		
Quartz	1	4
Heavy minerals	2	1
Clay	63	61
Pyrite	TR	TR
Calc. nannofossils	25	15
Diatoms	2	5
Radiolarians	1	5
Sponge spicules	5	6
Silicoflagellates	1	3

SITE 485 HOLE CORE 2 CORED INTERVAL 3.0–12.5 m

TIME – ROCK UNIT	BIOSTRATIGRAPHIC ZONE	FOSSIL CHARACTER: FORAMINIFERS	NANNOFOSSILS	RADIOLARIANS	DIATOMS
UPPER QUATERNARY	NN20–21 (N)		CM		
		FM-G		CM-G	

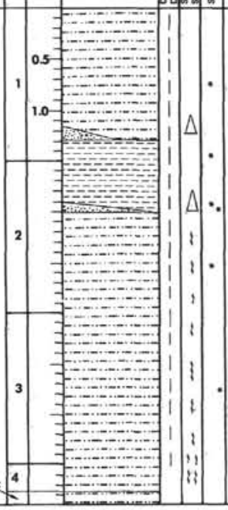

LITHOLOGIC DESCRIPTION

10Y 4/2

5GY 4/1

5B 5/1
10Y 4/2
and
5GY 4/1

10Y 4/2

Soft grayish olive CLAY and SILTY CLAY with occasional turbidite layers composed of SANDY SILT in Sections 1 and 2 and black streaks of pyrite at the base of the core.

SMEAR SLIDE SUMMARY

	1-75	1-148	2-41	2-48	2-104	3-75
TEXTURE:						
Sand	2	1	2	15	–	–
Silt	31	19	12	75	38.	21
Clay	67	80	86	10	62	79
COMPOSITION:						
Quartz	10	10	5	60	3	2
Feldspar	–	1	1	20	–	–
Mica	–	–	–	1	–	–
Heavy minerals	2	2	1	2	1	–
Clay	67	80	86	10	62	79
Volcanic glass	–	–	–	5	–	–
Pyroxenes	1	–	–	–	–	–
Pyrite	2	–	–	–	–	–
Carbonate unspec.	–	–	–	1	–	–
Foraminifers	–	1	–	1	–	–
Calc. nannofossils	10	5	7	–	7	10
Diatoms	5	–	–	–	8	5
Radiolarians	3	–	–	–	7	3
Sponge spicules	–	–	–	–	10	1
Silicoflagellates	–	–	–	–	2	–

SITE 485 HOLE CORE 3 CORED INTERVAL 12.5–22.0 m

TIME – ROCK UNIT	BIOSTRATIGRAPHIC ZONE	FOSSIL CHARACTER: FORAMINIFERS	NANNOFOSSILS	RADIOLARIANS	DIATOMS
UPPER QUATERNARY	NN20–21 (N)		CM		
		RM-G		RM-G	

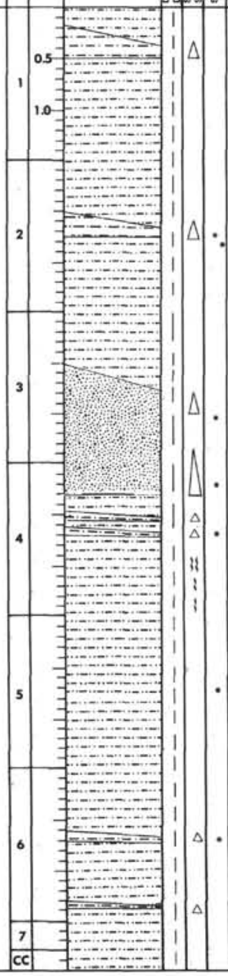

LITHOLOGIC DESCRIPTION

10Y 4/2

5Y 4/1

10Y 4/2

Soft grayish olive SILTY CLAY with grayish olive to olive gray turbidite layers composed of SANDY SILT, occasional small (mm) white patches composed of sponge spicules and black streaks of pyrite.

SMEAR SLIDE SUMMARY

	2-74	2-76	3-103	4-28	4-78	5-75	6-70
TEXTURE:							
Sand	10	–	35	20	–	–	20
Silt	44	40	50	55	22	27	44
Clay	46	60	15	25	78	73	36
COMPOSITION:							
Quartz	25	3	50	15	10	TR	15
Feldspar	5	–	10	2	–	–	–
Mica	1	–	TR	–	–	–	–
Heavy minerals	1	1	TR	1	–	–	TR
Clay	46	60	15	25	78	73	36
Volcanic glass	1	1	–	–	–	–	2
Pyrite	1	–	5	2	–	–	2
Foraminifers	5	–	15	–	–	–	30
Calc. nannofossils	15	25	5	35	10	15	15
Diatoms	–	5	–	10	1	7	TR
Radiolarians	–	–	–	10	–	–	–
Sponge spicules	–	5	–	–	–	3	TR
Silicoflagellates	–	–	–	–	–	1	–

SITE 485 HOLE CORE 4 CORED INTERVAL 22.0–31.5 m

TIME – ROCK UNIT: UPPER QUATERNARY

BIOSTRATIGRAPHIC ZONE: NN20–21 (N)

FOSSIL CHARACTER: FORAMINIFERS RG; NANNOFOSSILS CM; RADIOLARIANS AG; DIATOMS

SECTION: 1, 2, 3, CC

METERS: 0.5, 1.0

GRAPHIC LITHOLOGY / DRILLING DISTURBANCE / SEDIMENTARY STRUCTURES / SAMPLES

LITHOLOGIC DESCRIPTION

10Y 4/2

5Y 4/1

5Y 3/2

Soft grayish olive to olive gray SILTY CLAY with an olive gray turbidite layer composed of NANNOFOSSIL-bearing SANDY MUD at the top of Section 2.

SMEAR SLIDE SUMMARY

	2-34
TEXTURE:	
Sand	15
Silt	49
Clay	36
COMPOSITION:	
Quartz	10
Feldspar	1
Heavy minerals	1
Clay	36
Volcanic glass	2
Pyrite	2
Carbonate unspec.	2
Foraminifers	15
Calc. nannofossils	25
Diatoms	1
Sponge spicules	<1
Shell fragments	5

SITE 485 HOLE CORE 5 CORED INTERVAL 31.5–41.0 m

TIME – ROCK UNIT: UPPER QUATERNARY

BIOSTRATIGRAPHIC ZONE: Above extinction of *Axopyrunum angelinum* NN20–21 (N); NN19 (N)

FOSSIL CHARACTER: FORAMINIFERS RG; NANNOFOSSILS AM, AM, CM; RADIOLARIANS CG; DIATOMS

SECTION: 1, 2, 3, 4, CC 5

METERS: 0.5, 1.0

GRAPHIC LITHOLOGY / DRILLING DISTURBANCE / SEDIMENTARY STRUCTURES / SAMPLES

LITHOLOGIC DESCRIPTION

10Y 4/2

5Y 3/2

10Y 4/2

5Y 3/2

10Y 4/2

5Y 3/2

10Y 4/2

5Y 3/2

10Y 4/2

5Y 3/2

Firm, olive gray NANNOFOSSIL-bearing SILTY CLAY with numerous turbidite layers composed of SANDY MUD throughout the core and with layers of grayish olive MUDDY NANNOFOSSIL OOZE near the top of Section 3 and the base of the core. Plant debris and foraminifer are common at the base of many of the turbidites.

SMEAR SLIDE SUMMARY

	1-71	2-10	2-67	2-105	3-15	3-31	3-96	4-49	4-121	4-141
TEXTURE:										
Sand	–	5	–	5	10	–	–	20	–	1
Silt	45	23	–	32	29	71	29	46	38	44
Clay	55	72	–	63	61	29	71	34	62	55
COMPOSITION:										
Quartz	15	10	–	7	12	10	10	15	2	10
Feldspar	–	–	–	–	1	–	–	2	–	–
Mica	–	–	–	–	–	–	–	–	–	1
Heavy minerals	10	2	–	4	3	2	3	1	2	–
Clay	55	72	–	63	61	29	71	34	62	55
Volcanic glass	–	–	–	–	–	–	–	10	–	–
Pyrite	–	1	–	–	–	1	–	1	–	–
Carbonate unspec.	–	–	–	–	–	1	–	5	–	–
Foraminifers	–	–	–	–	–	–	–	15	–	–
Calc. nannofossils	20	10	–	25	20	50	10	15	30	30
Diatoms	–	1	–	1	2	3	5	2	2	3
Radiolarians	–	–	–	–	1	2	–	–	–	–
Sponge spicules	–	2	–	–	–	1	TR	–	TR	1
Silicoflagellates	–	2	–	–	–	1	–	–	TR	–
Plant Debris	–	–	100	–	–	–	–	–	–	–

SITE 485 HOLE CORE 6 CORED INTERVAL 41.0–50.5 m

TIME – ROCK UNIT: UPPER QUATERNARY

BIOSTRATIGRAPHIC ZONE: NN19 (N)

FOSSIL CHARACTER: FORAMINIFERS CM-G; NANNOFOSSILS CM; RADIOLARIANS CG; DIATOMS

SECTION: 1, 2, 3, 4, 5, 6, 7, CC

METERS: 0.5, 1.0

GRAPHIC LITHOLOGY / DRILLING DISTURBANCE / SEDIMENTARY STRUCTURES / SAMPLES

LITHOLOGIC DESCRIPTION

10Y 4/2 and 5Y 4/1

5Y 4/1

10Y 4/2

5Y 4/1

10Y 4/2

5Y 4/1

Firm, grayish olive SILTY CLAY with pieces of LIMESTONE or DOLOMITE in Sections 1 and 2 and fine-grained turbidites throughout. Foraminifer are common at the base of many of the turbidites.

SMEAR SLIDE SUMMARY

	1-85 (M)	2-80	5-80	6-140
TEXTURE:				
Sand	–	–	–	5
Silt	100	37	37	43
Clay	–	63	63	52
COMPOSITION:				
Quartz	–	12	10	5
Heavy minerals	–	3	3	5
Clay	–	63	63	52
Pyrite	1	1	–	–
Carbonate unspec.	99	–	–	–
Foraminifers	–	–	–	TR
Calc. nannofossils	–	15	20	30
Diatoms	–	2	2	3
Radiolarians	–	1	TR	1
Sponge spicules	–	3	1	1

SITE 485 HOLE A CORE 1 CORED INTERVAL 50.5–60.0 m

TIME – ROCK UNIT	BIOSTRATIGRAPHIC ZONE	FORAMINIFERS	NANNOFOSSILS	RADIOLARIANS	DIATOMS	SECTION	METERS	GRAPHIC LITHOLOGY	DRILLING DISTURBANCE	SEDIMENTARY STRUCTURES	SAMPLES
QUATERNARY	NN19 (N)	FM G	FM	RG		1, 2, 3, 4, 5, 6, 7, CC	0.5, 1.0				

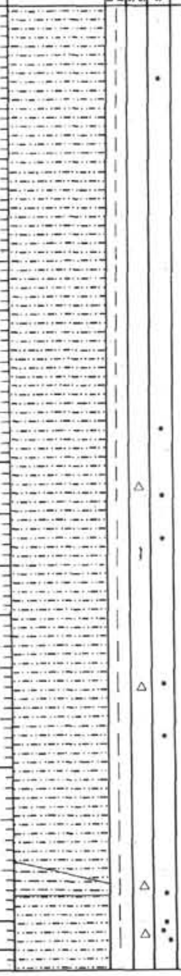

5Y 2/1

Firm, olive black NANNOFOSSIL-bearing CLAY and SILTY CLAY with thin olive gray turbidite layers composed of SILTY CLAY and SANDY MUD.

5Y 3/2
5Y 2/1
5Y 3/2
5Y 2/1
5Y 3/2
5Y 2/1

SMEAR SLIDE SUMMARY

	1-75	3-148	4-31	4-75	5-70	5-120	6-122	7-6	7-20	7-40
TEXTURE:										
Sand	4	7	7	5	1	1	15	2	–	–
Silt	37	23	21	9	20	50	55	33	38	46
Clay	59	70	72	86	79	49	30	65	62	54
COMPOSITION:										
Quartz	3	10	10	8	3	20	25	15	20	20
Feldspar	1	1	2	–	–	3	5	2	3	3
Mica	–	–	TR	–	–	–	1	–	–	TR
Heavy minerals	3	3	3	3	–	2	2	2	1	3
Clay	59	70	72	86	78	19	30	65	62	54
Pyrite	1	1	2	1	3	2	20	5	1	2
Carbonate unspec.	–	–	–	–	–	3	2	–	–	–
Foraminifers	–	TR	TR	TR	–	–	–	–	–	1
Calc. nannofossils	20	12	10	2	15	20	15	10	12	16
Diatoms	7	2	1	TR	–	–	1	1	1	1
Radiolarians	TR	TR	TR	TR	–	TR	–	–	–	–
Sponge spicules	5	1	TR	TR	–	TR	–	–	–	–
Silicoflagellates	1	TR	TR	TR	TR	–	–	–	–	–

SITE 485 HOLE A CORE 2 CORED INTERVAL 60.0–69.5 m

TIME – ROCK UNIT	BIOSTRATIGRAPHIC ZONE	FORAMINIFERS	NANNOFOSSILS	RADIOLARIANS	DIATOMS	SECTION	METERS	GRAPHIC LITHOLOGY	DRILLING DISTURBANCE	SEDIMENTARY STRUCTURES	SAMPLES
UPPER QUATERNARY	NN19 (N) Below extinction of *Axopruneum angelinum*	FM	CM	FG		1, 2, 3, 4, CC	0.5, 1.0				

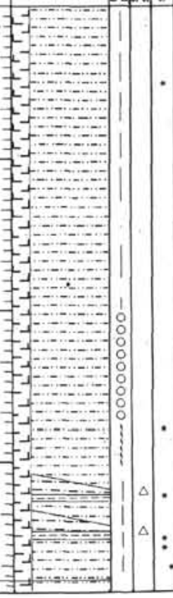

5Y 3/2

Firm, olive gray NANNOFOSSIL-bearing SILTY CLAY with turbidite layers composed of SANDY MUD near the base of the core. Each turbidite is underlain by a thin layer of grayish olive CLAY.

10Y 4/2
5Y 3/2
10Y 4/2
5Y 3/2

SMEAR SLIDE SUMMARY

	1-75	3-117	4-37	4-65	4-87	4-105
TEXTURE:						
Sand	–	1	20	20	–	2
Silt	45	44	27	24	42	28
Clay	55	55	53	56	58	72
COMPOSITION:						
Quartz	20	20	20	22	10	5
Feldspar	1	2	2	2	1	–
Mica	–	–	–	–	1	–
Heavy minerals	2	1	2	1	3	2
Clay	55	55	53	56	58	72
Pyrite	1	–	4	3	1	1
Carbonate unspec.	–	TR	5	2	–	–
Foraminifers	TR	1	1	TR	–	TR
Calc. nannofossils	20	20	10	10	25	16
Diatoms	1	1	1	1	1	3
Radiolarians	–	–	1	TR	–	TR
Sponge spicules	–	1	1	–	–	1
Silicoflagellates	–	–	–	1	–	TR

SITE 485 HOLE A CORE 3 CORED INTERVAL 69.5–79.0 m

TIME-ROCK UNIT: UPPER QUATERNARY
BIOSTRATIGRAPHIC ZONE: NN19 (N); Below extinction of *Axopranum angelinum*
FOSSIL CHARACTER: CM (nannofossils, Section 1); CC: CG (foraminifers), AG (radiolarians)
SECTIONS: 1, 2, 3, CC; METERS: 0.5, 1.0
GRAPHIC LITHOLOGY: VOID

LITHOLOGIC DESCRIPTION

10Y 4/2

Firm olive gray and grayish olive NANNOFOSSIL-bearing SILTY CLAY with a thin turbidite layer composed of CLAYEY SILT near the base of the core. Formainifer are abundant at the base of the turbidite. The sediments below the turbidite are stiff and dehydrated.

N2
5Y 3/2

SMEAR SLIDE SUMMARY

	1-77	1-140 (M)	2-120	3-56
TEXTURE:				
Sand	1	10	–	5
Silt	22	27	42	51
Clay	77	63	58	44
COMPOSITION:				
Quartz	5	20	20	20
Feldspar	TR	2	TR	2
Mica	–	1	–	–
Heavy minerals	2	1	1	–
Clay	77	63	58	44
Volcanic glass	–	–	–	TR
Pyrite	1	1	1	15
Carbonate unspec.	–	2	–	–
Foraminifers	–	–	–	5
Calc. nannofossils	15	10	15	10
Diatoms	–	TR	1	1
Radiolarians	–	TR	1	2
Sponge spicules	–	TR	2	1
Silicoflagellates	–	–	1	–

SITE 485 HOLE A CORE 4 CORED INTERVAL 79.0–88.5 m

TIME-ROCK UNIT: LOWER (?) QUATERNARY
BIOSTRATIGRAPHIC ZONE: NN19 (?)
FOSSIL CHARACTER: AM-G (foraminifers), RG (radiolarians)
SECTIONS: 1, CC; METERS: 0.5, 1.0

LITHOLOGIC DESCRIPTION

5Y 3/2

10Y 4/2
5Y 3/2

Firm, olive gray to grayish olive SILTY CLAY with thin turbidite layers composed of CLAYEY SILT.

SITE 485 HOLE A CORE 5 CORED INTERVAL 88.5–98.0 m

TIME-ROCK UNIT: QUATERNARY
BIOSTRATIGRAPHIC ZONE: NN19 (N)
FOSSIL CHARACTER: CM (nannofossils, Section 3); CC: RG (foraminifers), B (radiolarians)
SECTIONS: 1, 2, 3, 4, CC; METERS: 0.5, 1.0

LITHOLOGIC DESCRIPTION

5Y 3/2
and
10Y 4/2

Firm, olive gray to grayish olive NANNOFOSSIL-bearing SILTY CLAY with a NANNOFOSSIL-bearing CLAYEY SILT turbidite layer at the base of the core.

5Y 3/2

SMEAR SLIDE SUMMARY

	3-75	4-52
TEXTURE:		
Sand	–	3
Silt	25	32
Clay	75	65
COMPOSITION:		
Quartz	7	10
Feldspar	–	2
Heavy minerals	2	1
Clay	75	65
Pyrite	1	1
Foraminifers	TR	–
Calc. nannofossils	15	20
Diatoms	TR	1
Sponge spicules	–	TR

SITE 485 HOLE A CORE 6 CORED INTERVAL 98.0–107.5 m

TIME-ROCK UNIT: LOWER(?) QUATERNARY
BIOSTRATIGRAPHIC ZONE: NN19 (N)
FOSSIL CHARACTER: CM (nannofossils, Section 1); CC: AM-G (foraminifers), B (radiolarians)
SECTIONS: 1, 2, 3, CC; METERS: 0.5, 1.0

LITHOLOGIC DESCRIPTION

10Y 4/2

Firm, grayish olive NANNOFOSSIL-bearing SILTY CLAY underlain by a thin layer of SANDY MUD containing abundant (15%) foraminifers. The contact between these two lithologies is sharp and artifical (drilling-induced).

SMEAR SLIDE SUMMARY

	1-75	3-84	3-86
TEXTURE:			
Sand	–	–	6
Silt	30	25	39
Clay	70	75	55
COMPOSITION:			
Quartz	10	7	10
Feldspar	1	1	1
Mica	–	–	TR
Heavy minerals	3	1	–
Clay	70	75	55
Pyrite	1	1	1
Carbonate unspec.	–	–	15
Foraminifers	–	TR	1
Calc. nannofossils	15	15	15
Diatoms	TR	TR	1

5Y 3/2

SITE 485 HOLE A CORE 7 CORED INTERVAL 107.5–117.0 m

TIME – ROCK UNIT	BIOSTRATIGRAPHIC ZONE	FORAMINIFERS	NANNOFOSSILS	RADIOLARIANS	DIATOMS	SECTION	METERS
LOWER(?) QUATERNARY	NN19 (N)	CG	CM	RG		1, 2, CC	0.5, 1.0

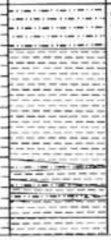

LITHOLOGIC DESCRIPTION

10Y 4/2, 5Y 3/2, 10Y 4/2, 5Y 3/2, 10Y 4/2

Firm, grayish olive NANNOFOSSIL-bearing CLAY and SILTY CLAY with soft, interbedded layers of disturbed SILTY CLAY and CLAYEY SILT in Section 1 and turbidites composed of firm CLAYEY SILT in Section 2.

SMEAR SLIDE SUMMARY

	1-73
TEXTURE:	
Sand	5
Silt	22
Clay	73
COMPOSITION:	
Quartz	6
Feldspar	TR
Mica	–
Heavy minerals	1
Clay	73
Pyrite	TR
Carbonate unspec.	10
Calc. nannofossils	10
Sponge spicules	TR
Silicoflagellates	TR

SITE 485 HOLE A CORE 8 CORED INTERVAL 117.0–126.5 m

TIME – ROCK UNIT	BIOSTRATIGRAPHIC ZONE	FORAMINIFERS	NANNOFOSSILS	RADIOLARIANS	DIATOMS	SECTION	METERS
QUATERNARY	NN19 (N)	RG	CM, B			1, 2, 3, CC	0.5, 1.0

LITHOLOGIC DESCRIPTION

10Y 4/2

Firm, homogeneous, grayish olive NANNOFOSSIL-bearing SILTY CLAY. The sediments in the Core-Catcher are dehydrated.

SMEAR SLIDE SUMMARY

	2-75
TEXTURE:	
Sand	–
Silt	33
Clay	67
COMPOSITION:	
Quartz	5
Heavy minerals	2
Clay	67
Pyrite	1
Carbonate unspec.	8
Foraminifers	TR
Calc. nannofossils	15
Diatoms	1
Radiolarians	1

SITE 485 HOLE A CORE 9 CORED INTERVAL 126.5–136.0 m

TIME – ROCK UNIT	BIOSTRATIGRAPHIC ZONE	FORAMINIFERS	NANNOFOSSILS	RADIOLARIANS	DIATOMS	SECTION	METERS
QUATERNARY	NN19 (N)	FM-G	FP, B			1, 2, 3, CC	0.5, 1.0

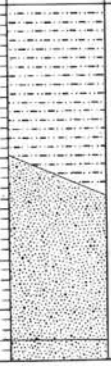

LITHOLOGIC DESCRIPTION

10Y 4/2

Firm, grayish olive SILTY CLAY grading with depth in the top of Section 2 to soft, grayish olive SILTY SAND.

SMEAR SLIDE SUMMARY

	2-75
TEXTURE:	
Sand	60
Silt	35
Clay	5
COMPOSITION:	
Quartz	65
Feldspar	TR
Mica	TR
Heavy minerals	1
Clay	5
Volcanic glass	TR
Pyrite	TR
Carbonate unspec.	25
Foraminifers	1
Calc. nannofossils	3

SITE 485 HOLE A CORE 10 CORED INTERVAL 136.0–145.5 m

TIME – ROCK UNIT	BIOSTRATIGRAPHIC ZONE	FORAMINIFERS	NANNOFOSSILS	RADIOLARIANS	DIATOMS	SECTION	METERS
QUATERNARY	NN19 (N)	RG	FM, B			1, 2, 3, CC	0.5, 1.0

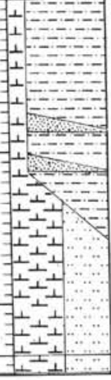

LITHOLOGIC DESCRIPTION

10Y 4/2

Firm, grayish olive NANNOFOSSIL-bearing SANDY MUD with small turbidite layers of NANNOFOSSIL-bearing SANDY SILT, grading with depth in Section 2 to a SILTY NANNOFOSSIL OOZE containing silt-sized grains of calcite and minor dolomite.

SMEAR SLIDE SUMMARY

	1-75	1-130	2-75
TEXTURE:			
Sand	10	15	–
Silt	37	61	99
Clay	53	24	1
COMPOSITION:			
Quartz	15	30	20
Feldspar	TR	5	2
Mica	TR	TR	2
Heavy minerals	2	1	2
Clay	53	24	1
Voclanic glass	TR	TR	TR
Glauconite	–	TR	TR
Pyrite	5	5	10
Carbonate unspec.	TR	15	10
Foraminifers	TR	TR	–
Calc. nannofossils	25	20	50
Diatoms	TR	–	3

SITE 485 HOLE A CORE 11 CORED INTERVAL 145.5–155.0 m

TIME – ROCK UNIT	BIOSTRATIGRAPHIC ZONE	FOSSIL CHARACTER: FORAMINIFERS	NANNOFOSSILS	RADIOLARIANS	DIATOMS	SECTION	METERS	GRAPHIC LITHOLOGY	DRILLING DISTURBANCE	SEDIMENTARY STRUCTURES	SAMPLES
LOWER(?) QUATERNARY	NN19 (N)	CG	CP	B		1	0.5, 1.0	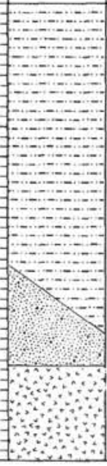			*
						2					*
						3					*

LITHOLOGIC DESCRIPTION

5Y 3/2

Section 1, 0 cm–Section 3, 55 cm: Stiff, olive gray CALCAREOUS CLAYEY SILT grading with depth to CALCAREOUS SILTY SAND overlying BASALT. Dehydration is pronounced in the uppermost sediments and increases with depth to the base of the sediment section.

Section 3, 55–150 cm: BASALT with a thin glassy margin and a crust of brecciated, indurated sediments composed of SILTY SAND containing deformed foraminifers, shards of glass and feldspar.

SMEAR SLIDE SUMMARY

	1-75	2-75	3-35
TEXTURE:			
Sand	2	2	60
Silt	60	65	35
Clay	38	33	5
COMPOSITION:			
Quartz	33	20	40
Feldspar	5	3	15
Mica	2	TR	5
Heavy minerals	2	1	5
Clay	38	33	5
Volcanic glass	TR	TR	–
Pyroxenes	–	–	TR
Pyrite	1	2	5
Carbonate unspec.	10	20	10
Foraminifers	2	1	5
Calc. nannofossils	7	20	5
Diatoms	TR	TR	–

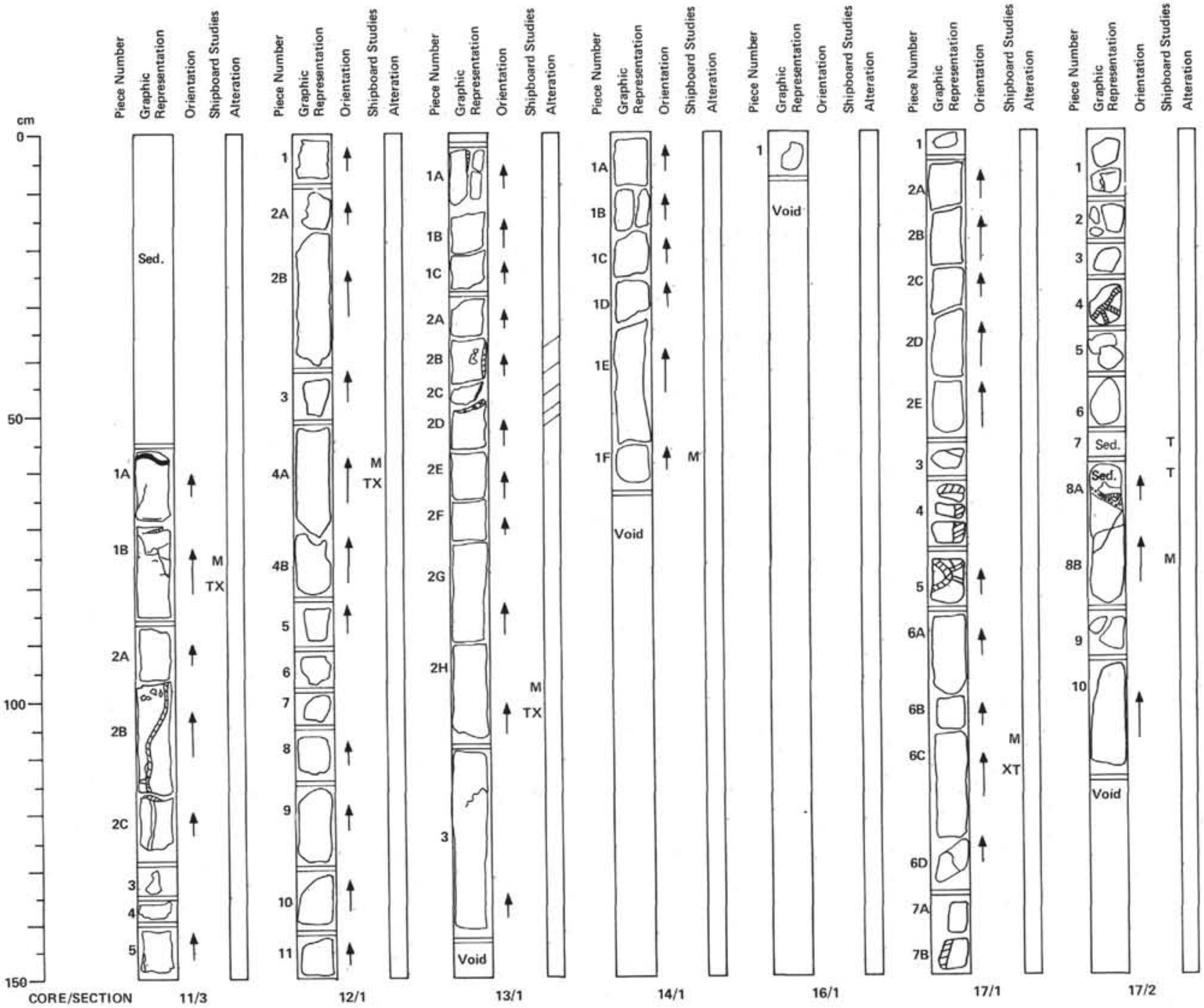

HOLE 485A, CORE 11

Visual Description

Section 1, 0 cm–Section 3, 56 cm: Sediment.

Section 3, 56 cm–base of core: Gray, very sparsely phyric, massive basalt. Plagioclase phenocrysts <1%, <4 mm, subhedral, fresh. Groundmass very fine- to medium-grained, grain size increases gradually downward from glass selvedge at 56 cm, Section 3. Vesicles common near upper contact with sediment, < 1 mm, round, filled with carbonate; elsewhere vesicles sparse. Veins and fractures fairly common, steep, filled with carbonate.

Thin Section Description

Location: Section 3, 82–83 cm:

Texture: Very sparsely phyric, fine- to medium-grained, intergranular to intersertal

Phenocrysts: Plagioclase < 1%, < 2 mm, anhedral, fresh, zoned; olivine 2%, < 1 mm, subhedral, mostly fresh, some alteration to smectite, $2V_z \sim 90°$.

Groundmass: Plagioclase 50%, 0.5–0.8 mm, subhedral, fresh; olivine 5%, 0.1–0.2 mm, anhedral, mostly fresh with some alteration to smectite; clinopyroxene 45%, 0.2–0.5 mm, acicular, fresh, $2V_z \sim 40°$; opaques 2%, 0.05–0.1 mm, subhedral; interstitial material 2–3%, replaced by smectite.

Vesicles: <1%, 0.5 mm, round to irregular, filled with carbonate.

Alteration: Olivine and interstitial material partly replaced by smectite.

HOLE 485A, CORE 12

Visual Description

Gray, very sparsely phyric, massive basalt. Plagioclase phenocrysts < 1%, < 3 mm, subhedral, fresh; olivine(?) phenocrysts < 1%, < 1 mm, replaced by smectite. Groundmass fine- to medium-grained, fresh. *Veinlets and fractures sparse, steep, filled with carbonate, smectite,* and minor pyrite.

Thin Section Description

Location: Section 1, 62–64 cm

Texture: Sparsely to moderately phyric, quench

Phenocrysts: Plagioclase 8–10%, 0.6–1 mm, subhedral, fresh; olivine 2–3%, 0.4–0.6 mm, subhedral, mostly altered to smectite; clinopyroxene 2%, 0.3–0.5 *mm, anhedral, fresh,* $2V_z \sim 40°$; phenocrysts typically intergrown in glomerophyric clusters.

Groundmass: *Dark brown, partly devitrified glass with sparse plagioclase* and magnetite crystals.

Alteration: Olivine partly replaced by smectite.

HOLE 485A, CORE 13

Visual Description

Gray, sparsely phyric, massive basalt. Plagioclase phenocrysts <1%, *<2 mm, subhedral, fresh; olivine phenocrysts 2–3%,* <1 mm, subhedral, replaced by smectite. Groundmass fine-grained, uniform, fresh. Vesicles <1%, < 1 mm, round, filled with smectite; one large irregular vesicles at 40 cm, Section 1. Fractures and veinlets sparse, hairline to 1 mm, filled with carbonate and minor pyrite.

Thin Section Description

Location: Section 1, 103–105 cm

Texture: Aphyric, medium-grained, intergranular to intersertal

Groundmass: Plagioclase 50%, 0.5–1 mm, subhedral, fresh; olivine 1–2%, 0.5 mm, subhedral, partly replaced by smectite; clinopyroxene 40%, 0.3–0.5 mm, subhedral, fresh, $2V_z \sim 40°$; opaques 2–3%, 0.1–0.3 mm, subhedral, probably magnetite; interstitial material, 5%, brown microcrystalline material, fresh.

Veins and Fractures: Sparse, 0.2 mm wide, filled with carbonate.

Alteration: Olivine partly replaced by smectite.

HOLE 485A, CORE 14

Visual Description

Gray, sparsely phyric, massive basalt. Plagioclase phenocrysts <1%, <3 mm, subhedral, fresh; olivine phenocrysts 1%, < 1 mm, subhedral, replaced by smectite. Groundmass fine-grained, uniform, fresh. Fractures and veinlets sparse, hairline to 1 mm, filled with smectite and carbonate.

HOLE 485A, CORE 15

Visual Description

NO RECOVERY

HOLE 485A, CORE 16

Visual Description

Gray, sparsely phyric, massive basalt. Plagioclase phenocrysts < 1%, < 2 mm, subhedral, fresh. Groundmass fine-grained, uniform, fresh. Vesicles < 1%, < 0.5 mm, round, filled with carbonate.

HOLE 485A, CORE 17

Visual Description

Section 1, 0 cm–Section 2, 53 cm: Gray, aphyric, massive basalt. Plagioclase phenocrysts < 1%, < 2 mm, subhedral, fresh. Rock is fine- to medium-grained, fresh. Vesicles < 1%, < 0.5 mm; round, filled with carbonate. Fractures and veinlets common, hairline to 12 mm wide, filled with carbonate.

Section 2, 53–57 cm: Medium gray limestone.

Section 2, 57 cm–base of core: Gray, fine-grained, fresh, aphyric, massive basalt.

Thin Section Description

Location: Section 1, 112–114 cm

Texture: Aphyric, medium- to coarse-grained, intergranular to intersertal.

Groundmass: Plagioclase 50%, 0.5–1.5 mm, subhedral, fresh; olivine 5–8%, 0.3–0.5 mm, subhedral, replaced by carbonate and smectite; clinopyroxene 35%, 0.3–0.6 mm, subhedral, fresh, $2V_z \sim 40°$; opaques 3%, 0.05–0.2 mm, subhedral, some acicular cyrstals, probably magnetite-ilmenite; interstitial material 5%, microcrystalline plagioclase and clinopyroxene, partly replaced by smectite.

Vesicles: <1%, 0.5 mm, round, filled with carbonate

Veins and Fractures: Hairline vein filled with brown smectite

Alteration: Olivine and minor interstitial material replaced by smectite and carbonate.

Location: Section 2, 60–65 cm (Depositional contact of sediment on basalt)

Texture: Aphyric, medium-grained, intersertal to subophitic

Groundmass: Plagioclase 35%, 0.5–1 mm, subhedral, fresh; olivine 2%, 0.3 mm, subhedral, altered to smectite and carbonate; clinopyroxene 30%, 0.3–0.5 mm, anhedral, fresh, except at immediate contact where it is partly altered to smectite, $2V_z \sim 40°$; opaques 3%, 0.05–0.2 mm, granular to acicular, magnetite-ilmenite; interstitial material 30%, quenched material, partly replaced by smectite particularly near contact

Alteration: Olivine, some pyroxene, and interstitial material replaced by smectite

SITE 485 HOLE A CORE 18 CORED INTERVAL 183.5–188.0 m

TIME – ROCK UNIT	BIOSTRATIGRAPHIC ZONE	FOSSIL CHARACTER: FORAMINIFERS	NANNOFOSSILS	RADIOLARIANS	DIATOMS	SECTION	METERS	GRAPHIC LITHOLOGY	DRILLING DISTURBANCE	SEDIMENTARY STRUCTURES	SAMPLES		LITHOLOGIC DESCRIPTION
QUATERNARY	NN19 (N)		FM			1	0.5 1.0				*	5Y 3/2	Section 1, 0–58 cm: Massive BASALT. Section 1, 58–63 cm: BASALT breccia. Section 1, 63–150 cm: Soft olive gray SANDY MUD.

SMEAR SLIDE SUMMARY

	1-95
TEXTURE:	
Sand	25
Silt	31
Clay	44
COMPOSITION:	
Quartz	35
Feldspar	5
Mica	TR
Heavy minerals	2
Clay	44
Pyrite	2
Carbonate unspec.	3
Foraminifers	1
Calc. nannofossils	7
Diatoms	1

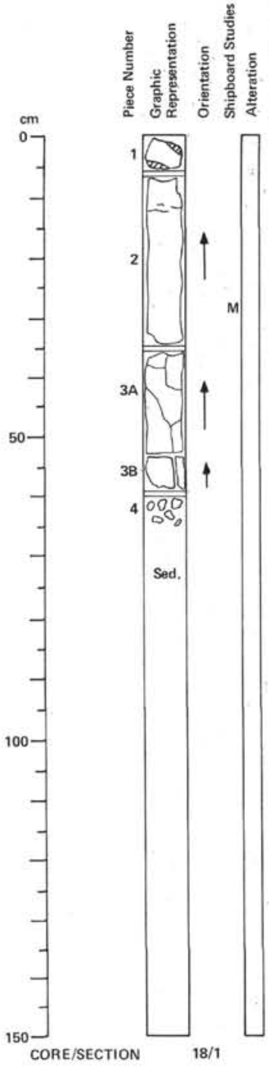

HOLE 485A, CORE 18

Visual Description

Section 1, 0–58 cm: Gray, fine- to medium-grained, aphyric, massive basalt. Plagioclase and olivine phenocrysts < 1%, < 1 mm; plagioclase fresh, olivine altered to smectite. Veins sparse, filled with smectite and carbonate.

Section 1, 58 cm–base of core: Olive-gray, soft, sandy clay.

SITE 485 HOLE A CORE 19 CORED INTERVAL 188.0–192.5 m

TIME-ROCK UNIT	BIOSTRATIGRAPHIC ZONE	FORAMINIFERS	NANNOFOSSILS	RADIOLARIANS	DIATOMS	SECTION	METERS	GRAPHIC LITHOLOGY
QUATERNARY	NN19 (N)	AM-G	CM	B		1	0.5 / 1.0	VOID
		FM-G		RG		2		

5Y 3/2

LITHOLOGIC DESCRIPTION

Section 1, 135 cm–Section 2, 75 cm: Firm to stiff olive gray SANDY MUD containing visible foraminifer and framboidal grains of pyrite.

Section 2, 75–150 cm: Stiff, dehydrated olive gray SILTY NANNOFOSSIL CHALK containing framboidal concretions of pyrite.

SMEAR SLIDE SUMMARY

	2-2	2-73	2-142
TEXTURE:			
Sand	25	20	–
Silt	14	21	83
Clay	61	59	17
COMPOSITION:			
Quartz	20	10	30
Feldspar	2	2	TR
Mica	–	3	–
Heavy minerals	3	2	1
Clay	61	59	17
Pyrite	2	15	1
Carbonate unspec.	5	–	–
Foraminifers	1	TR	–
Calc. nannofossils	5	7	50
Diatoms	1	1	1
Radiolarians	–	1	–
Sponge spicules	TR	–	–

SITE 485 HOLE A CORE 20 CORED INTERVAL 192.5–197.0 m

TIME-ROCK UNIT	BIOSTRATIGRAPHIC ZONE	FORAMINIFERS	NANNOFOSSILS	RADIOLARIANS	DIATOMS	SECTION	METERS	GRAPHIC LITHOLOGY
QUATERNARY	NN19 (N)		CM			1	0.5 / 1.0	
		RM		B		2		
						CC		

5Y 3/2

LITHOLOGIC DESCRIPTION

Section 1, 0 cm–Section 2, 35 cm: Hard, olive gray MUDDY NANNOFOSSIL CHALK containing small burrows(?) filled with pyrite and rimmed with calcite.

Core-Catcher: Olive gray MUDDY NANNOFOSSIL CHALK with small pieces of light gray, SILTY CALCAREOUS CHALK at the base of the core.

SMEAR SLIDE SUMMARY

	1-52	CC
TEXTURE:		
Sand	–	–
Silt	60	61
Clay	40	39
COMPOSITION:		
Quartz	25	20
Heavy minerals	1	1
Clay	40	39
Pyrite	1	–
Carbonate unspec.	–	30
Calc. nannofossils	30	10
Diatoms	3	–

SITE 485 HOLE A CORE 21 CORED INTERVAL 197.0–201.5 m

TIME-ROCK UNIT	BIOSTRATIGRAPHIC ZONE	FORAMINIFERS	NANNOFOSSILS	RADIOLARIANS	DIATOMS	SECTION	METERS	GRAPHIC LITHOLOGY
QUATERNARY	NN19 (N)					1		

LITHOLOGIC DESCRIPTION

Large fragment of coarse-grained HYALOCLASTITE or HYDROTHERMALLY ALTERED SANDSTONE(?) with well-developed layering in a matrix of disturbed MUDSTONE.

SITE 485 HOLE A CORE 22 CORED INTERVAL 201.5–211.5 m

TIME-ROCK UNIT	BIOSTRATIGRAPHIC ZONE	FORAMINIFERS	NANNOFOSSILS	RADIOLARIANS	DIATOMS	SECTION	METERS	GRAPHIC LITHOLOGY
QUATERNARY	NN19 (N)		CM			1	0.5 / 1.0	
						2		
						3		
						4		
						5		
			CP			6		
		CP		B		CC		

5Y 3/2

5GY 3/2

5Y 3/2

5GY 3/2

5GY 2/1

LITHOLOGIC DESCRIPTION

Firm to hard, olive gray MUDDY NANNOFOSSIL CHALK containing pieces of glassy BASALT near the top of Section 1, pyrite-filled burrows near the base of Section 1 and layers of grayish olive green SANDY MUD near the middle of the core.

SMEAR SLIDE SUMMARY

	1-10	2-100	3-18	3-135	4-20	4-122	6-80
TEXTURE:							
Sand	1	–	–	40	2	–	TR
Silt	45	62	57	21	60	68	67
Clay	54	38	43	39	38	32	32
COMPOSITION:							
Quartz	12	20	10	30	15	10	12
Feldspar	1	2	–	5	1	TR	TR
Mica	TR	–	–	–	TR	TR	TR
Heavy minerals	1	1	3	3	1	2	1
Clay	54	38	43	39	38	32	32
Pyrite	1	2	1	3	2	5	4
Carbonate unspec.	TR	5	–	–	TR	TR	TR
Foraminifers	TR	TR	–	2	1	–	–
Calc. nannofossils	30	30	40	15	40	50	50
Diatoms	–	1	3	3	2	1	1
Radiolarians	TR	–	–	–	–	–	–
Sponge spicules	–	–	–	–	–	TR	–
Silicoflagellates	–	–	TR	–	–	–	–

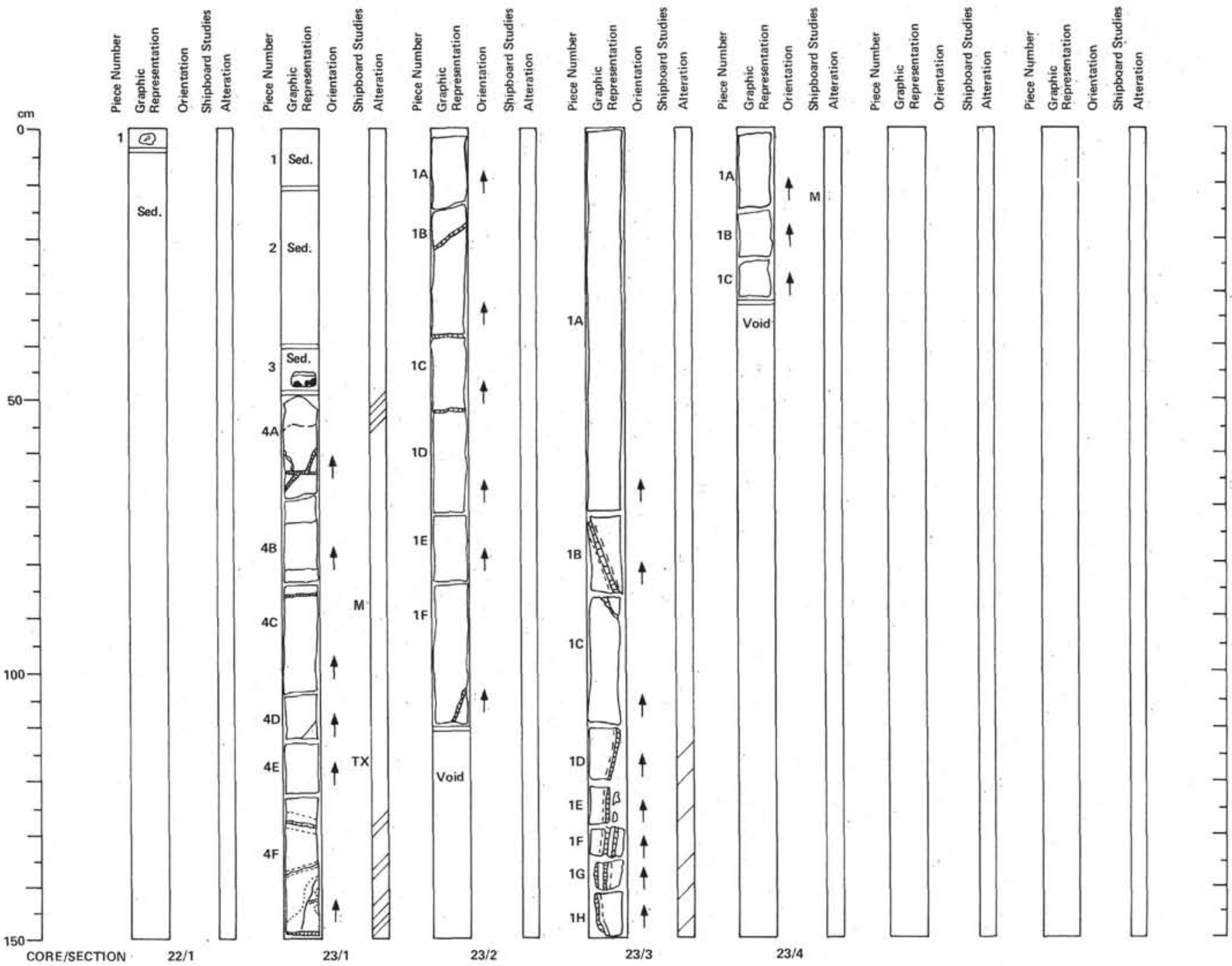

HOLE 485A, CORE 22

Visual Description

Olive gray, stiff, nannofossil-rich clay, with bioturbations filled with pyrite. Fragments of aphyric basalt at top of core.

HOLE 485A, CORE 23

Visual Description

Section 1, 0–50 cm: Olive gray to dark brown indurated siltstone. Sediment appears baked against basalt at 50 cm.

Section 1, 50 cm–base of core: Gray, sparsely phyric, massive basalt. Plagioclase phenocrysts <2%, ≤3 mm, subhedral, fresh; olivine microphenocrysts <1%, <1 mm, altered to smectite. Groundmass very fine- to medium-grained, grain size increases downward, fresh. Vesicles < 1%, < 1 mm, round; filled with smectite and carbonate. Fractures and veins common, subvertical, 1–10 mm, filled with carbonate, zeolite(?), and minor smectite.

Thin Section Description

Location: Section 1, 118–120 cm

Texture: Very sparsely phyric, medium-grained, intergranular

Phenocrysts: Plagioclase 1%, 1–3 mm, subhedral to anhedral, fresh.

Groundmass: Plagioclase 50%, 0.5–0.8 mm, subhedral, fresh; olivine 5%, 0.3–0.5 mm, subhedral, replaced by smectite; clinopyroxene 35–40%, 0.4–0.7 mm, anhedral, fresh, $2V_z - 40°$; opaques 3–4%, 0.05–0.1 mm, subhedral, probably magnetite; interstitial material 2–3%, quartz, feldspar and apatite, fresh.

Alteration: Olivine replaced by smectite.

SITE 485 HOLE A CORE 23 CORED INTERVAL 211.5–216.0 m

TIME – ROCK UNIT	BIOSTRATIGRAPHIC ZONE	FOSSIL CHARACTER: FORAMINIFERS	NANNOFOSSILS	RADIOLARIANS	DIATOMS	SECTION	METERS	GRAPHIC LITHOLOGY	DRILLING DISTURBANCE	SEDIMENTARY STRUCTURES	SAMPLES
QUATERNARY	NN19 (N)		CP			1	0.5 1.0	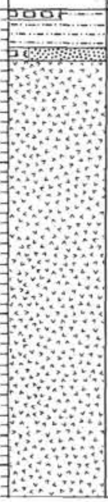			•
						2					
						3					
						4					

LITHOLOGIC DESCRIPTION

5Y 3/2
5YR 2/1

Section 1, 0–10 cm: Soft, olive gray SILTY CALCAREOUS OOZE composed of calcite and minor dolomite(?) in a matrix of clayey silt.

Section 1, 10–40 cm: Firm SILTY CLAY containing minor carbonate.

Section 1, 40–50 cm: Light green, finely layered CALCAREOUS SANDSTONE overlying BASALT. The sandstone contains partially dissolved calcareous nannofossils and is cemented by carbonates.

Section 1, 50 cm–Section 4, 30 cm: BASALT with a devitrified glassy margin in direct contact with the overlying sediments.

SMEAR SLIDE SUMMARY

	1-23
TEXTURE:	
Sand	5
Silt	64
Clay	31
COMPOSITION:	
Quartz	10
Feldspar	3
Clay	31
Pyrite	3
Carbonate unspec.	50
Calc. nannofossils	3
Diatoms	TR
Radiolarians	TR

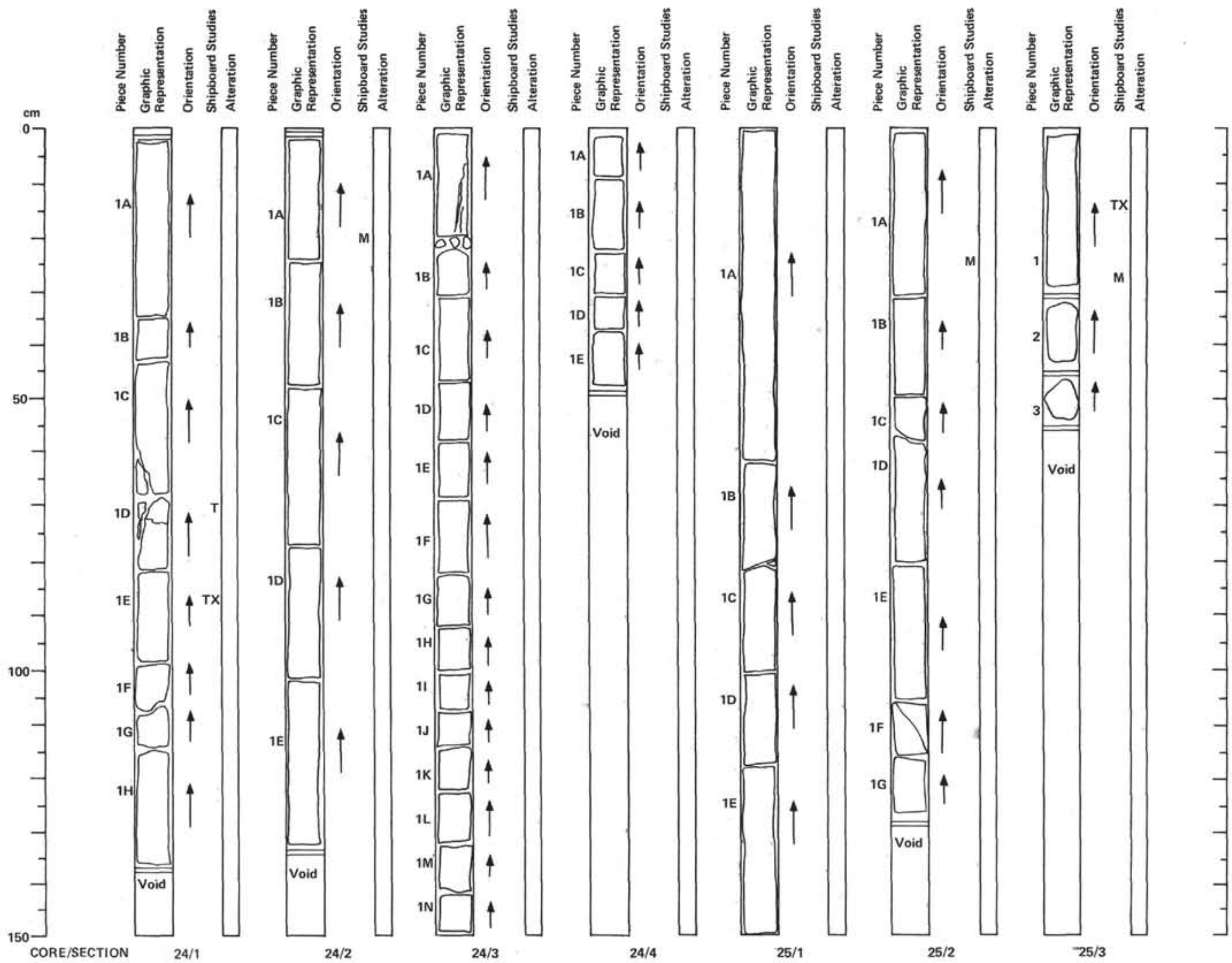

HOLE 485A, CORE 24

Visual Description

Gray, sparsely phyric, massive basalt. Plagioclase phenocrysts < 2%, 1–3 mm, subhedral, fresh, some glomerophyric blusters; clinopyroxen phenocrysts <1%, <1 mm, fresh. Groundmass medium- to coarse-grained, holocrystalline, fresh. Fractures sparse, subvertical, hairline to 1 mm, lined with smectite and minor pyrite.

Thin Section Description

Location: Section 1, 68–70 cm

Texture: Aphyric, very coarse-grained, subophitic

Groundmass: Plagioclase 50%, 1–3 mm, subhedral, partly altered to smectite; clinopyroxene 40%, <3 mm, anhedral, subophitic crystals, $2V_z \sim 40°$; partly replaced by smectite; opaques 2%, 0.1–0.3 mm, often skeletal, probably magnetite; interstitial material 10–15%, replaced by smectite

Alteration: Rock highly altered; plagioclase, clinopyroxene, and interstitial material partly to completely replaced by smectite. Unknown mineral also present, possibly scapolite.

HOLE 485A, CORE 25

Visual Description

Gray, sparsely phyric, massive basalt. Plagioclase phenocrysts 2–3%, 1–3 mm, subhedral, fresh, some glomerophyric clusters with clinopyroxene; clinopyroxene phenocrysts 1%, 1 mm, anhedral, mostly intergrown with plagioclase. Groundmass medium- to coarse-grained, uniform, fresh. Fractures and veinlets sparse, mostly subvertical, hairline to 1 mm, filled with smectite, carbonate and minor pyrite.

Thin Section Description

Location: Section 1, 89–91 cm

Texture: Aphyric, very coarse-grained, ophitic to intersertal

Groundmass: Plagioclase 45%, < 2 mm, subhedral laths, fresh, often zoned; clinopyroxene 40%, <4 mm, subhedral, ophitic plates, fresh, $2V_z \sim 40°$; opaques 3–4%, 0.2–1 mm, skeletal, probably magnetite; interstitial material 10–12%, mostly altered to smectite, may include some altered olivine

Alteration: Interstitial material partly altered to smectite

Location: Section 3, 14–16 cm

Texture: Aphyric, medium-grained, subophitic to intersertal

Groundmass: Plagioclase 45%, 0.5–2 mm, subhedral, fresh; olivine 5%, < 0.5 mm, subhedral, replaced by smectite; clinopyroxene 40%, <1 mm, anhedral, fresh, $2V_z \sim 40°$; opaques 2–3%, 0.05–0.2 mm, subhedral, probably magnetite; interstitial material 5–10%, mostly replaced by smectite.

Alteration: Olivine and interstitial material replaced by smectite.

SITE 485 HOLE A CORE 26 CORED INTERVAL 226.0–230.5 m

TIME–ROCK UNIT	BIOSTRATIGRAPHIC ZONE	FOSSIL CHARACTER: FORAMINIFERS	NANNOFOSSILS	RADIOLARIANS	DIATOMS	SECTION	METERS	GRAPHIC LITHOLOGY	DRILLING DISTURBANCE	SEDIMENTARY STRUCTURES	SAMPLES	LITHOLOGIC DESCRIPTION
QUATERNARY	NN19 (N)	FP	FM	B		1, 2	0.5, 1.0				• • •	5Y 3/2

5Y 3/2

Section 1, 0–21 cm: Massive BASALT.

Section 1, 21 cm–Section 2, 115 cm: Very firm; olive gray *MUDDY NANNOFOSSIL CHALK*. The sediments are strongly dehydrated and display a tendency toward fissile parting.

SMEAR SLIDE SUMMARY

	1-40	1-75	2-14
TEXTURE:			
Sand	–	–	–
Silt	62	51	46
Clay	38	49	54
COMPOSITION:			
Quartz	5	7	5
Feldspar	TR	1	TR
Mica	TR	1	–
Heavy minerals	TR	TR	TR
Clay	38	49	54
Volcanic glass	–	TR	TR
Pyrite	7	3	1
Carbonate unspec.	TR	TR	1
Foraminifers	–	TR	–
Calc. nannofossils	50	40	40
Diatoms	TR	TR	–

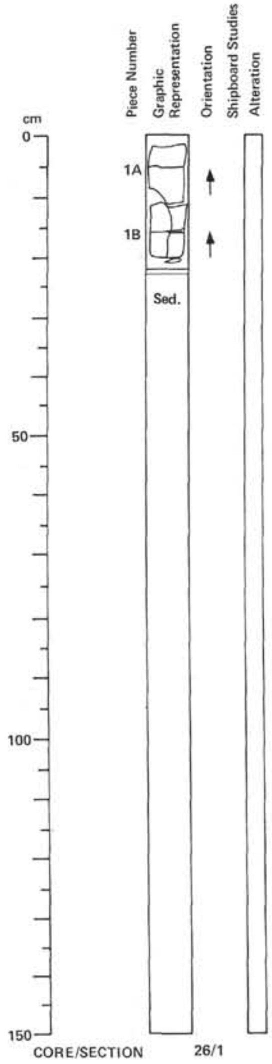

HOLE 485A, CORE 26

Visual Description

Section 1, 0–21 cm: Gray, sparsely phyric, massive basalt. Plagioclase phenocrysts 1–2%, < 4 mm, subhedral, fresh; olivine phenocrysts 1–2%, < 4 mm, subhedral, altered to smectite. Groundmass fine-grained, uniform, fresh. Fractures sparse, subvertical, hairline, filled with carbonate.

Section 1, 21 cm–base of core: Olive gray, firm, nannofossil marl.

SITE 485 HOLE A CORE 27 CORED INTERVAL 230.5–235.0 m

TIME – ROCK UNIT	BIOSTRATIGRAPHIC ZONE	FOSSIL CHARACTER: FORAMINIFERS	NANNOFOSSILS	RADIOLARIANS	DIATOMS	SECTION	METERS	GRAPHIC LITHOLOGY	DRILLING DISTURBANCE	SEDIMENTARY STRUCTURES	SAMPLES	LITHOLOGIC DESCRIPTION
QUATERNARY	NN19 (N)	FP	CM	B		1	0.5, 1.0				*	5Y 2/1
						CC					*	

Hard, olive black NANNOFOSSIL-bearing SILTY CLAYSTONE.

SMEAR SLIDE SUMMARY

	1-20	1-126
TEXTURE:		
Sand	–	–
Silt	32	40
Clay	68	60
COMPOSITION:		
Quartz	10	5
Feldspar	1	TR
Heavy minerals	TR	TR
Clay	68	60
Volcanic glass	TR	TR
Pyrite	–	5
Carbonate unspec.	1	TR
Foraminifers	TR	–
Calc. nannofossils	20	30
Diatoms	–	TR

SITE 485 HOLE A CORE 28 CORED INTERVAL 235.0–239.5 m

TIME – ROCK UNIT	BIOSTRATIGRAPHIC ZONE	FOSSIL CHARACTER: FORAMINIFERS	NANNOFOSSILS	RADIOLARIANS	DIATOMS	SECTION	METERS	GRAPHIC LITHOLOGY	DRILLING DISTURBANCE	SEDIMENTARY STRUCTURES	SAMPLES	LITHOLOGIC DESCRIPTION
QUATERNARY	NN19 (N)	RM	CM	B		1	0.5, 1.0	VOID			*	5Y 2/1
						CC						

Hard, olive black NANNOFOSSIL-bearing SILTY CLAYSTONE.

SMEAR SLIDE SUMMARY

	1-125
TEXTURE:	
Sand	–
Silt	41
Clay	59
COMPOSITION:	
Quartz	5
Feldspar	TR
Heavy minerals	1
Clay	59
Volcanic glass	TR
Pyrite	15
Carbonate unspec.	TR
Calc. nannofossils	20
Diatoms	TR

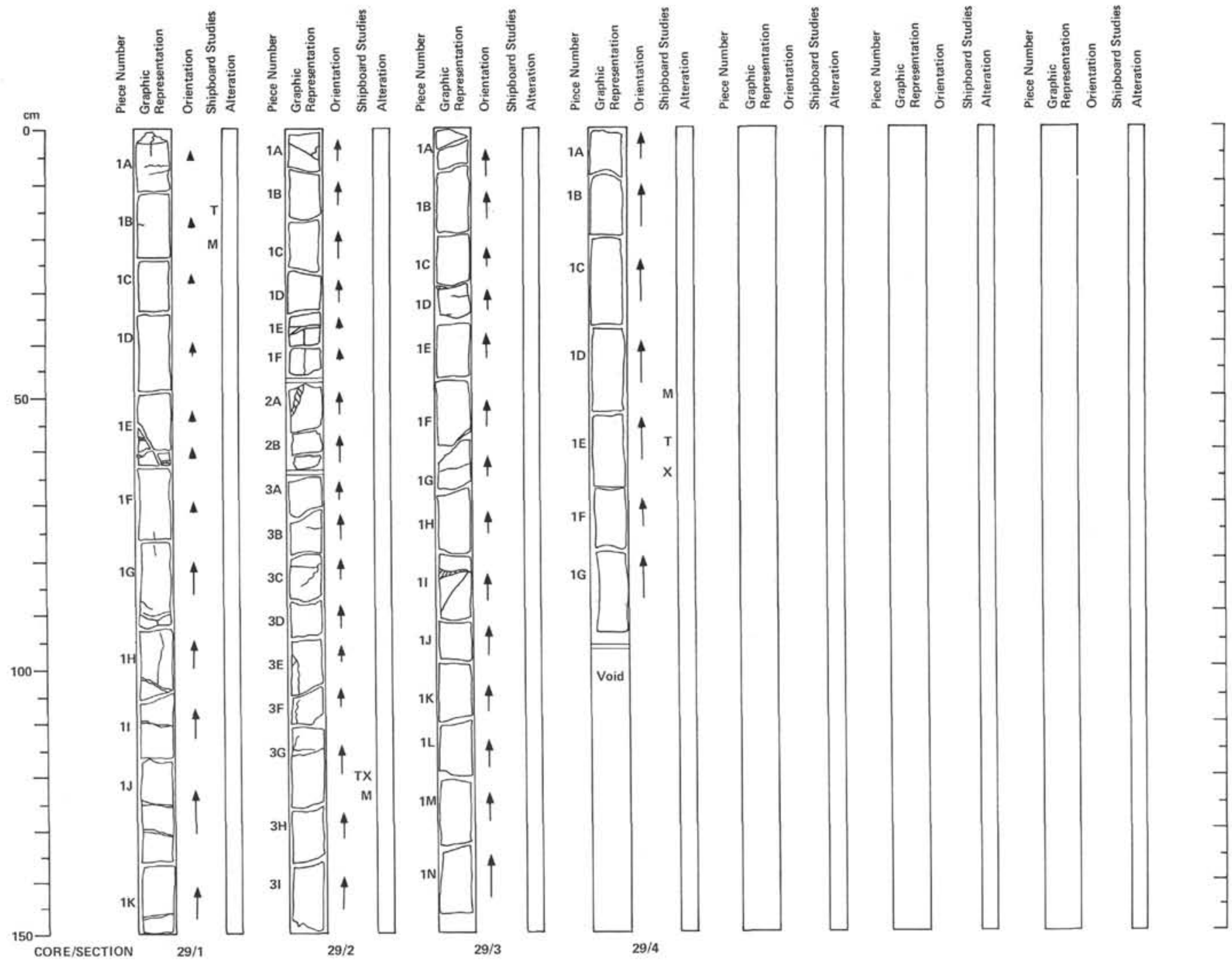

HOLE 485A, CORE 29

Visual Description

Gray to greenish-gray, very sparsely phyric, massive basalt. Plagioclase phenocrysts < 1%, 1–3 mm, subhedral, fresh, some glomerophyric clusters with traces of clinopyroxene; rare plagioclase megacrysts to 7 mm. Groundmass fine- to medium-grained, grain size increases gradually with depth; groundmass greenish-gray, locally altered to smectite and chlorite(?) with minor carbonate and pyrite. Vesicles <1%, < 0.5 mm, round, filled with smectite and carbonate. Fractures and veinlets fairly common, subvertical, hairline to 2 mm, filled with smectite and carbonate.

Thin Section Description

Location: Section 1, 15–17 cm

Texture: Aphyric, fine- to medium-grained, intergranular to intersertal

Groundmass: Plagioclase 45%, 0.4–1 mm, subhedral, fresh; olivine 2–3%, 0.2–0.4 mm, subhedral, replaced by smectite and carbonate; clinopyroxene 40–45%, 0.2–0.4 mm, anhedral, fresh, $2V_z \sim 40°$; opaques 2%, 0.05–0.1 mm, granular, probably magnetite; interstitial material 5–10%, replaced by green smectite(?).

Alteration: Olivine and interstitial material replaced by smectite and minor carbonate

Location: Section 2, 122–124 cm

Texture: Aphyric, fine- to medium-grained, intergranular to intersertal

Groundmass: Plagioclase 45%, 0.4–1 mm, subhedral, fresh; olivine 2–4%, 0.2–0.4 mm, subhedral, replaced by smectite and carbonate; clinopyroxene 40–45%, 0.2–0.4 mm, anhedral, fresh, $2V_z \sim 40°$; opaques 2%, 0.05–0.1 mm, granular, probably magnetite; interstitial material 5–10%, replaced by green smectite.

Alteration: Olivine and interstitial material replaced by smectite and minor carbonate.

Location: Section 4, 59–61 cm

Texture: Aphyric, coarse-grained, subophitic to intersertal

Groundmass: Plagioclase 45%, 1–4 mm, subhedral, fresh; clinopyroxene 40–45%, 1–2 mm, subophitic plates, marginally altered to green smectite, $2V_z \sim 40°$; opaques 2%, 0.5–1 mm, skeletal, probably magnetite; interstitial material 10%, mostly quartz, feldspar, and apatite, partly replaced by smectite.

Alteration: Pyroxene and interstitial material partly replaced by smectite.

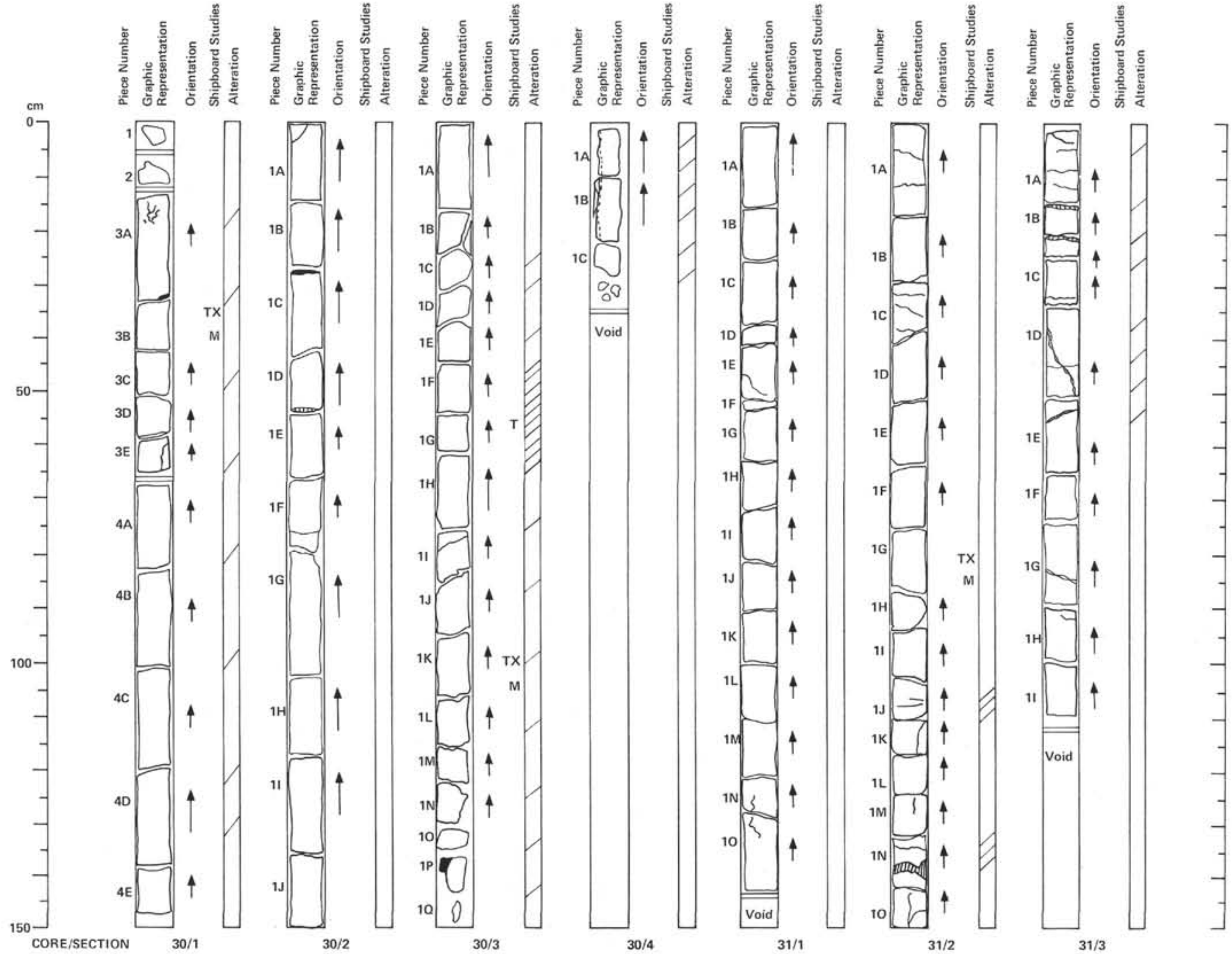

HOLE 485A, CORE 30

Visual Description

Gray to greenish-gray, aphyric, massive basalt. Rock is fine- to coarse-grained, grain size increases gradually downward, some altered zones with smectite, chlorite(?), carbonate and pyrite. Veins and fractures sparse, filled with smectite and carbonate.

Thin Section Description

Location: Section 1, 39–41 cm

Texture: Aphyric, coarse-grained, intergranular to subophitic

Groundmass: Plagioclase 45–50%, 1–3 mm, subhedral, fresh; clinopyroxene 45%, 0.2–0.5 mm, subhedral, fresh; $2V_z \sim 40°$, some sector zoning, some crystals may have cores of pigeonite; opaques 2–3%, 0.2–0.5 mm, subhedral, probably magnetite; interstitial material 5%, quartz, feldspar, and apatite, partly replaced by smectite.

Alteration: Minor interstitial material replaced by smectite; some altered material may be after olivine.

Location: Section 3, 55–58 cm

Texture: Aphyric, very coarse-grained, ophitic

Groundmass: Plagioclase 30–35%, 4–7 mm, subhedral, often curved crystals, partly replaced by smectite; clinopyroxene 60–65%, 5–10 mm, ophitic plates, partly replaced by smectite, $2V_z \sim 40°$; opaques 1–2%, 0.5 mm, subhedral, probably magnetite.

Alteration: Plagioclase and clinopyroxene partly replaced by smectite

Location: Section 3, 103–105 cm

Texture: Aphyric, very coarse-grained, ophitic to intersertal

Groundmass: Plagioclase 45–50%, 1–3 mm, subhedral, fresh; olivine 3–4%, 1 mm, subhedral, replaced by smectite; clinopyroxene 25–45%, 0.5–5 mm, anhedral, subophitic, twinned, often zoned, $2V_z \sim 40°$, some with probable cores of pigeonite; opaques 1–2%, 0.5–1.5 mm, skeletal, probably magnetite; interstitial material 5–20%, quartz, feldspar, and apatite, partly replaced by smectite

Alteration: Olivine and some interstitial material replaced by smectite

HOLE 485A, CORE 31

Visual Description

Gray, aphyric, massive basalt. Rock very coarse-grained, subophitic, generally uniform, with patchy alteration to smectite. Fractures and veinlets sparse, mostly subhorizontal, hairline to 3 mm, filled with smectite.

Thin Section Description

Location: Section 1, 81–83 cm

Texture: Aphyric, coarse-grained, subophitic to intergranular

Groundmass: Plagioclase 55%, 0.5–3 mm, subhedral, fresh; olivine 2–3%, < 0.5 mm, replaced by brown smectite; clinopyroxene 30–35%, 0.5–2 mm, subhedral, often zoned, marginally altered to amphibole and smectite, $2V_z \sim 40°$, many crystals with cores of pigeonite, $2V_z \sim 5°$; opaques 3%, < 1.5 mm, skeletal, probably magnetite; interstitial material 5–10%, quartz, feldspar and minor apatite, partly replaced by smectite.

Alteration: Olivine and some interstitial material altered to smectite; clinopyroxene rimmed with amphibole and smectite.

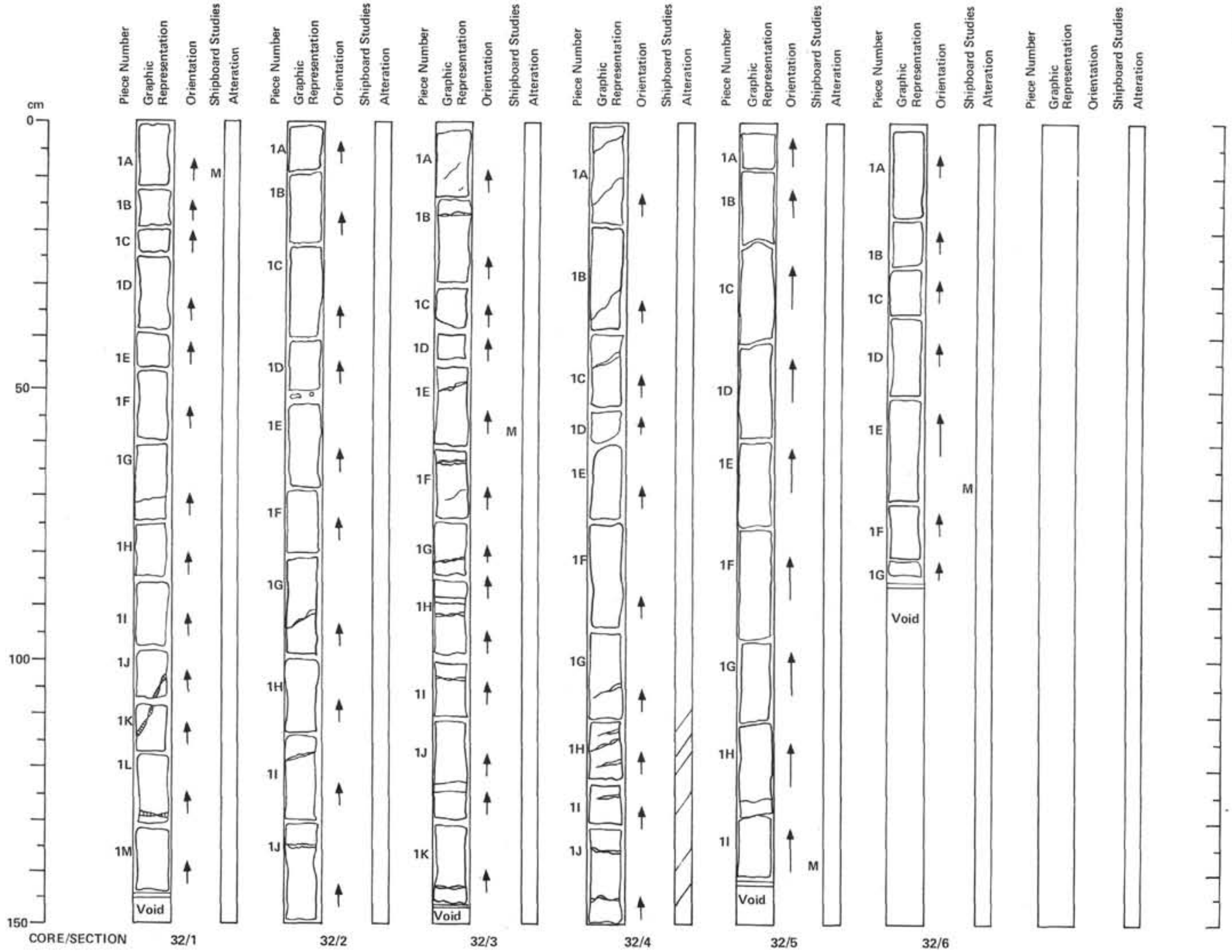

HOLE 485A, CORE 32

Visual Description

Gray, aphyric, massive basalt. Rock coarse-grained, uniform, massive, generally fresh; grain size decreases somewhat downwards. Scattered round plagioclase megacrysts to 15 mm. Fractures fairly common, subhorizontal, hairline to 2 mm, filled with smectite.

SITE 485 HOLE A CORE 33 CORED INTERVAL 268.0–277.0 m

TIME – ROCK UNIT	BIOSTRATIGRAPHIC ZONE	FOSSIL CHARACTER: FORAMINIFERS	FOSSIL CHARACTER: NANNOFOSSILS	FOSSIL CHARACTER: RADIOLARIANS	FOSSIL CHARACTER: DIATOMS	SECTION	METERS	GRAPHIC LITHOLOGY	DRILLING DISTURBANCE	SEDIMENTARY STRUCTURES	SAMPLES	LITHOLOGIC DESCRIPTION
QUATERNARY	NN19 (N)		B			1 2	0.5 1.0				*	N1

Section 1, 0 cm–Section 2, 95 cm: Massive BASALT.

Section 2, 95–100 cm: Hard, black CLAYSTONE.

SMEAR SLIDE SUMMARY

	2-99
TEXTURE:	
Sand	3
Silt	10
Clay	87
COMPOSITION:	
Quartz	4
Heavy minerals	2
Clay	87
Pyrite	2
Zeolite	5
Calc. nannofossils	TR

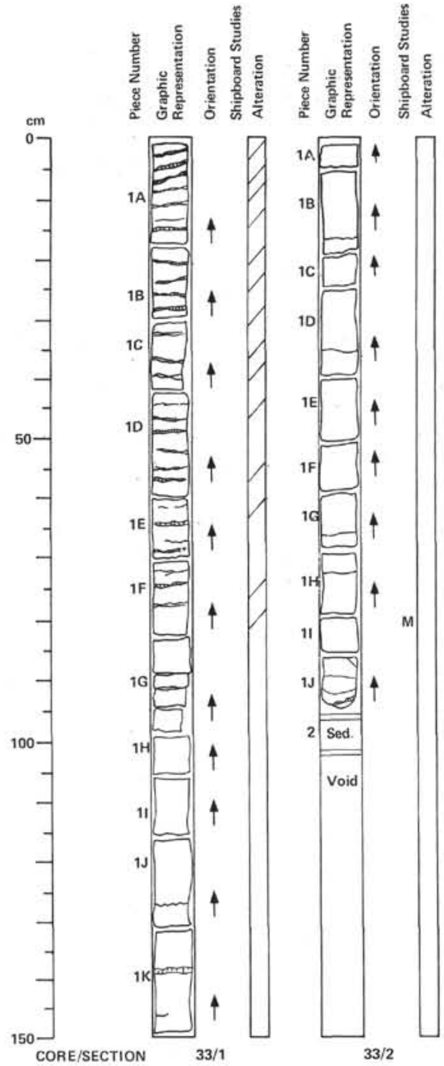

HOLE 485A, CORE 33

Visual Description

Section 1, 0 cm–Section 2, 93 cm: Gray, very sparsely phyric, massive basalt. Plagioclase phenocrysts 1–2%, 5 mm, subhedral, fresh; some rounded crystals to 10 mm; olivine phenocrysts < 1%, < 3 mm, subhedral, altered to smectite. Groundmass fine- to medium-grained, generally fresh. Fractures common, subhorizontal, hairline to 2 mm, filled with smectite.

Section 2, 93 cm–base of core: Dark brown, soft siltstone

SITE 485 HOLE A CORE 34 CORED INTERVAL 277.0–286.0 m

TIME – ROCK UNIT	BIOSTRATIGRAPHIC ZONE	FORAMINIFERS	NANNOFOSSILS	RADIOLARIANS	DIATOMS	SECTION	METERS	GRAPHIC LITHOLOGY	DRILLING DISTURBANCE	SEDIMENTARY STRUCTURES	SAMPLES	LITHOLOGIC DESCRIPTION
QUATERNARY	NN19 (N)	FM B	RP	RM B		1	0.5, 1.0				• •	N1 Hard, black CLAYSTONE overlying massive BASALT.

SMEAR SLIDE SUMMARY

	1-14	1-55
TEXTURE:		
Sand	–	4
Silt	11	11
Clay	89	85
COMPOSITION:		
Quartz	5	7
Heavy minerals	1	2
Clay	89	85
Pyrite	2	2
Zeolite	–	3
Carbonate unspec.	TR	1
Calc. nannofossils	1	TR
Diatoms	TR	–

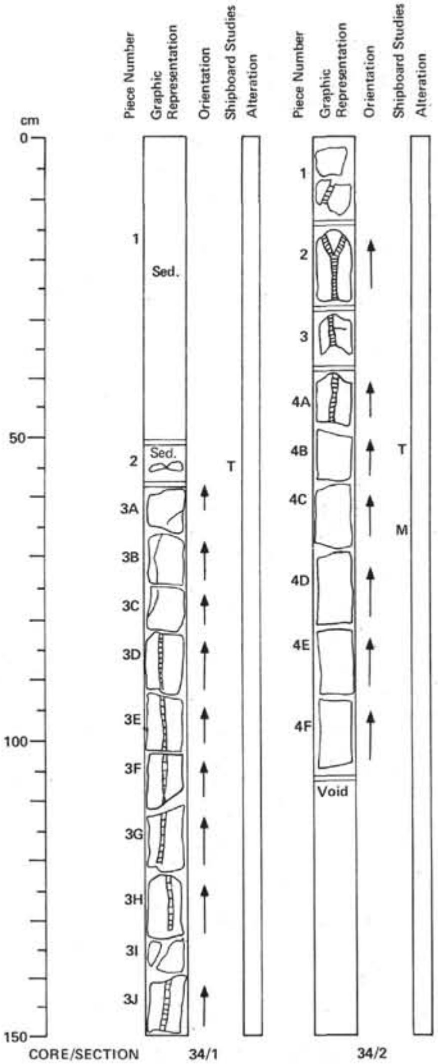

HOLE 485A, CORE 34

Visual Descripton

Section 1, 0–55 cm: Brownish-black, indurated silty claystone.

Section 1, 55 cm–base of core: Gray, aphyric, massive, basalt. Rock very fine-grained to medium-grained, with grain size increasing downward; some glassy fragments at sediment contact. Rock generally fresh. Vesicles 1–2%, < 1 mm, round, filled with carbonate and smectite. Fractures common, steep, hairline to 5 mm, filled with carbonate, smectite, and minor pyrite.

Thin Section Description

Location: Section 1, 55–57 cm

Texture: Very sparsely phyric, quench

Phenocrysts: Plagioclase 2–3%, < 1 mm, skeletal laths, fresh

Groundmass: Traces of feldspar microlites, minute crystals of altered olivine, and tiny grains of magnetite in a matrix of brown, devitrified glass

Alteration: Olivinve replaced by smectite

Location: Section 2, 48–50 cm

Texture: Aphyric, fine-grained, intergranular to intersertal

Groundmass: Plagioclase 55%, 0.2–1 mm, subhedral, fresh; olivine 1–2%, 0.2–0.5 mm, subhedral, replaced by smectite; clinopyroxene 30–35%, 0.1–0.4 mm, anhedral, fresh, $2V_z \sim 40°$; opaques 2–3%, 0.05–0.3 mm, skeletal, probably magnetite; interstitial material, 5–10%, quartz, feldspar and apatite, partly replaced by smectite.

Alteration: Olivine and some interstitial material replaced by smectite.

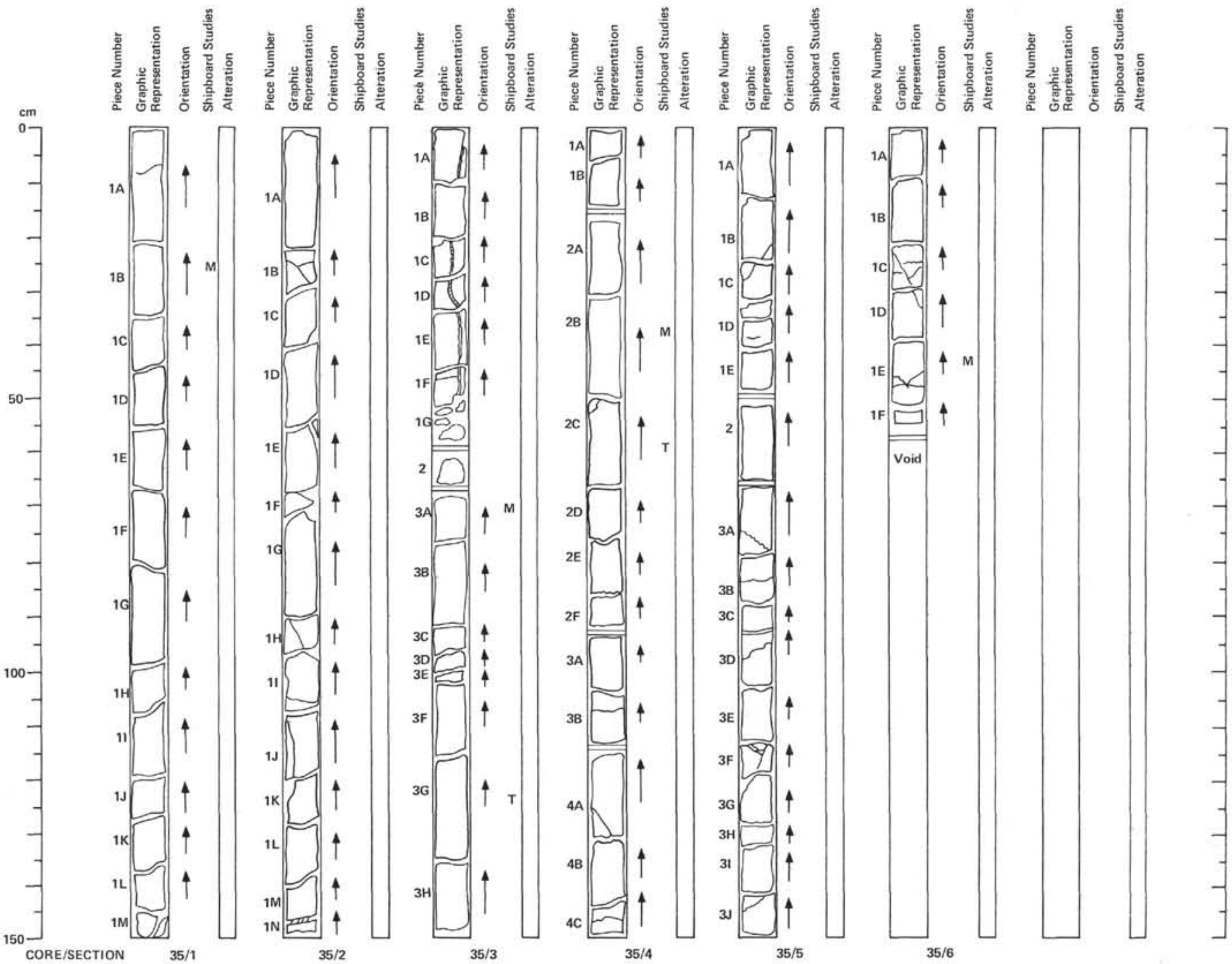

HOLE 485A, CORE 35

Visual Description

Gray, very sparsely phyric, massive basalt. Plagioclase phenocrysts < 1%, < 8 mm, subhedral, fresh; olivine phenocrysts < 1%, < 3 mm, subhedral, altered to smectite. Groundmass fine- to medium-grained, generally uniform, fresh. Vesicles 1%, < 1 mm, filled with smectite. Fractures sparse, to common, steep, hairline to 2 mm, filled with smectite and carbonate.

Thin Section Description

Location: Section 3, 131–135 cm

Texture: Aphyric, fine-grained, intergranular to intersertal

Groundmass: Plagioclase 55%, 0.2–1 mm, subhedral, fresh; olivine 5%, 0.2–0.5 mm, subhedral, replaced by smectite; clinopyroxene 30%, 0.1–0.4 mm, anhedral, fresh, $2V_z$ ~40°; opaques 2–3%, 0.05–0.3 mm, skeletal, probably magnetite; interstitial material 5–10%, quartz, feldspar and apatite, partly replaced by smectite.

Alteration: Olivine and some interstitial material replaced by smectite.

Location: Section 4, 63–66 cm

Texture: Aphyric, fine-grained, intergranular to intersertal

Groundmass: Plagioclase 55%, 0.2–1 mm, subhedral, fresh; olivine 5%, 0.2–0.5 mm, subhedral, replaced by smectite; clinopyroxene 30%, 0.1–0.4 mm, anhedral, fresh, $2V_z$ ~ 40°; opaques 2–3%, 0.05–0.2 mm, skeletal, probably magnetite; interstitial material 5–10%, microcrystalline material, partly altered to smectite.

Alteration: Olivine and some interstitial material replaced by smectite.

SITE 485 HOLE A CORE 36 CORED INTERVAL 295.0–304.0 m

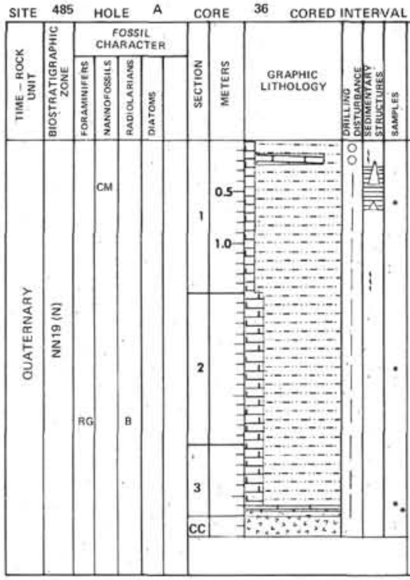

LITHOLOGIC DESCRIPTION

5Y 2/1

Section 1, 0 cm–Section 3, 65 cm: Hard, olive black NANNOFOSSIL-bearing SILTY CLAYSTONE containing a large fragment of limestone at a depth of 17–22 cm in Section 1 and a thin layer of dark, pyrite-rich LIMESTONE in contact with BASALT at the base of the sediments. The sediments between 22–64 cm in Section 1 contain thin intervals of finely laminated SANDY MUDSTONE and occasional burrows filled with pyrite and foraminifers.

Section 3, 65–70 cm: BASALT with a devitrified, glassy margin in direct contact with the limestone at the base of the sediments.

SMEAR SLIDE SUMMARY

	1-66	2-82	3-62	3-71
TEXTURE:				
Sand	–	–	–	–
Silt	14	26	56	100
Clay	86	74	44	–
COMPOSITION:				
Quartz	3	1	TR	–
Heavy minerals	1	–	–	–
Clay	86	74	44	–
Pyrite	1	5	15	15
Zeolite	3?	–	–	–
Carbonate unspec.	–	TR	20	85
Calc. nannofossils	10	20	20	–
Diatoms	TR	–	–	–

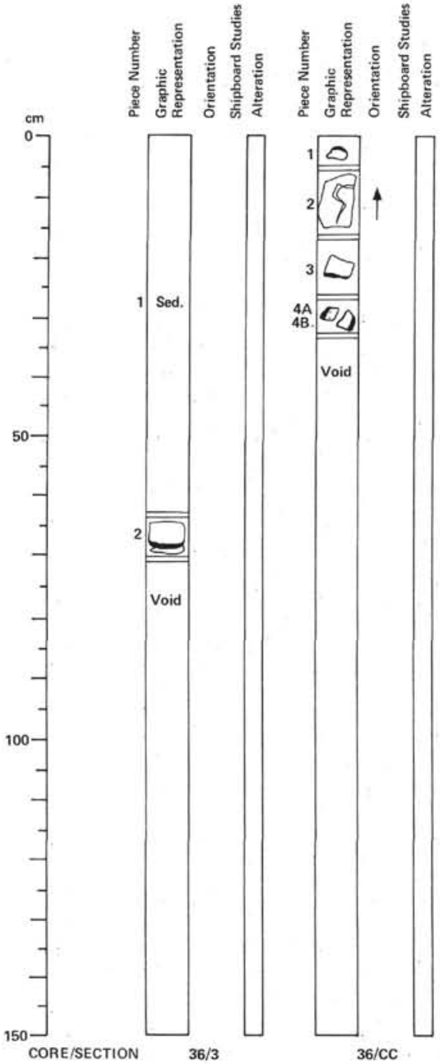

HOLE 485A, CORE 36

Visual Description

Section 1, 0cm–Section 3, 64 cm: Olive-black mudstone.

Section 3, 64 cm–base of core: Dark gray, sparsely phyric, massive(?) basalt. Plagioclase phenocrysts 3%, < 3 mm, subhedral, fresh; some rounded crystals to 6 mm. Veins and fractures sparse, filled with smectite and carbonate.

SITE 485 HOLE A CORE 37 CORED INTERVAL 304.0–313.0 m

TIME – ROCK UNIT	BIOSTRATIGRAPHIC ZONE	FORAMINIFERS	NANNOFOSSILS	RADIOLARIANS	DIATOMS	SECTION	METERS	GRAPHIC LITHOLOGY	DRILLING DISTURBANCE	SEDIMENTARY STRUCTURES	SAMPLES
QUATERNARY	NN19 (N)	B	CP	B		1 CC	0.5 1.0	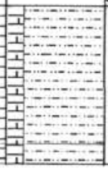			*

5Y 2/1

Homogeneous, olive black NANNOFOSSIL-bearing SILTY CLAYSTONE.

SMEAR SLIDE SUMMARY

	1-75
TEXTURE:	
Sand	–
Silt	21
Clay	79
COMPOSITION:	
Quartz	3
Feldspar	1
Heavy minerals	TR
Clay	79
Pyrite	2
Zeolite	3?
Calc. nannofossils	15

SITE 485 HOLE A CORE 38 CORED INTERVAL 313.0–322.0 m

TIME – ROCK UNIT	BIOSTRATIGRAPHIC ZONE	FORAMINIFERS	NANNOFOSSILS	RADIOLARIANS	DIATOMS	SECTION	METERS	GRAPHIC LITHOLOGY	DRILLING DISTURBANCE	SEDIMENTARY STRUCTURES	SAMPLES
QUATERNARY	NN19 (N)	RM	CP B B	B		1 2 3 4 5 6	0.5 1.0	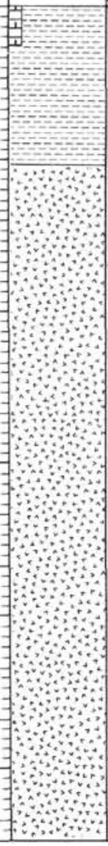			* * * *

N1

Section 1, 0 cm–Section 2, 1 cm: Firm to hard, black CLAYSTONE and SILTY CLAYSTONE with a sulfide-filled vein cutting across the core near the base of the sediments at a dip of about 60°. The basal sediments in contact with the underlying BASALT consist of an indurated mixture of glass and fine-grained basalt fragments, carbonate, sulfide, smectite, chalcedony and silty clay.

Section 2, 1 cm–Section 6, 70 cm: Massive BASALT.

SMEAR SLIDE SUMMARY

	1-10	1-85	1-146	2-5
TEXTURE:				
Sand	–	–	–	–
Silt	27	20	27	22
Clay	73	80	73	78
COMPOSITION:				
Quartz	10	15	12	10
Feldspar	2	TR	2	1
Heavy minerals	1	–	1	1
Clay	73	80	73	78
Pyrite	3	5	10	10
Carbonate unspec.	TR	–	–	TR
Calc. nannofossils	10	–	2	–

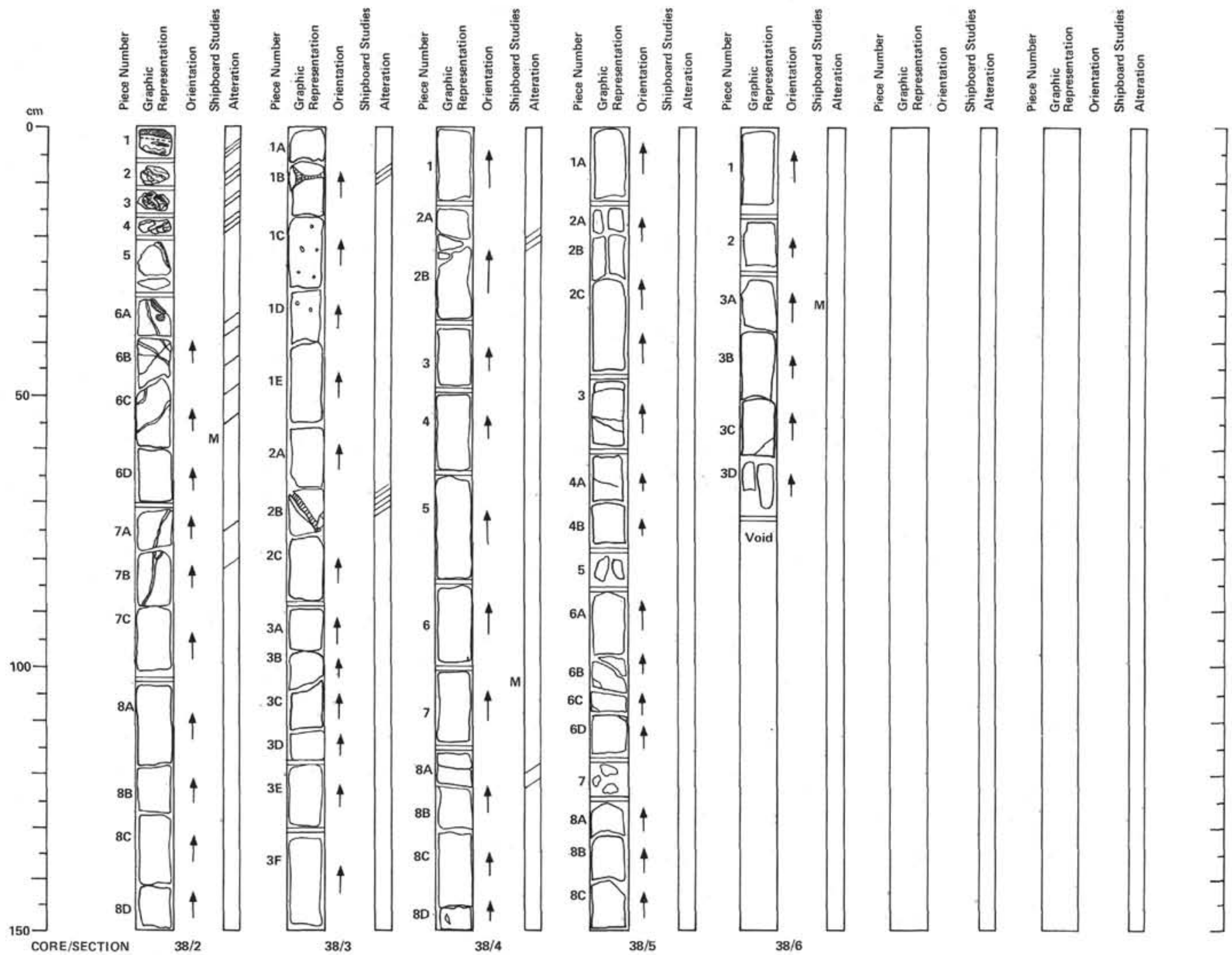

HOLE 485A, CORE 38

Visual Description

Section 1, 0 cm–Section 2, 2 cm: Black, indurated mudstone with minor pyrite.

Section 2, 2 cm–base of core: Gray, sparsely phyric massive basalt. Plagioclase phenocrysts 3–5%, <10 mm, subhedral, fresh. Groundmass, fine- to medium-grained, increasing slightly in grain size downward, generally fresh. Vesicles <1%, <0.5 mm, round, filled with smectite. Veinlets sparse, steep, hairline to 5 mm, filled with smectite.

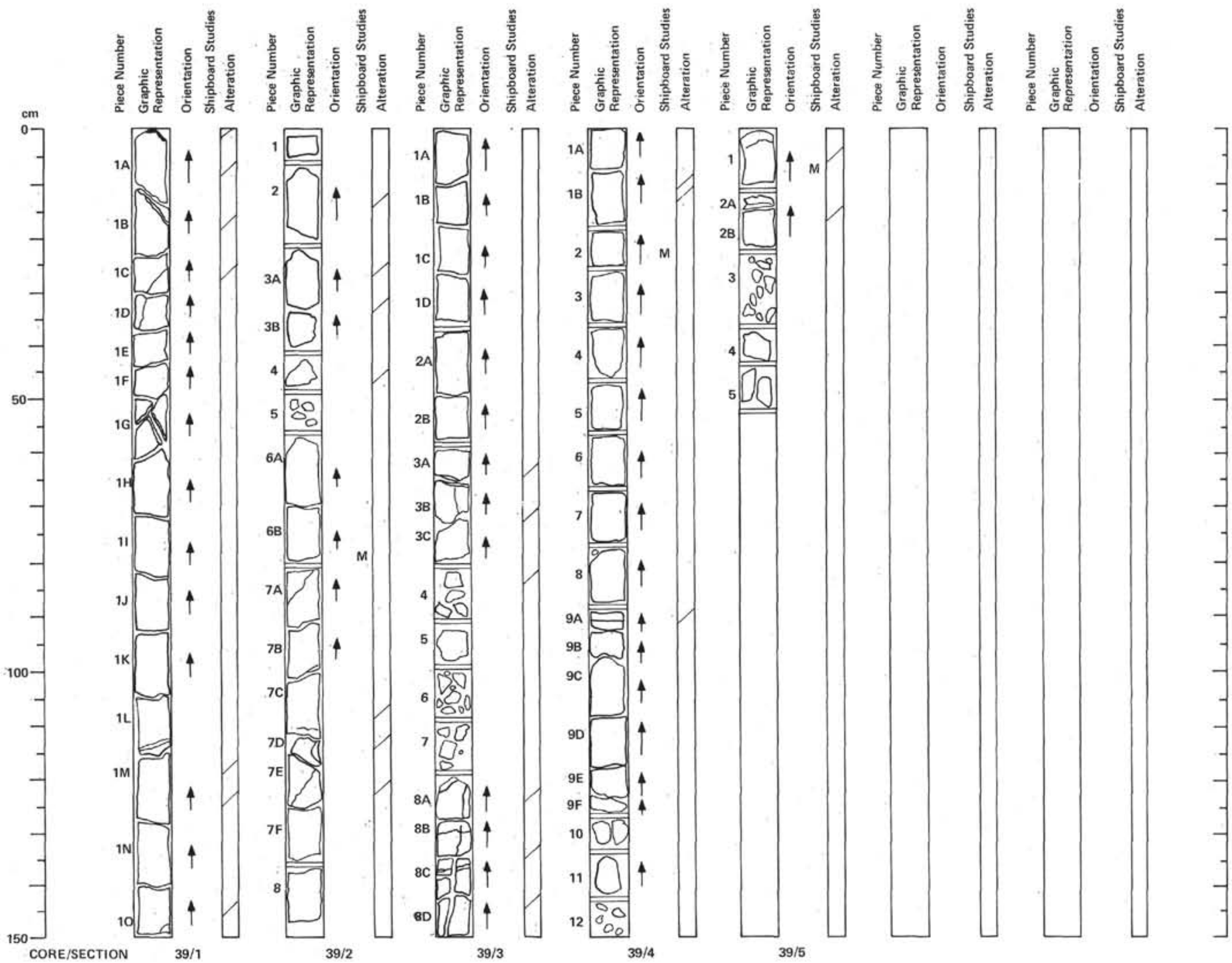

HOLE 485A, CORE 39

Visual Description

Gray, very sparsely phyric, massive basalt. Plagioclase phenocrysts < 1%, < 5 mm, subhedral, fresh. Groundmass medium-grained to coarse-grained, generally fresh, grain size increases somewhat downward. Vesicles < 1%, irregularly distributed, 1–2 mm, round, filled with smectite. Veins and fractures sparse, steep, hairline to 3 mm, filled with smectite, carbonate and pyrite.

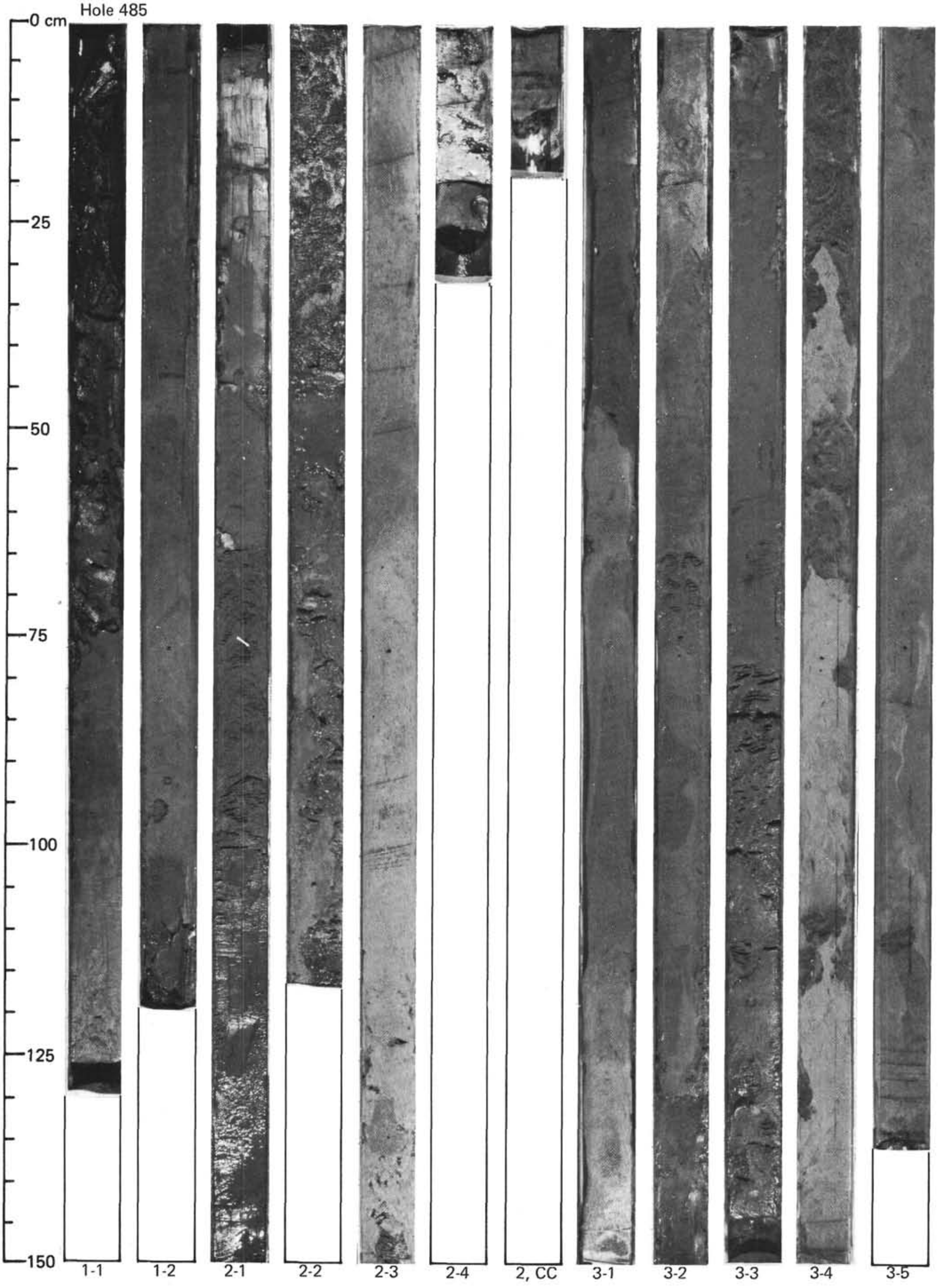
Hole 485
0 cm
25
50
75
100
125
150
1-1
1-2
2-1
2-2
2-3
2-4
2, CC
3-1
3-2
3-3
3-4
3-5

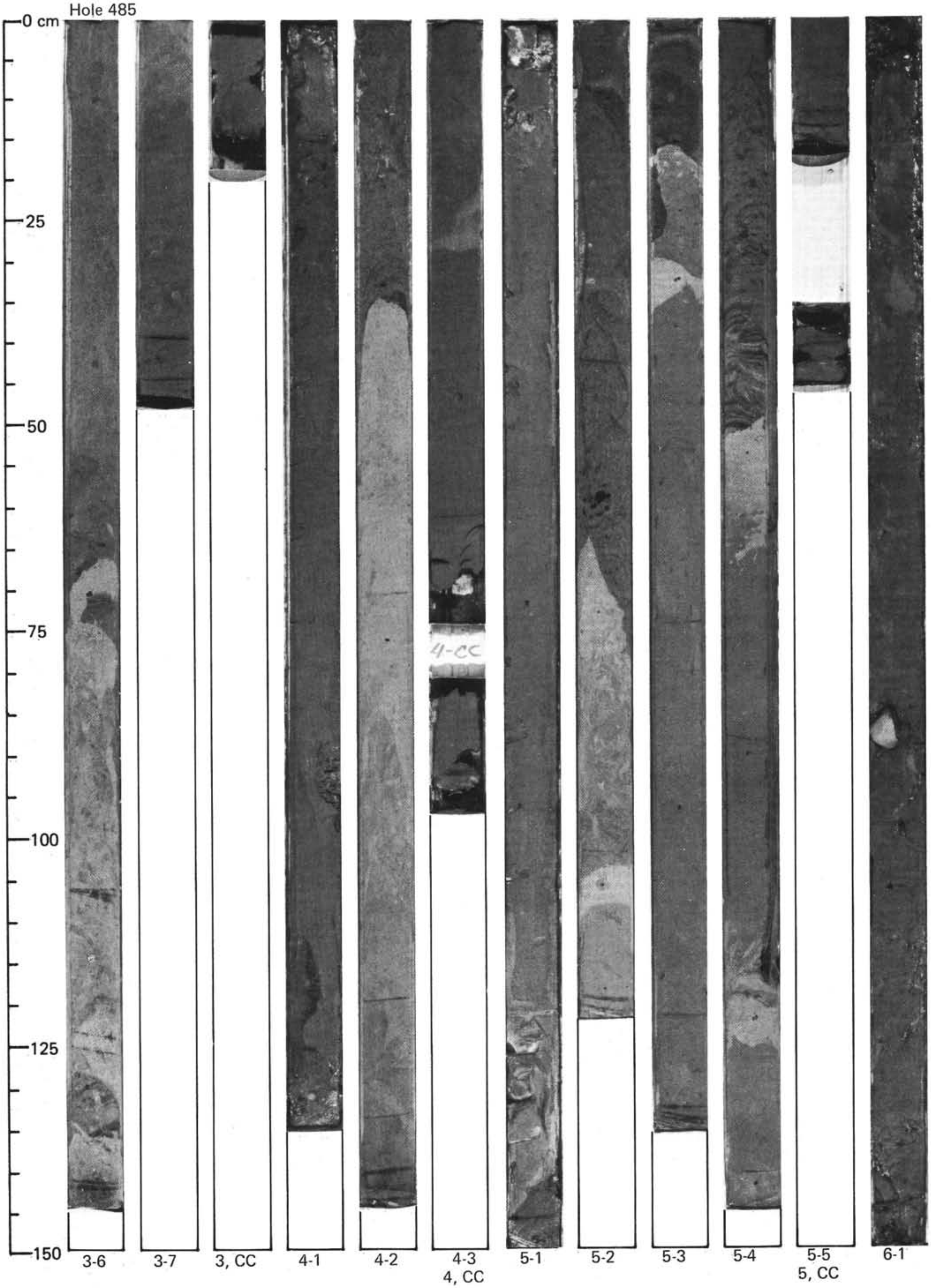
Hole 485
0 cm
25
50
75
100
125
150
4-CC
3-6
3-7
3, CC
4-1
4-2
4-3
4, CC
5-1
5-2
5-3
5-4
5-5
5, CC
6-1

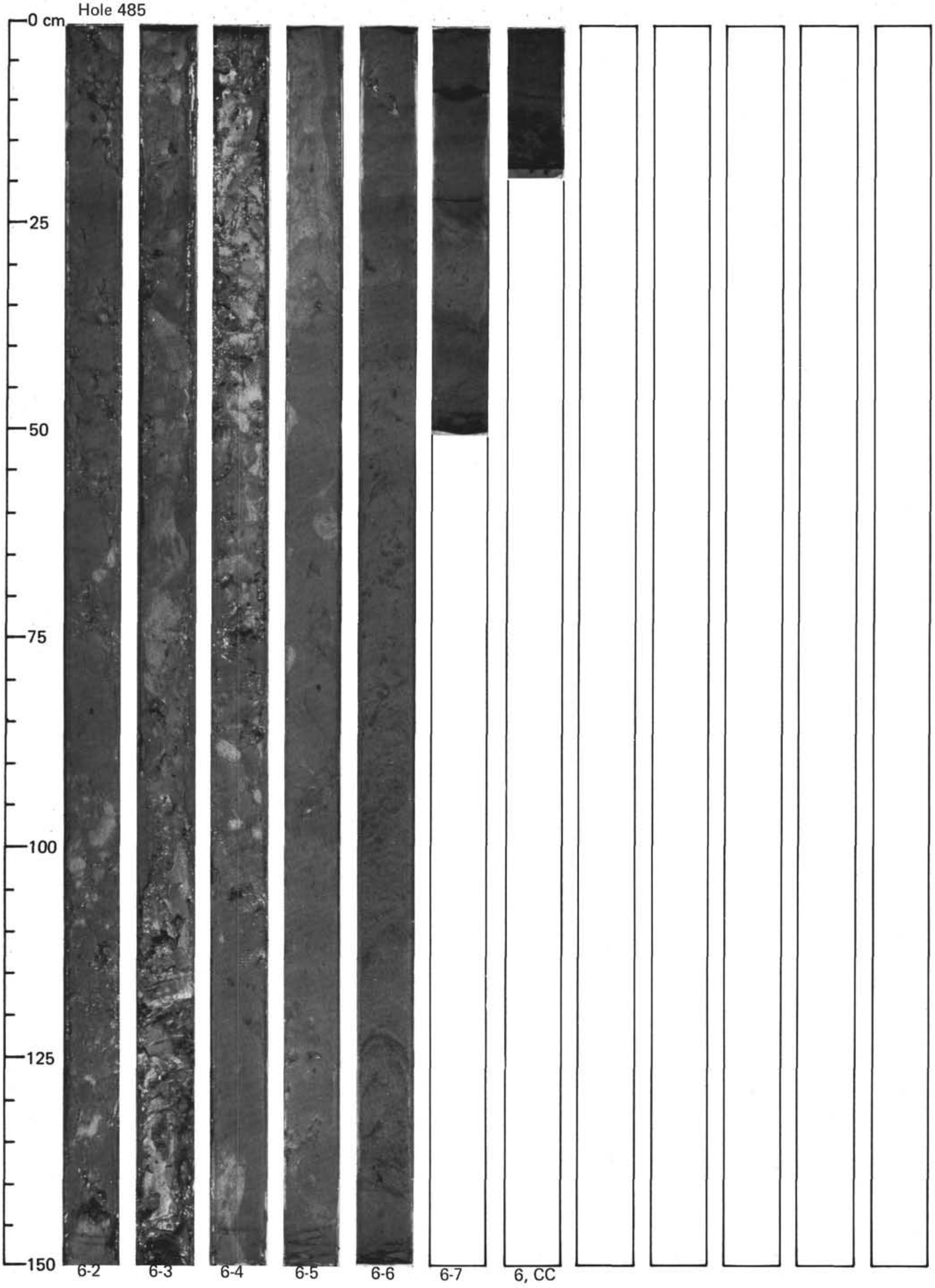
Hole 485
0 cm
25
50
75
100
125
150
6-2
6-3
6-4
6-5
6-6
6-7
6, CC

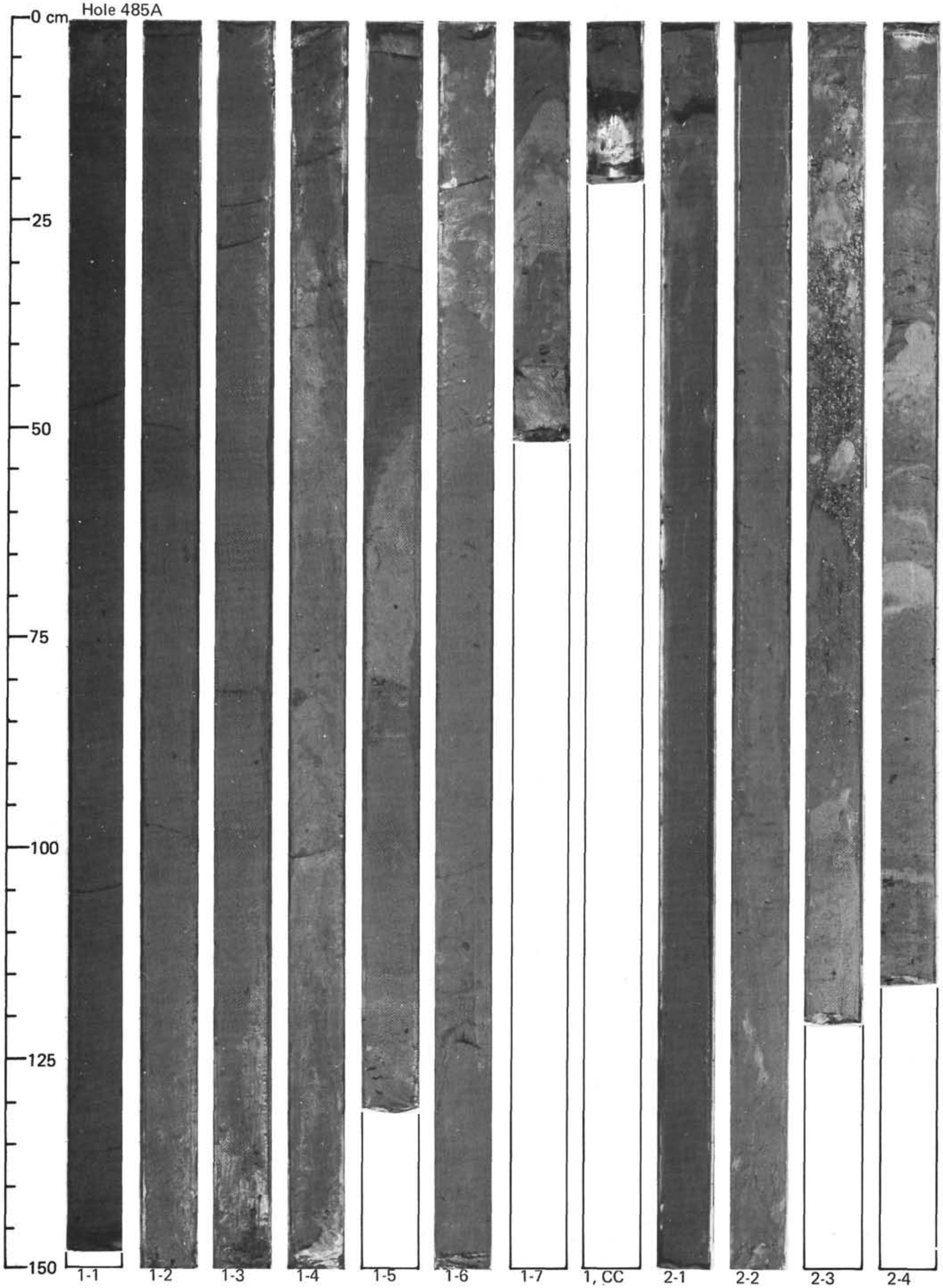
0 cm
Hole 485A
25
50
75
100
125
150
1-1
1-2
1-3
1-4
1-5
1-6
1-7
1, CC
2-1
2-2
2-3
2-4

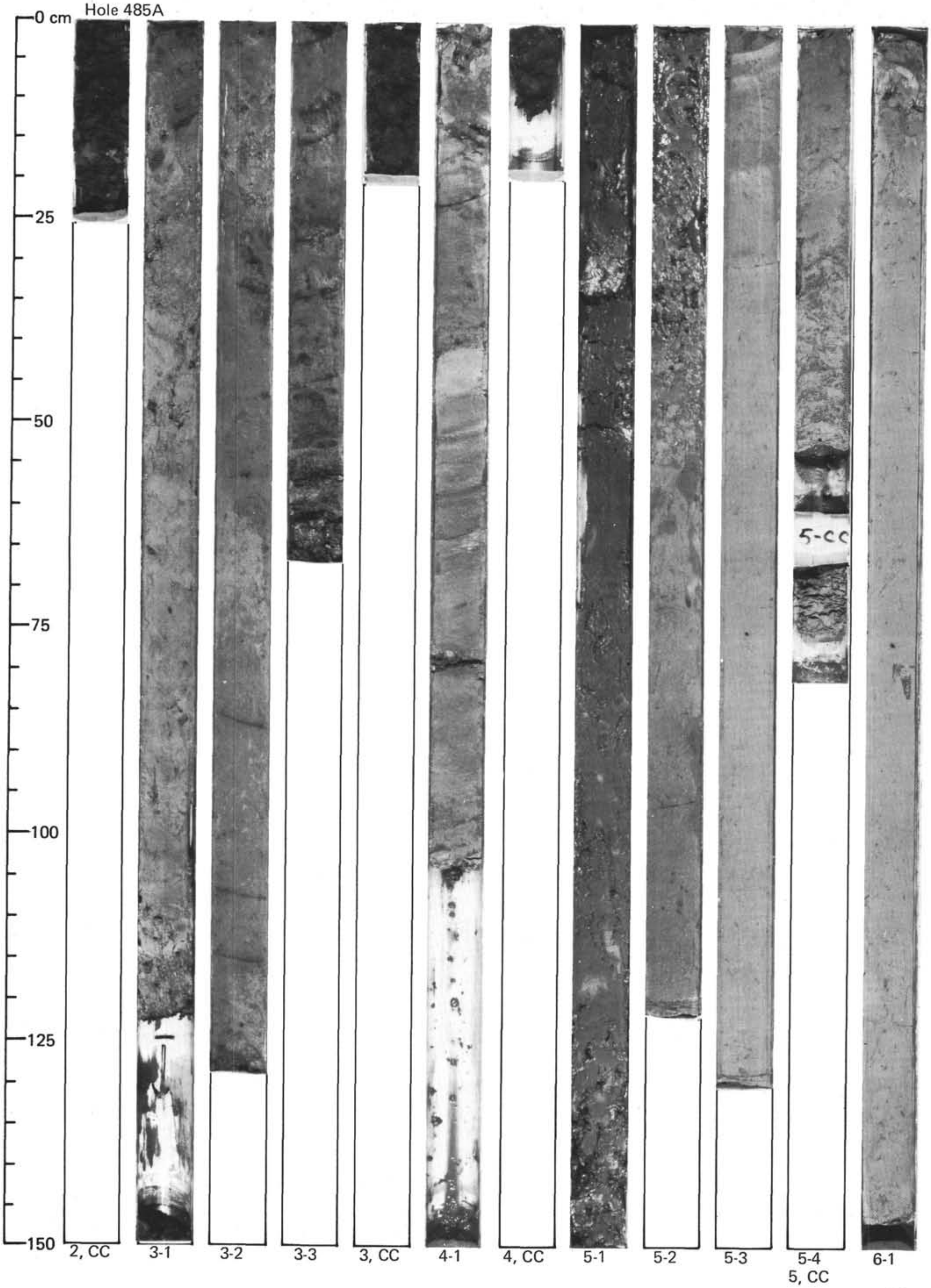
Hole 485A
0 cm
25
50
75
100
125
150
2, CC
3-1
3-2
3-3
3, CC
4-1
4, CC
5-1
5-2
5-3
5-4
5, CC
6-1
5-CC

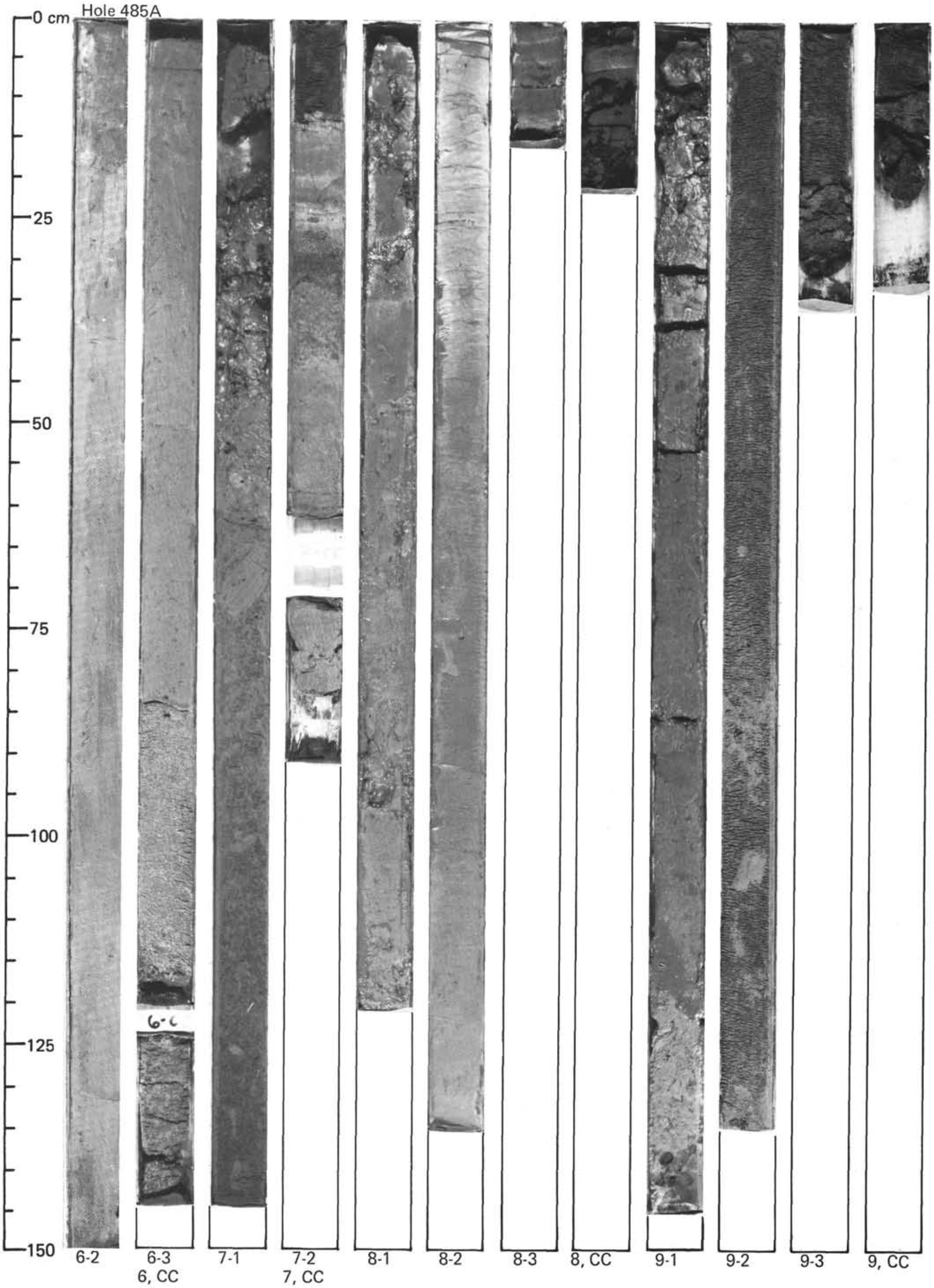
0 cm
Hole 485A
25
50
75
100
125
150
6-C
6-2
6-3
6, CC
7-1
7-2
7, CC
8-1
8-2
8-3
8, CC
9-1
9-2
9-3
9, CC

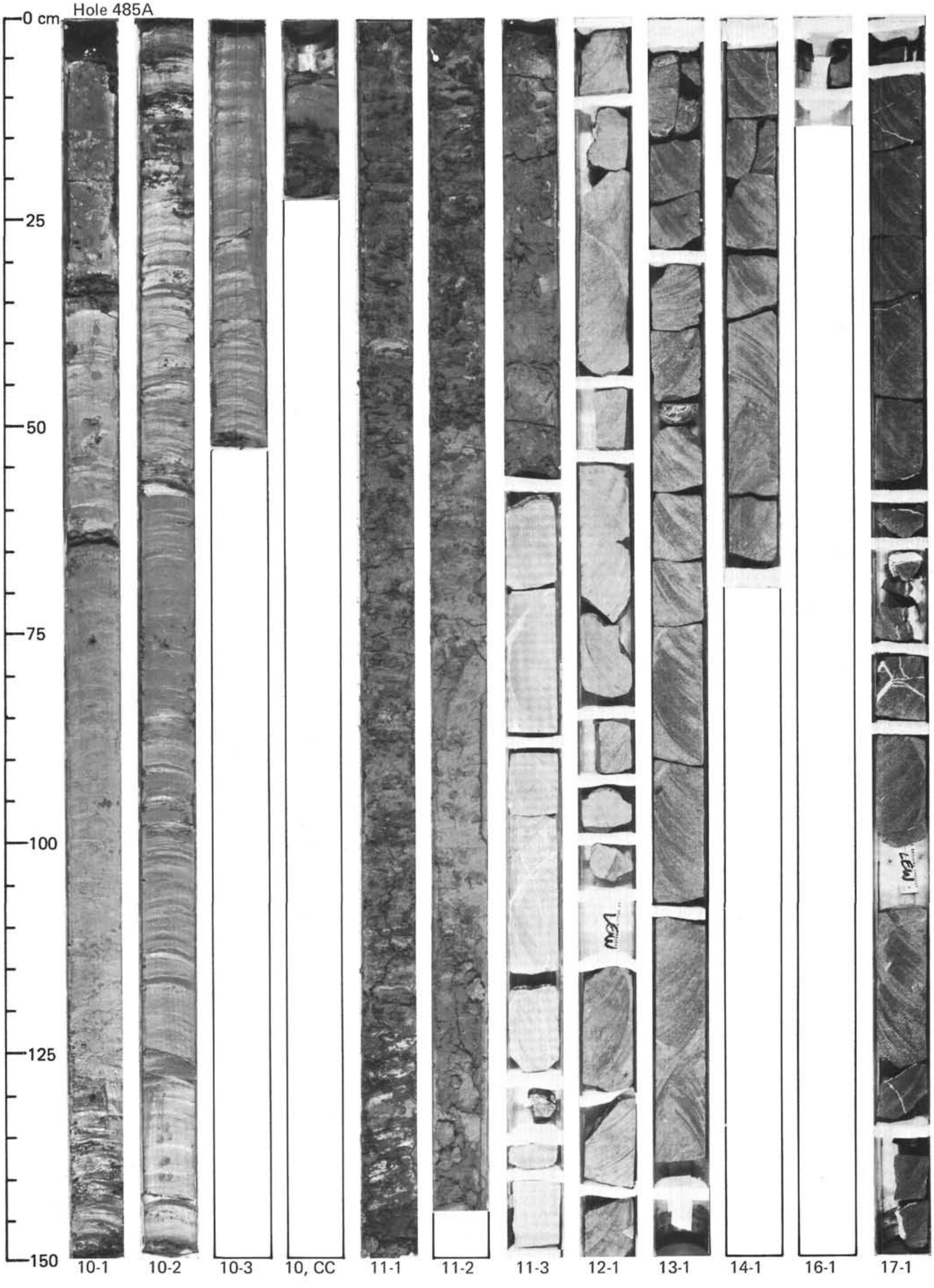
0 cm
Hole 485A
25
50
75
100
125
150
10-1
10-2
10-3
10, CC
11-1
11-2
11-3
12-1
13-1
14-1
16-1
17-1

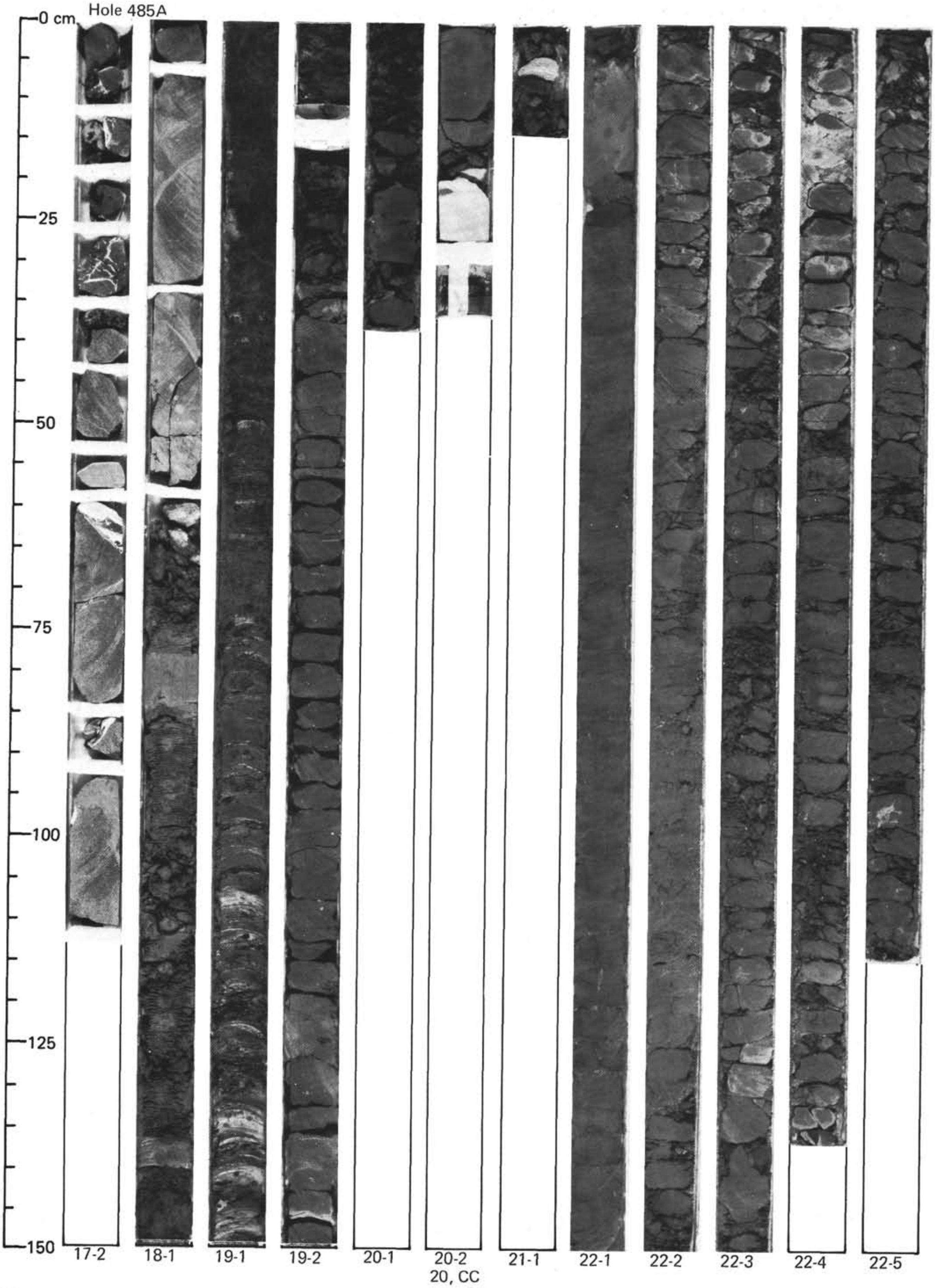
Hole 485A
0 cm
25
50
75
100
125
150
17-2
18-1
19-1
19-2
20-1
20-2
20, CC
21-1
22-1
22-2
22-3
22-4
22-5

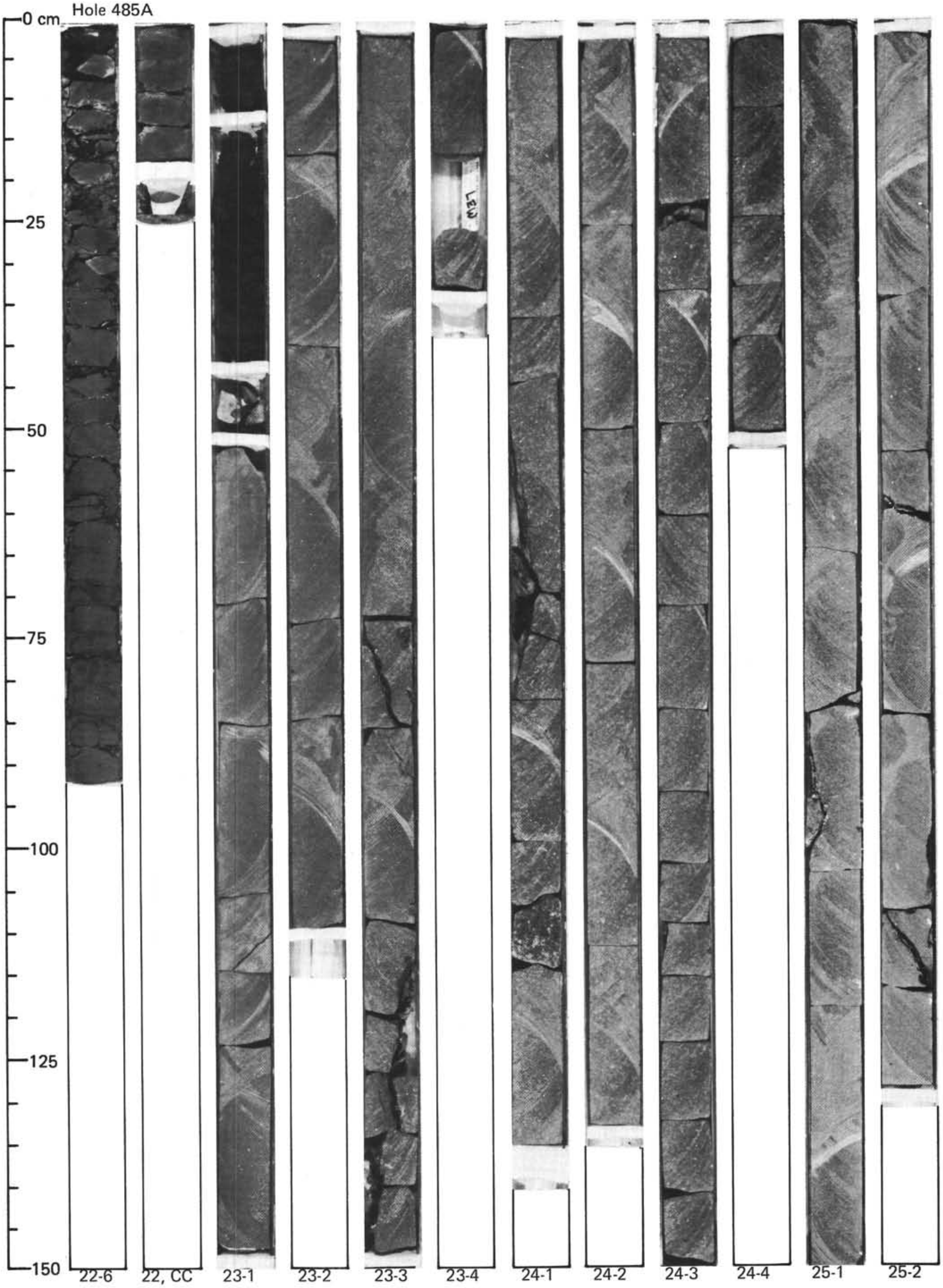
Hole 485A
0 cm
25
50
75
100
125
150
22-6
22, CC
23-1
23-2
23-3
23-4
24-1
24-2
24-3
24-4
25-1
25-2

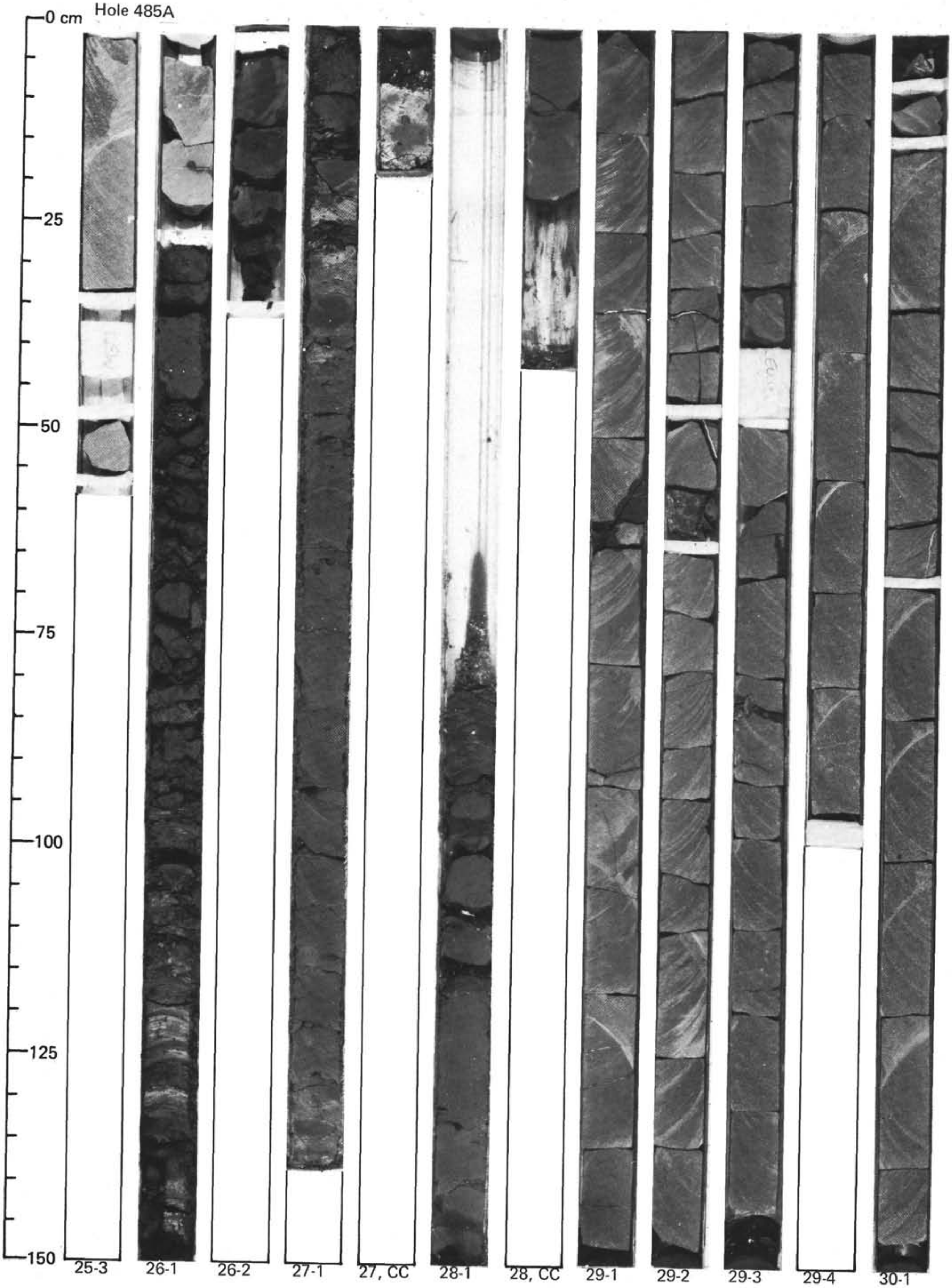
0 cm
Hole 485A
25
50
75
100
125
150
25-3
26-1
26-2
27-1
27, CC
28-1
28, CC
29-1
29-2
29-3
29-4
30-1

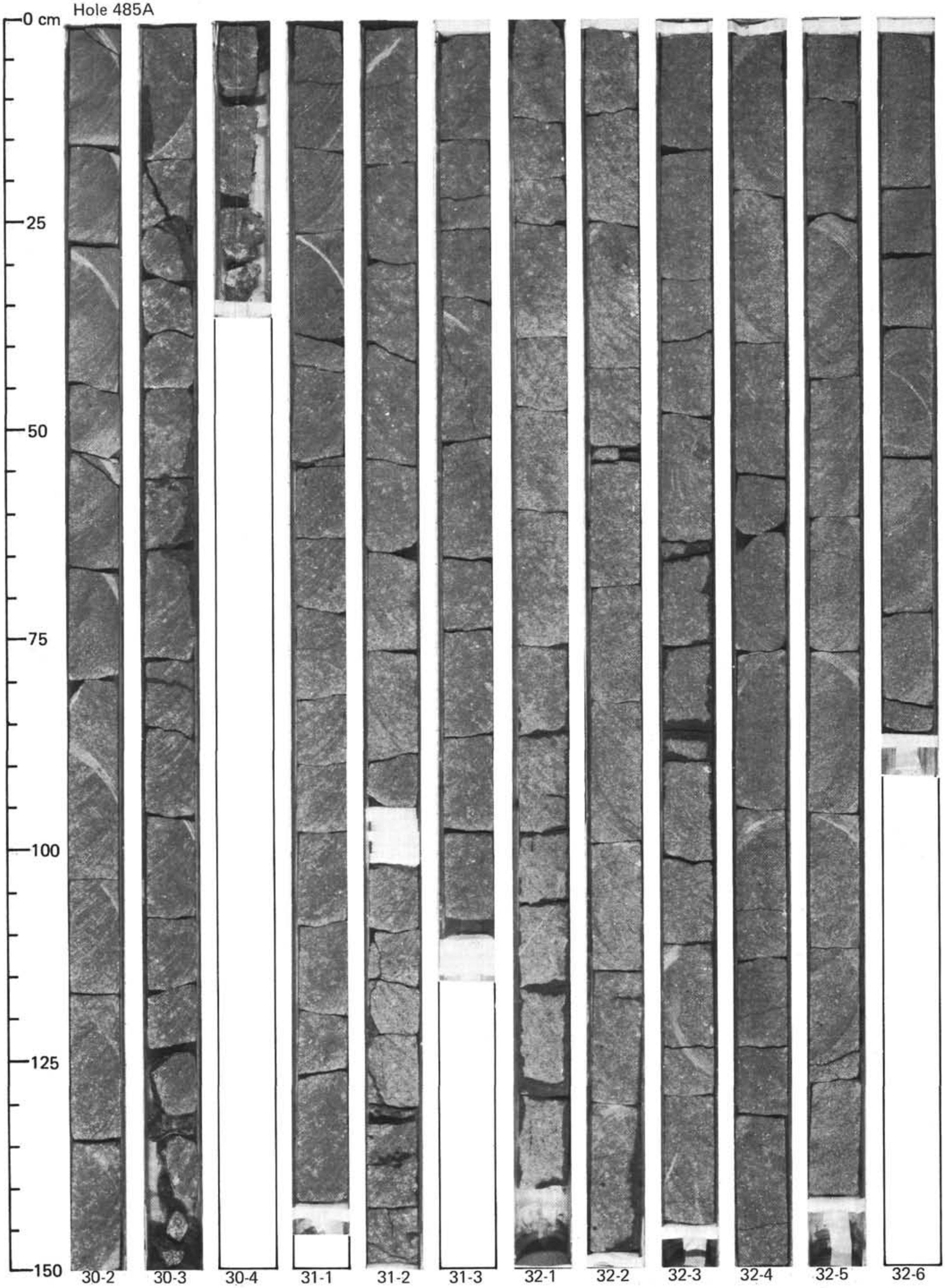
Hole 485A
0 cm
25
50
75
100
125
150
30-2
30-3
30-4
31-1
31-2
31-3
32-1
32-2
32-3
32-4
32-5
32-6

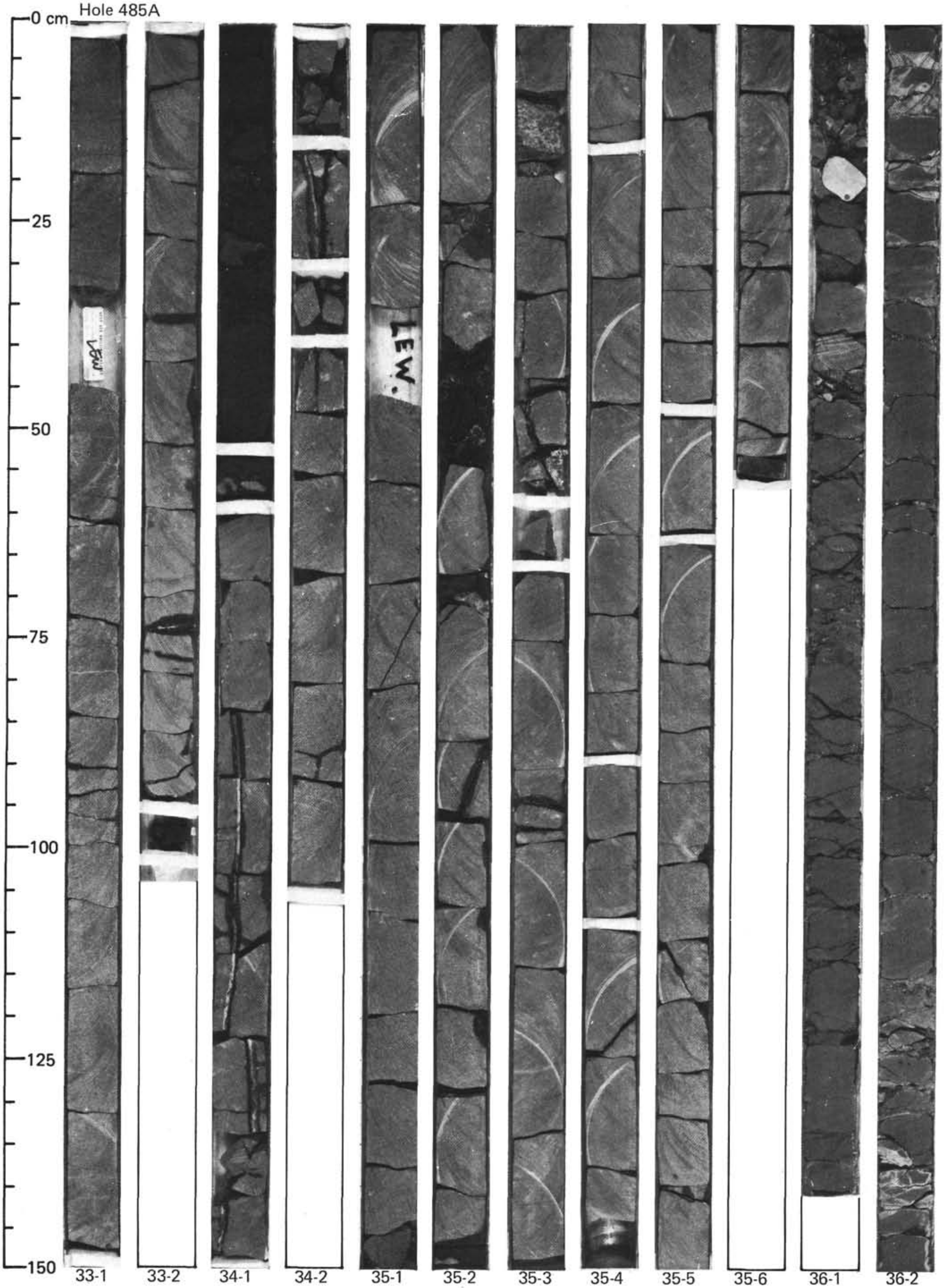

Hole 485A
0 cm
25
50
75
100
125
150
33-1
33-2
34-1
34-2
35-1
35-2
35-3
35-4
35-5
35-6
36-1
36-2

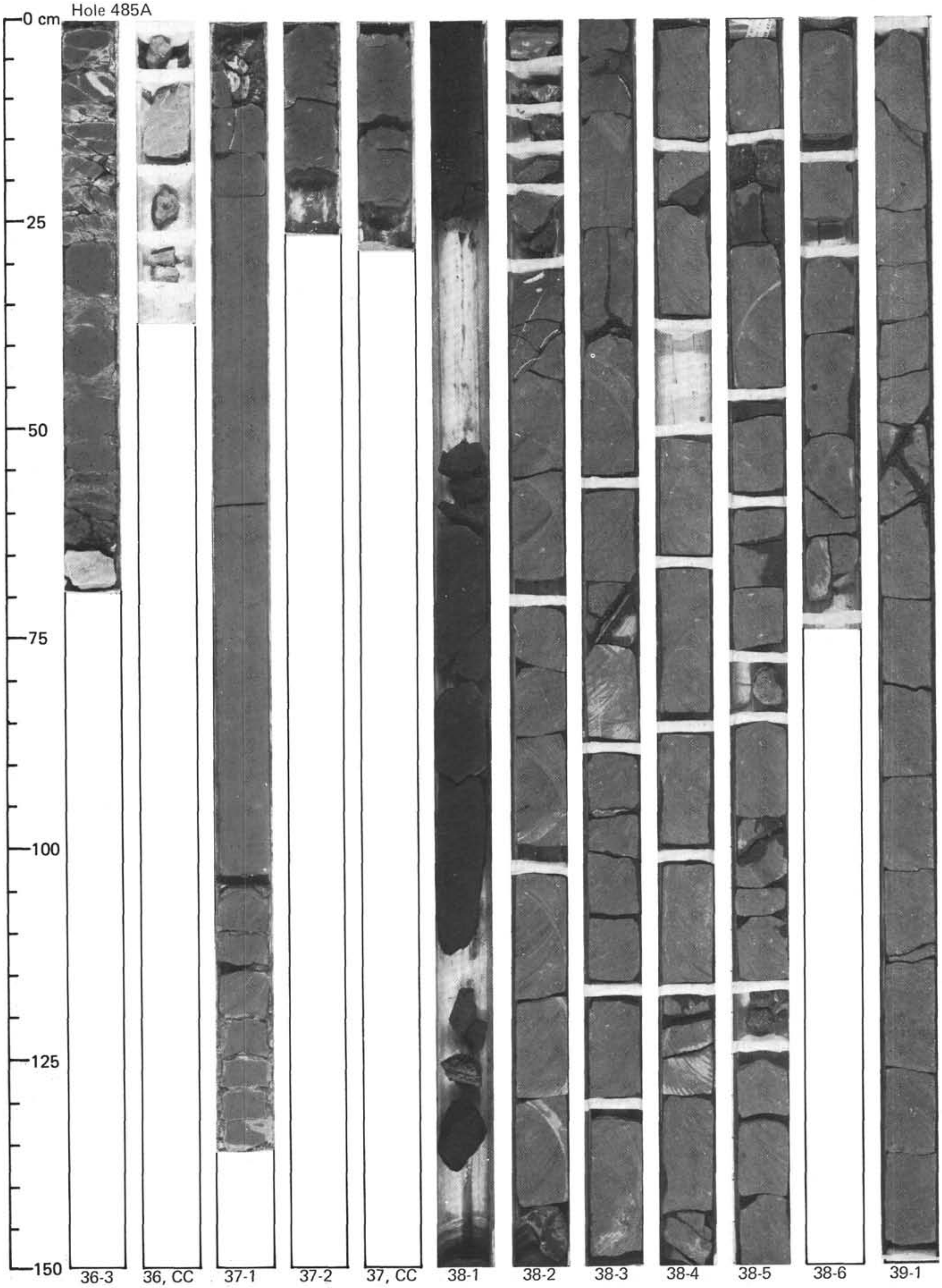
Hole 485A
0 cm
25
50
75
100
125
150
36-3
36, CC
37-1
37-2
37, CC
38-1
38-2
38-3
38-4
38-5
38-6
39-1

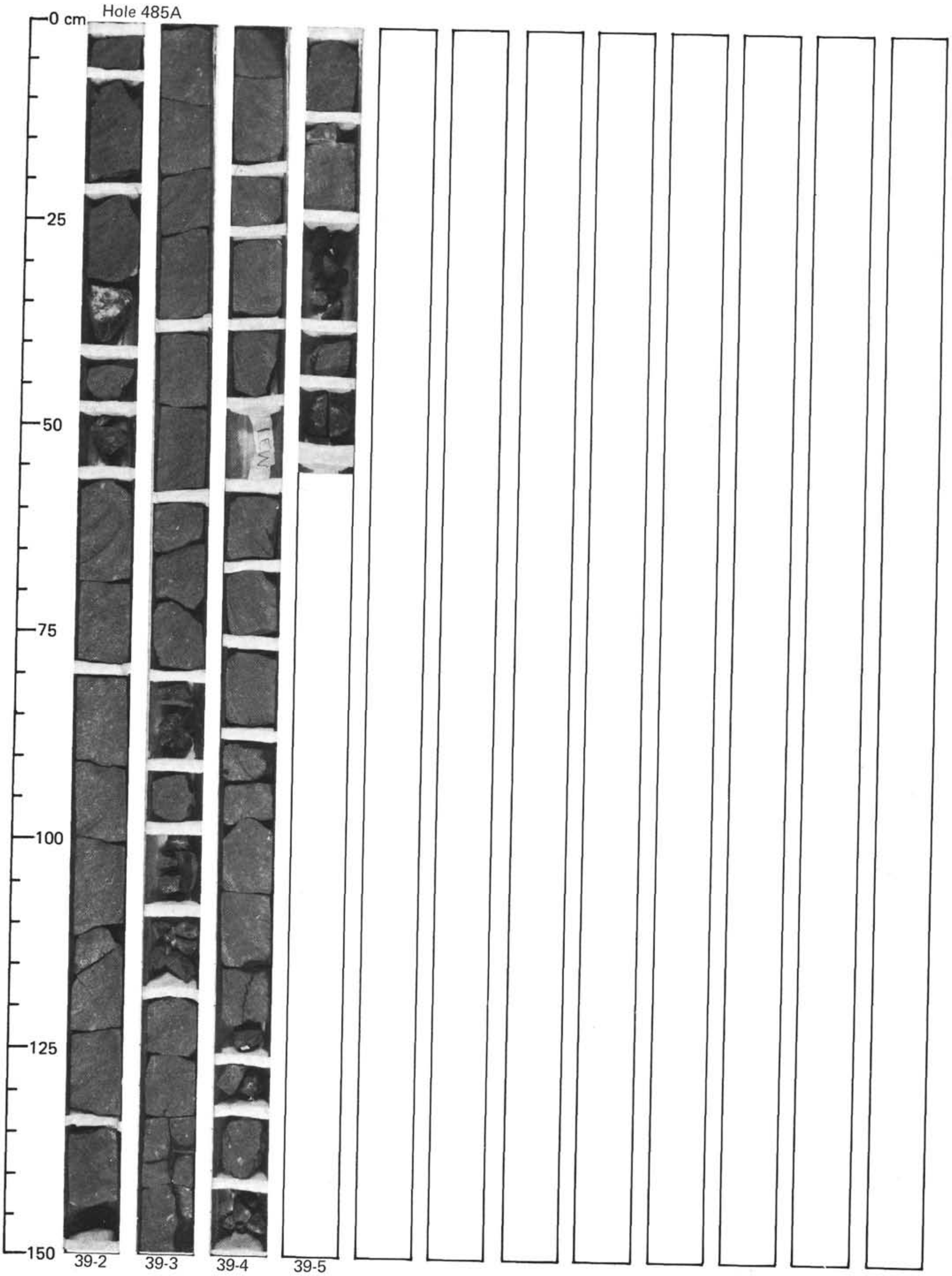
0 cm
Hole 485A
25
50
75
100
125
150
39-2
39-3
39-4
39-5